

**Alma Mater Studiorum - Università di Bologna**

---

Department of Physics and Astronomy  
Master degree in Astrophysics and Cosmology

**Bayesian Models and Biomarker Detection in  
Astrobiology**

Master thesis

Presenter:  
**Flavio Turrini**

Supervisor:  
**Leonardo testi**

---

Academic year 2023-2024

*Dedication...*

## Abstract

Since the confirmation of the first exoplanet in 1992 , exoplanetary science has expanded significantly , with over 5600 confirmed planets in the NASA database. A central goal of the field is to understand habitability and identify biomarkers for life detection. However , the science of biosignature currently lacks a universally accepted theoretical framework to make rigorous life detection claims. My thesis focuses on the application of the Bayesian framework to biosignature detection and highlights both its strengths and limitations. The Bayesian framework offers a flexible and quantitative tool for evaluating life-detection claims, but currently his reliability seems to be hindered by the uncertainties on prior probability of life  $P(life)$ , which remains poorly constrained due to the absence of a robust theoretical framework. Furthermore the application of Bayesian model shows that in the scenario where  $P(molecule|life) \ll P(molecule|nolife)$  , a high posterior probability of life can only be achieved if the prior probability is already very high, which is a rarely realistic assumption. In such cases repeated observations lead to a steep decline in posterior probability rather than an increase. Only eliminating false positives or selecting biomarkers with no false positives , combined with large statistical samples, can lead to high-confidence detection over time. The results obtained from sensitivity analysis highlight the necessity of detecting multiple biosignatures to reduce the dependency on prior assumptions , making high-confidence life-detection claims more attainable.

Finally ,as a case study ,in the last chapter I analyzed the alleged detection of Phosphine in Venus, highlighting the challenges in life-detection and how the lack of application of a Bayesian framework makes it difficult to rigorously establish confidence in life detection claims.

# Contents

<b>Contents</b>	<b>i</b>
<b>1 The study of exoplanetary atmospheres</b>	<b>1</b>
1.1 A brief history and current state of the field . . . . .	1
1.2 Properties comparison between Solar system planets and Exoplanets .	6
1.3 different types of rocky exoplanets . . . . .	9
1.4 The different detection methods for exoplanets . . . . .	11
1.4.1 Transit Spectroscopy . . . . .	11
1.4.2 High resolution Doppler Spectroscopy . . . . .	15
1.4.3 direct imaging . . . . .	17
1.4.4 timing . . . . .	18
1.4.5 microlensing . . . . .	20
1.4.6 comparison of the different methods . . . . .	21
1.4.7 Summary . . . . .	23
1.5 The modelling of the exoplanetary atmospheres . . . . .	23
<b>2 Addressing the Challenge of Defining Reliable Biomarkers in Exo- planetary Atmosphere Studies</b>	<b>25</b>
2.1 The search for gaseous biomarkers . . . . .	25
2.1.1 potential biosignature gases . . . . .	28
2.2 Phosphine $\text{PH}_3$ . . . . .	29
2.2.1 Phosphine as a biomarker in spectroscopic observations . . . . .	29
2.2.2 spectral properties of of Phosphine . . . . .	30
2.2.3 phosphine Surface fluxes required for detection . . . . .	31
2.2.4 Sensitivity to temperature and radiation levels . . . . .	32
2.2.5 Phosphine spectral distinguishability . . . . .	33
2.2.6 Phosphine false positives . . . . .	35
2.2.7 conclusion:phosphine as a biosignature gas . . . . .	36
2.3 chemical imbalance as a biomarker . . . . .	36
2.4 critical aspects of the concept of biosignature . . . . .	38
<b>3 Application of the Bayesian statistics to the inference of gaseous biomarkers</b>	<b>43</b>
3.1 The use of a Bayesian approach . . . . .	43
3.1.1 The different ways of seeing probability . . . . .	43
3.1.2 General properties of probability . . . . .	45
3.1.3 What is the Bayesian approach to probability theory . . . . .	46

3.1.4	Bayesian approach applied to astrobiology . . . . .	49
3.1.5	Statistical approaches to characterizing atmospheres of non-Earth like worlds . . . . .	53
3.1.6	$P(data abiotic)$ . . . . .	55
3.1.7	$P(data life)$ . . . . .	57
3.1.8	$P(life)$ . . . . .	59
3.1.9	Bayesian framework example: building a toy model for phosphine detection . . . . .	63
3.2	Expanding the model . . . . .	67
3.2.1	Application to Phosphine case . . . . .	72
3.2.2	Quantifying the error . . . . .	75
3.3	Sensitivity analysis . . . . .	77
3.3.1	application of the sensitivity analysis to the model . . . . .	79
3.3.2	Search Strategies Based on Bayesian Approach . . . . .	83
3.4	critical aspects of the Bayesian approach to astrobiology . . . . .	85
3.5	Signal detection theory . . . . .	89
3.5.1	Bayesian Hypothesis testing . . . . .	91
3.5.2	possible application of SDT and BHT to gaseous biomarkers . . . . .	92
3.6	Ladders for life detection . . . . .	93
<b>4</b>	<b>The case of detecting Phosphine in the atmosphere of Venus</b>	<b>95</b>
4.1	Venus properties and habitability . . . . .	95
4.2	venus and the search for life . . . . .	100
4.2.1	The alleged discovery of Phosphine in the atmosphere of Venus	100
4.2.2	JCMT and ALMA observations . . . . .	101
4.2.3	further analysis from the ground . . . . .	103
4.2.4	The debate around the line . . . . .	104
4.3	hypothesis on the origins of Phosphine on Venus . . . . .	107
4.4	The future of Phosphine study on Venus . . . . .	109
4.4.1	Earth and space based studies . . . . .	109
4.5	conclusion: Bayesian life detection on Venus . . . . .	111
<b>5</b>	<b>conclusions</b>	<b>113</b>
	<b>Bibliography</b>	<b>116</b>

# Chapter 1

## The study of exoplanetary atmospheres

### 1.1 A brief history and current state of the field

The study of planetary atmospheres through telescopes is probably the only method we will ever have in order to be able to study the composition of the exoplanets. It is indeed very hard to think of the time when we will be able to study them with in situ observations. The last decades of observations have brought us enormous advancements. Thousands of exoplanets have now been found, and we are beginning to appreciate with increasing precision their diversity, from the chemical composition to the processes by which they begin to form. Since the first discovery of an exoplanet in 1992[58], around a pulsar, many others have followed: 51 Pegasi b in 1995[2], which was the first discovered around a main sequence star, indirectly found using stellar Doppler shift, classified later as a gas giant, with  $0.5 M_{\odot}$  and a 4.23-day orbit. From the beginning, it was clear that the next step would be to try to study the atmosphere using spectroscopy. One of the main challenges to face in this type of analysis is dealing with the planet-star contrast, which is very low, of the order of  $10^{-6}$ . This is one of the reasons why from 1999, when we obtained a spectrum for the first time, until 2008, there have been no significant advancements in the study of exoplanetary atmospheres with high-resolution spectroscopy.

The first studies regarding atmospheric absorption from a transiting exoplanet can be found in [14], for what concerns thermal emission instead in [15]. When exoplanetary spectra are combined with bulk parameters of the planets and host star it is possible to obtain important informations about the planet atmosphere

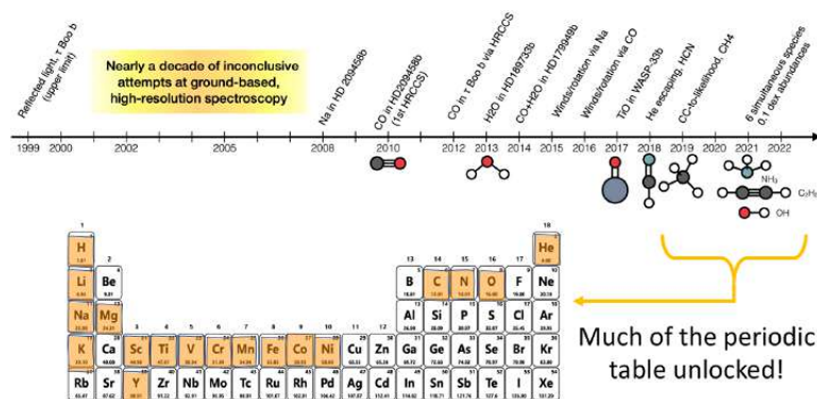


**Figure 1.1:** timeline of high spectral resolution history

, internal properties and formation history. The observables that you can obtain from an exoplanets are strongly dependent upon the detection method, but for what concerns transiting exoplanets they can include: bulk parameters (mass and radius), atmospheric spectra and host star spectra. The atmospheric spectra taken individually are able to give us information about chemical composition , temperature profiles and energy distributions in the atmospheres, which in turn give us information about chemical atmospheric processes as equilibrium processes, presence or not of chemical inversion , atmospheric dynamics and aerosol. [37]

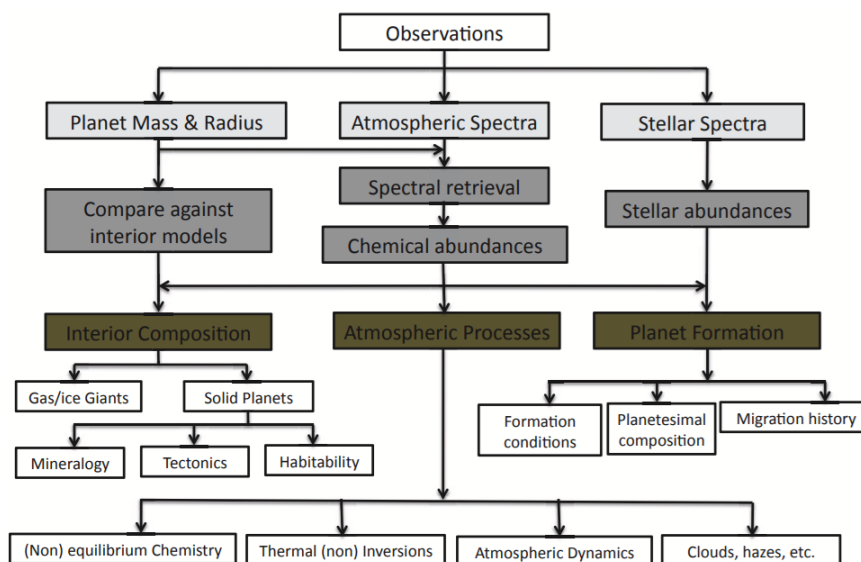


**Figure 1.2:** Schematic diagram of exoplanets characterization. from observables to various aspects of planets. from [37]

In the last decades , with the discovery of thousands of different exoplanets , it

was clear that there is a big variety in exoplanetary zoo. The range of values that the properties span is much larger than the one we are familiar in the solar system.

The measured temperatures go from 200 to 4000K , radius and mass go from 0.5-20  $R_{\odot}$  to  $1 - 10^4 M_{\odot}$ . In the Solar system instead the temperatures stay between 50 and 500K and only Venus stays above 300K. A possible exoplanet size and mass classification can be found in 1.1 and 1.8 later in the chapter. Currently it is believed that the transition between planets that must have an atmosphere , and smaller rocky planets that might or might not have atmospheres, is close to  $1.5R_{\odot}$  and  $1.7R_{\odot}$ .

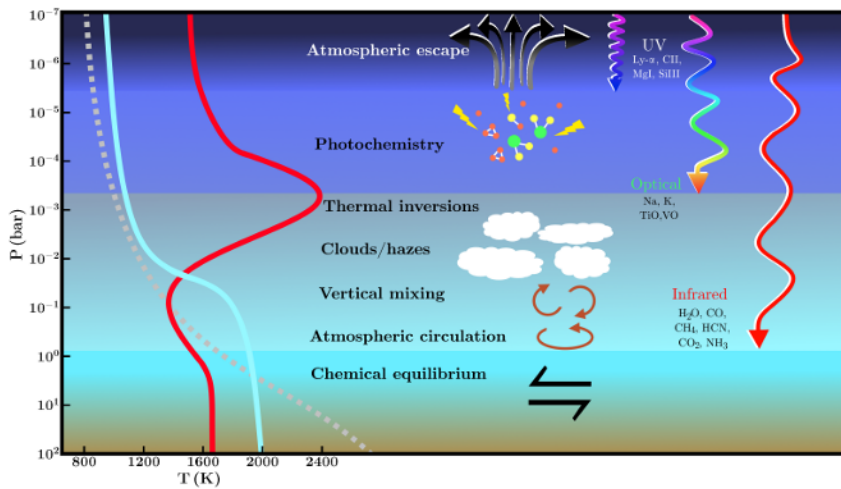


**Figure 1.3:** process in exoplanetary atmospheres and how they are probed by different parts of the EM spectrum, the chemical species whose signatures can be detected in each wavelength range are also indicated. On the left are shown three types of temperature profile which can arise as a result of atmospheric processes: the profile of a highly-irradiated planet with a thermal inversion (red), that of an irradiated planet without a thermal inversion (cyan), and the temperature profile of a poorly irradiated planet (grey, dashed), taken from [72]

As shown in 1.3 different spectral ranges probe different region of the atmosphere, so gaining informations on different processes. This can be studied as a function of pressure  $P$  in the atmosphere [72]. In the depths of the atmosphere ( $P > 1bar$ ) the pressure and temperature, and so density and opacity are sufficiently big so that the thermochemical equilibrium and radiative convective equilibrium prevail and so the chemical reactions occur at a higher rate than kinetical processes. The resulting composition is then the one that minimizes the free gibbs energy of the system for a given temperature, pressure and elemental abundance. In the high region of the atmosphere , between 1 mbar and 1 bar , different processes begin to be



prevail , including atmospherical dynamical processes like clouds and temperature inversions, as a result of the complex interaction between incident radiation field, chemical composition and others planetary properties. These processes strongly influence and are influenced by chemical composition and the temperature structure of the atmosphere and both can be out of the equilibrium. Higher in the atmosphere ( $P = 10^{-6} - 10^{-3}$  bar ) the low density and the high radiation field cause the photochemical processes to prevail in the atmosphere trough photodissociation of prominent molecules. Finally at very low pressures , the atmospherical escape of atomical species brings to mass loss in the atmosphere. This is why every atmospherical region probes different chemical and physical processes, as outlined by [72].

At the same time different chemical species are accessible from different region of the EM spectrum. The prominent chemical species ( $H_2O$ ,  $CO$ ,  $CO_2$ ,  $CH_4$ , etc.) absorb mainly in infrared due to the rotovibrational transitions, except some metal species ( $TiO$ ;  $VO$ ,  $TiH$ , etc.) that have a strong absorb features in the optical. Instead, the atomic species absorb mainly in optical and UV, depending on the excitation states and ionization. So while observation in UV probe the upper region of the atmosphere where the composition is mainly atomic, the observations in infrared probe low regions in the atmosphere where the composition is mainly molecular, where the molecular spectra probe intermedial regions. [72]

The study of exoplanetary atmospheres has had a rapid progress since 2008, only few years ago less than 25 planets were known transiting and the first images from direct imaging have been obtained. Only a handful of atomic species had been measured robustly, manly in the two gaseous giants HD 209458b and HD 189733b using transmission spectra in optical and UV obtained from Hubble.[14] [52] Besides this, the first observations of exoplanetary atmospheres were made using multi band space-based infrared photometry and spectroscopy with Spitzer and HST. [3] [26] In [50] for the first time it was claimed the possible presence of methane in an exoplanetary atmosphere. It is important to say that these first observation were made with instruments like HST NICMOS spectrograph and spitzer photometric instruments that had not been designed to study exoplanets, which require very high sensitivities( with a photometric precision of at least  $10^{-4}$ ). For this reason many of these observation have been debated and some of them also corrected. An analysis and summary of these arguments can be found in [7]. Today the situation

is changed a lot, the HST telescope has allowed to obtain high quality exoplanetary spectra frequently enough to allow a fast advancement in the field.

In those years, at the same time the first attempts of transit spectroscopy were being made. [81] However, the inferences on molecular absorption and pressure-temperature profile were based primarily on forward models with solar like elemental composition and equilibrium conditions. In those years the retrieval methods were still at the beginning and the statistical constrain of the atmospherical properties not feasible yet.

In the last decades a combination of technically challenge observation of transiting exoplanets and theoretical advancements have brought us to the rapid development we see nowadays. The Nasa database counts more than 5600 exoplanets discovered using different techniques both from ground and space observations.

Today more than a Hundred of exoplanets spectra have been obtained.

Besides the improvement of the detection methods, the development of the retrieval techniques has allowed to study the atmosphere of exoplanets and obtain statistical information as a standard procedure. Such inversion techniques have allowed us to obtain initial constraints about the key properties of the atmosphere such as molecular and atomical species. Elemental ratios (O/H, C/O), temperature profiles, cloud/hazes, circulation patterns and exospheres. [72].As outlined by [72] The most successful studies have focused on 3 different techniques:

1. Extensive high precision transit spectroscopy with HST from UV to NIR, which brought to many characterization of transiting exoplanets. The spectrograph WXF3 of the HST in NIR in particular has made observation of H<sub>2</sub>O in the exoplanetary atmospheres and has observed dozens of exoplanets from hot jupiters to exoneptunes and even super Earths. A remarkable achievements because even in the solar system is hard to characterize this molecule in gaseous giants due to low temperatures at which H<sub>2</sub>O condensates.
2. direct imaging and spectroscopy of exoplanets
3. high resolution Doppler spectroscopy in the NIR has allowed to observe molecules in the exoplanetary atmospheres, both in transit and not, using cross correlation with template spectra.

## 1.2 Properties comparison between Solar system planets and Exoplanets

As we can see from figures 1.4,1.6,1.7, there seems to be very few exoplanets discovered in the region of the parameter space where Solar system planets lay. Partially it is caused by a selection effect due to the fact that the radial velocity, transit, and direct imaging methods are currently not sensitive to planets in this region of parameter space, as highlighted by [60]. However, in the study of exoplanet demographics, it is still unclear how common Earth-analog planetary systems actually are. A surprising result of the Kepler analyses was precisely discovering that most stars seem to host close-in super-Earths and/or sub-Neptunes. Since our planetary system does not host this type of planets, this result would suggest that planetary systems like ours—i.e., with small rocky planets in the temperate zone and gas giants beyond the ice line—might not be common. One of the main goals will be to combine different detection methods that are complementary to each other, in order to derive constraints across the entire parameter space. For what concerns the Exoplanet classification there is not a universally accepted one. The size classification adopted by [11] is the following:

<b>Planet Type</b>	<b>Planet Size</b>
Earth size	$< 1.25R_{\oplus}$
Super Earth size	$1.25 - 2R_{\oplus}$
Neptune size	$2 - 6R_{\oplus}$
Jupiter size	$6 - 15R_{\oplus}$

**Table 1.1:** Planet size classification, as proposed by [11]

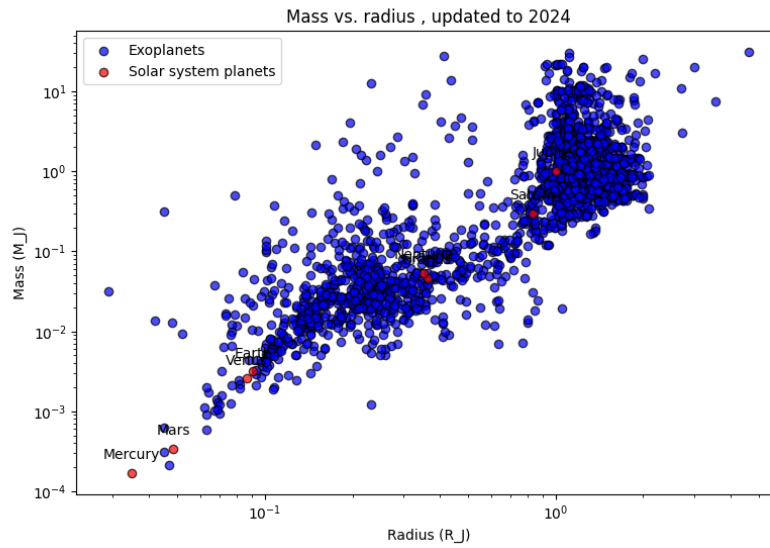


**Figure 1.4:** comparison between Solar system planets mass and radius with exoplanets. The exoplanets data come from NASA archive: <https://exoplanetarchive.ipac.caltech.edu/index.html>. The data are updated to 23/07/2024.

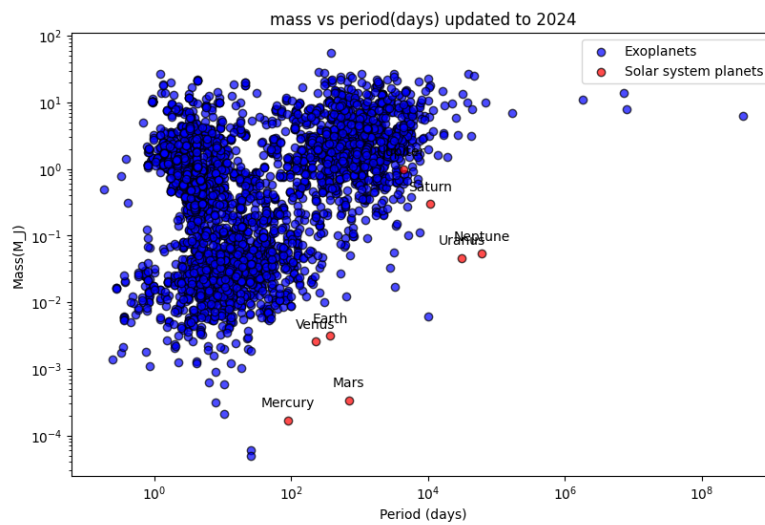


**Figure 1.5:** comparison between Solar system planets mass and period with exoplanets. The exoplanets data come from NASA archive: <https://exoplanetarchive.ipac.caltech.edu/index.html>, The data are updated to 23/07/2024.

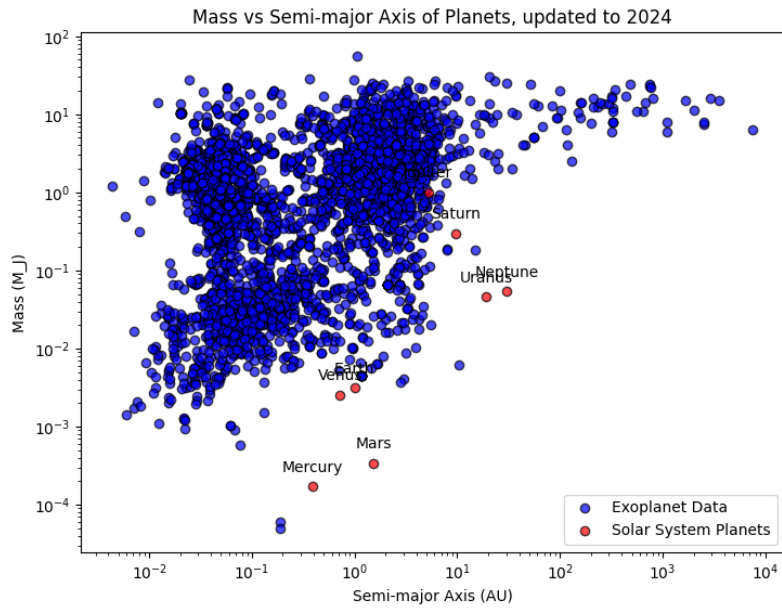


**Figure 1.6:** comparison between Solar system planets mass and major semiaxes with exoplanets. The exoplanets data come from NASA archive: <https://exoplanetarchive.ipac.caltech.edu/index.html>, The data are updated to 23/07/2024.

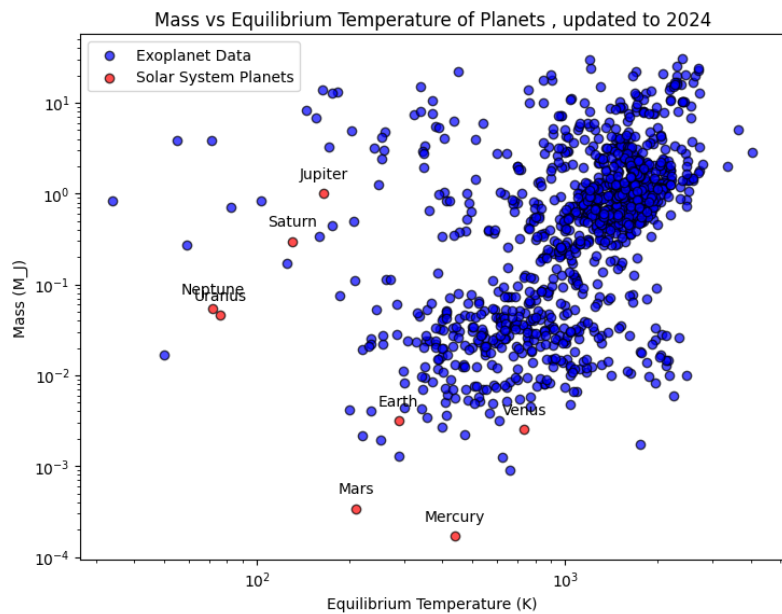


**Figure 1.7:** comparison between Solar system planets mass and temperature with exoplanets. The exoplanets data come from NASA archive: <https://exoplanetarchive.ipac.caltech.edu/index.html>, The data are updated to 23/07/2024.

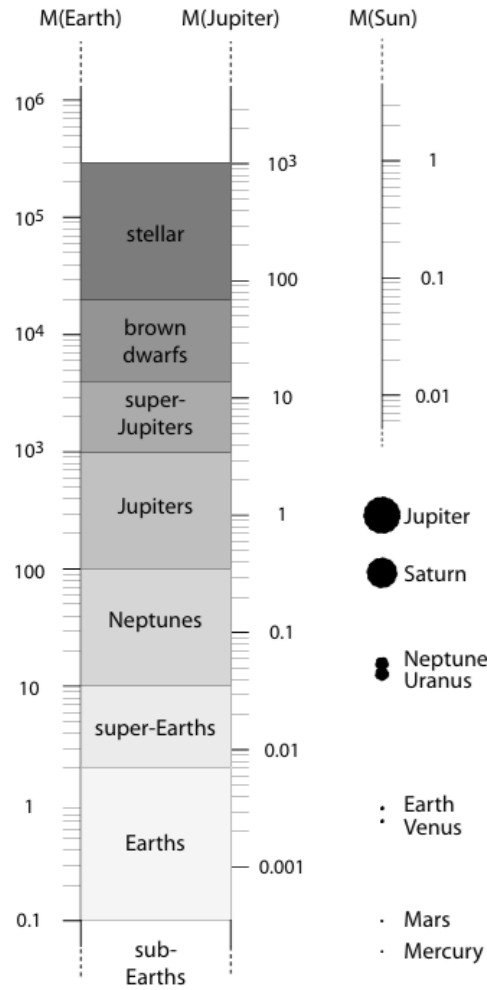


**Figure 1.8:** Classification of planet masses. From [77], the classification follows the proposal by Stevens and Gaudì (2013)

### 1.3 different types of rocky exoplanets

since when we are looking for biosignature and habitable planets we look for rocky exoplanets in the habitable zone, it is useful to list the different types of rocky exoplanets discovered. In 1.2 I show the types classification used by [68].

**Table 1.2:** Rocky Exoplanets Types

Rocky planet type	Atmospheric phenomena occurring	Possible chemical composition
<b>Lava worlds: boiling hot</b>	Extremely high temperatures > 1500K. The atmosphere comes from vaporization of lava with gradients both in pressure and composition.	Na, SiO, O, O <sub>2</sub>
<b>Searing-hot planets</b>	Orbital and stellar insolation similar to Mercury. If any water is present, it exists as steam. Water can be lost via photolysis and H escape. Silicate materials dissolve readily in steam atmospheres.	Si(OH) <sub>4</sub> , KCl, ZnS, CO <sub>2</sub> , N <sub>2</sub> (if water has been lost)
<b>Exo-Earth or Exo-Venus</b>	Often within the habitable zone. Possible abiotic O <sub>2</sub> atmosphere for planets that start with water but lose hydrogen. At habitable temperatures, water should condensate and make oceans H <sub>2</sub> could act as an efficient greenhouse gas that may extend the HZ if life is present, disequilibrium atmosphere may be present	H <sub>2</sub> O, CO <sub>2</sub> , N <sub>2</sub>
<b>Exo-Titan and Beyond: Cold</b>	Planets beyond the HZ (very few have been discovered) water is no longer a volatile species, behaving more like silicate rocks for HZ planets gases like N <sub>2</sub> , NH <sub>3</sub> and CO <sub>2</sub> become less volatile at greater distances and may be stable as ices or liquid at planetary surfaces	N <sub>2</sub> , H <sub>2</sub>

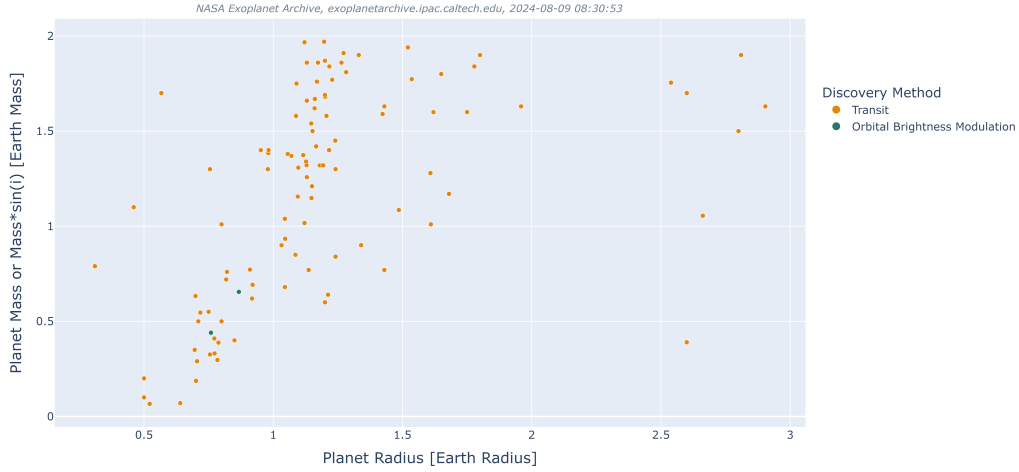


**Figure 1.9:** plot of exoplanets discovered with masses  $< 2M_{\text{Ter}}$ , made using the NASA database archive. Mass vs. radius.

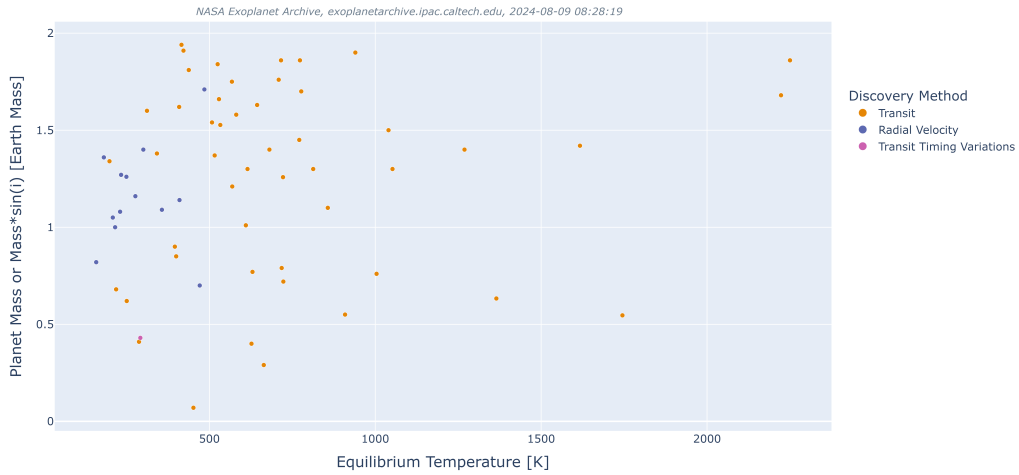


**Figure 1.10:** plot of exoplanets discovered with masses  $< 2M_{\text{Ter}}$ , made using the NASA database archive. Mass vs. equilibrium temperature.

## 1.4 The different detection methods for exoplanets

### 1.4.1 Transit Spectroscopy

The transit occurs when an exoplanet passes in front of its host star and blocks part of the light. What we observe is a drop in the star’s brightness. This is the observable we are going to work with. From this we can obtain different parameters:  $P$  (transit period),  $\Delta F$  (variation in luminosity in the host star),  $t_T$  (time duration



of the transit),  $t_F$  (duration of the period of minimum luminosity). With these parameters, we can obtain the fundamental properties: the planet's radius  $R_p$ , the semi-major axis of the orbit  $a$ , the radius of the star  $R_*$ , the mass of the host star  $M_*$ , eccentricity  $e$ , angle of inclination  $i$ . For example, it is possible to calculate  $R_p$  if the radius of the host star  $R_*$  is known: [4]

$$\Delta F = \left( \frac{R_p}{R_*} \right)^2 \quad (1.1)$$

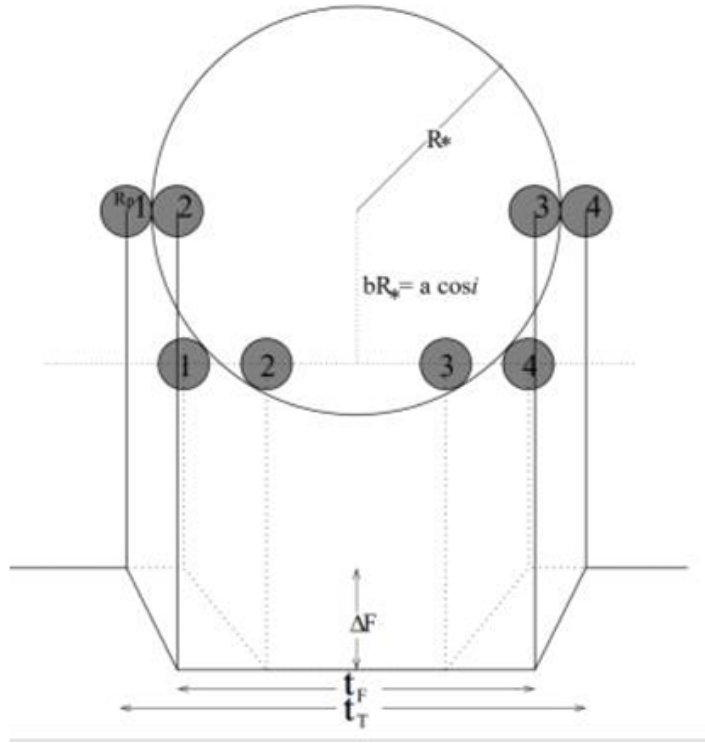


**Figure 1.11:** The light curve and position of the exoplanet relative to its host star, from [4]

The transit spectroscopy has revealed to be the most successful method for their atmospheric characterization both by number of exoplanets observed (more than 4000) and the range of atmospheric constraints obtained [72]. The reason is that the favourable geometry makes it relatively easier for atmospheric observation compared to other methods. The transit method allows three configurations to observe a planet's atmosphere:

- a transmission spectrum when the planet transits in front of the host star ,  
i.e. a primary eclipse

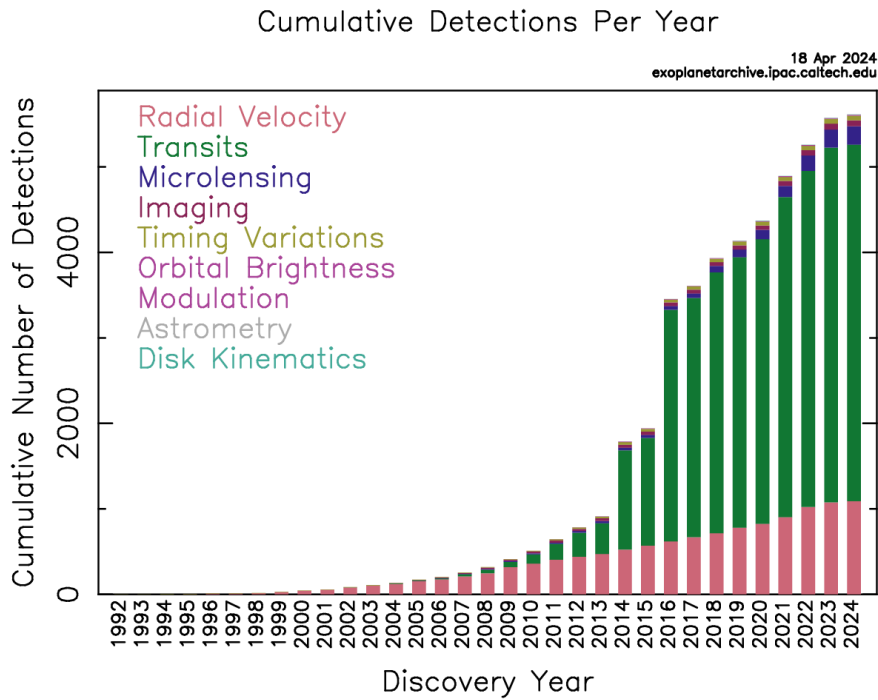


**Figure 1.12:** cumulative graph of exoplanets discovered by method, plot taken from NASA archive

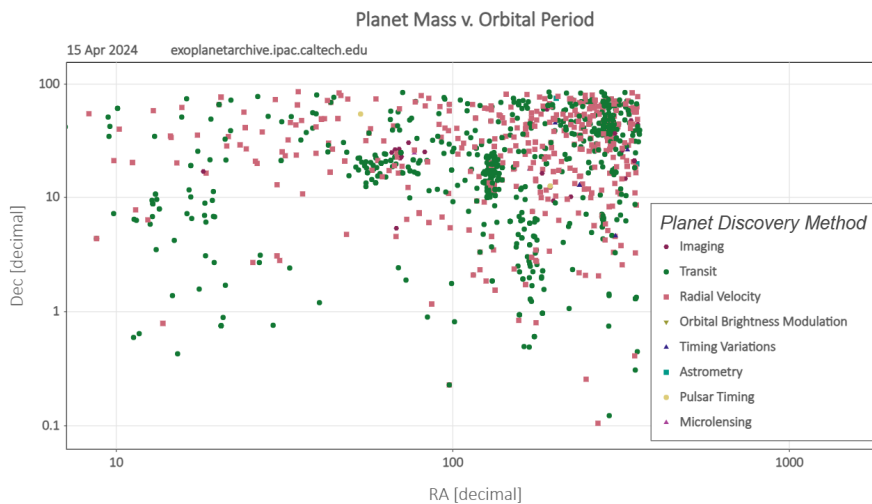


**Figure 1.13:** exoplanets found by different method; the green islands corresponds to the period of observation of Kepler , plot taken from NASA archive

- an emission spectrum as the planet passes behind the host star , at secondary eclipse
- a phase curve as the planet orbits between the primary and secondary eclipses

During the first eclipse , the light of the star towards the line of sight passes through the atmosphere at the day-night terminator of the planet. The resulting spectra observed contains absorption features of the planetary atmosphere imprinted

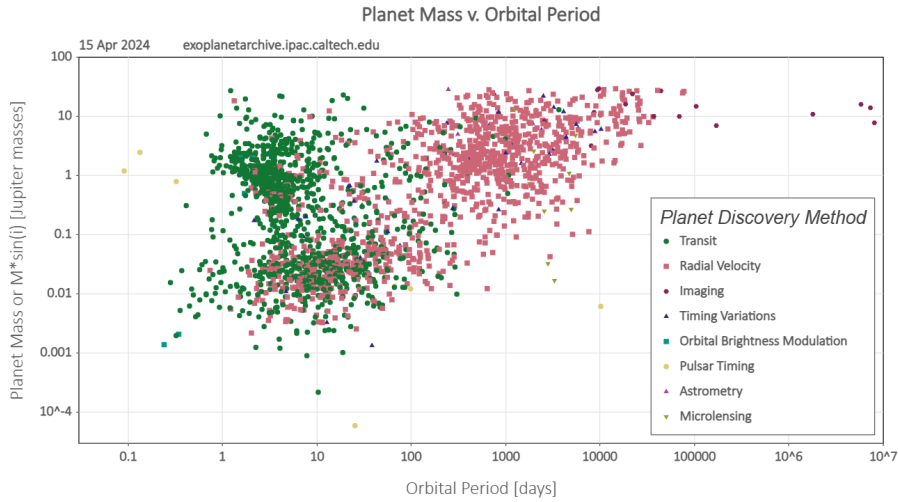


**Figure 1.14:** discovered planets, orbital period vs. planet mass plot taken from NASA archive

in the stellar spectrum. The difference between in-transit and out-of-transit spectrum, normalized from the out of transit spectrum, brings to transmission spectrum. That is a measure of the extinction because of the planetary atmosphere at his day-night terminator region. The secondary eclipse spectrum measures the emergent spectra from the dayside atmosphere of the planet. Just prior to secondary eclipse the combined spectrum of both the star and the planetary dayside is observed. This combined spectrum, when subtracted by stellar spectrum, which is observed during secondary eclipse, yields the primary spectrum. Finally the phase curve gives us a spectra of the planet at different phases. Each of these configurations of transit spectroscopy gives us different and complementary constraints on the atmospherical properties of a transient planet. [72]. A transmission spectra is essentially a measure of the thickness of the atmosphere probed perpendicular at the line of sight as a function of wavelength. It gives us constraints primarily on the chemical composition of the atmosphere at the day-night terminator region, together with the mean molecular weight and temperature through the scale height. As said before, different spectral regions give us constraints on different chemical species.

An emission spectra probes directly the temperature structure of the dayside atmosphere of the planet together with the chemical composition. In principle, the planetary spectra observed at the secondary eclipse contains both reflection and emission. Where instead the reflection dominates at higher optical wavelengths correspondingly with the peak of the stellar spectra for stars FGK. The planetary emission typically dominates in infrared at lower temperature. The planet star flux

contrast dominates in infrared due to much lower temperatures. The planet-star flux contrast increases with the wavelength with the star becoming weaker and the planets that becomes brighter. So most of the observations in the dayside of the exoplanetary atmospheres have been reported in infrared. The observed spectra probe the brightness temperature of the planet at different wavelengths, which means measuring the temperature at different depths in the atmosphere [72].

## 1.4.2 High resolution Doppler Spectroscopy

A detailed review of this method can be found in [1]. If a stellar system is made of one or more planets , the system will rotate around the centre of mass of the entire system. This will make the star rotate in a circular or elliptical orbit. Observed from Earth, the system will include a star that has a velocity in respect to the line of sight and has periodic variations. This brings to periodic blue shifts and red shifts of the spectra of the planet , that can be observed from a telescope on Earth. Measuring the shift in a specific wavelength ,  $\Delta\lambda$  and his original wavelength  $\lambda$ , the speed at the line of sight of the star  $v$ , can be calculated with the following formula: [4]

$$\frac{\delta\lambda}{\lambda} = \frac{v}{c} \quad (1.2)$$

where  $c$  is the speed of light. From a plot velocity-time is possible to obtain the maximum velocity of the star  $K$ , and the period of the motion of the star,  $t$ . The minimum mass of the planet can be calculated: [4]

$$K = \left(\frac{2G\pi}{T}\right)^{1/3} * \frac{M_p \sin i}{M_p + M_s} \frac{1}{\sqrt{1 - e^2}} \quad (1.3)$$

Where  $G$  is the gravitational universal constant ,  $M_p$  the mass of the planet,  $i$  the orbital inclination (The angle between observers and the axes of revolution of the planet),  $M_s$  the mass of the host star , and  $e$  represents the eccentricity of the orbit of the exoplanets. The high resolution Doppler spectroscopy of planets has also offered a powerful tool to discover chemical species in the atmosphere of the exoplanets, particularly hot jupiters.

This method involves phase resolved high resolution (  $R = 10^5$ ) spectroscopy of the star-planet system to deduce the Doppler motion of the planet using the

planetary spectral lines. The combined spectra, observed using large ground based facilities, contains contributes both from stellar and planetary spectra together with telluric features because of the Earth's atmosphere. For a typical hot Jupiter the RV semi-amplitude of the planets is a 1000 times bigger of that of the star. So the stellar and telluric features are relatively not modified during the observations, if compared with the planetary spectral lines that have significant Doppler shifts. The firsts 2 are removed using different methods, that leave only the time varying signal from the planet. The residual spectra, after detrending are then cross correlated with the template planetary spectra containing the expected prominent molecules. For the matching planet spectrum the orbital motion of the planet can be reconstructed , the radial velocity semi-amplitude of the planet  $K_p$  and the systematic velocity  $V_{sys}$  are constrained. An high significance peak in the plane  $K_p$ - $V_{sys}$  constitutes a detection of the molecule present in the model template. Typically a  $5\sigma$  is considered a strong detection. This method has been used to find chemical species in a certain number of hot jupiters. For example CO [55], H<sub>2</sub>O[10]. Besides Molecular detection , this technique has also brought infromations on the profiles of temperature and atmospheric velocity of the winds. This technique is also been used to characterize the atmospheres of directly imaged exoplanets at big orbital separations. For example the observation of CO in  $\beta$  Pic b [47], using a combination of high contrast imaging and high resolution spectroscopy. Given the big orbital separation we don't expect these planets to be tidally locked. So their rotational speed can be measured with the broadening of the spectral lines. For  $\beta Pic b$  has been measured a 25 km/s velocity using CO spectral features. The combination of high resolution spectroscopy and high contrast imaging improves the sensitivities of flux contrasts beyond what is achievable with other methods. Besides this the combination of cross correlation technique with adaptive optics assisted integral field spectrographs at medium resolution can be used to discover chemical species in the two dimensional field of the image. Such a molecular mapping has been showed to be a strong method with high significance detection of prominent molecular species like H<sub>2</sub>O and CO in directly imaged planets.

### 1.4.3 direct imaging

A detailed review of this method can be found in [90]. The only method that is able to directly catch the photons directly emitted by the planetary bodies is direct imaging. It's a very useful method for analyze nascent planetary systems. This method requires high contrast imaging(HCI) , to resolve objects millions of times fainter than the parent star. So extreme adaptive optics systems, telescopes exceeding 8 meters in diameter, coronagraphs and modern imagers. The HCI requires the coronagraphs to block the light of the primary star. There are two main categories of coronagraphs: occulting masks and phase masking coronagraphs. The first class uses an opaque mask that attenuates the first peak of the Airy function, the second exploits the principle of the destructive interference of the on-axis light. In the infrared the exoplanets emit light coming from their own heat. Even if the luminosity is still very faint in this band is possible to observe the exoplanet. The exact orbit can be determined from the observation and the temperature can be inferred from the radiation emitted by the planet. The first exoplanet detected with this technique is 2M1207b . It was discovered using NACO (NAOS CONICA) on the VLT. In 2004 the first epoch was obtained observing the star 2MASSW J1207334-393254 , an M8 type star of the TW Hydra association. The age is around 8Myr. The object is separated from the host star by about  $0.78''$  ( $=55\text{au}$ ). The nature of the planet has been confirmed one year later. The estimated mass is  $M = 5 \pm 2 M_{\text{jup}}$  and the  $T_{\text{eff}} = 1250 \pm 200\text{K}$ . Now it's considered a binary system of low-mass objects, rather than a planetary system.

One of the main challenge with this method has to do with the high sensitivity required and the inner working angle, which is the radius where the peak flux of the star is attenuated by 50%. The goal of the new coronagraphs is to lower as much as possible this value , in order to be able to detect planets orbiting at small separations. For example , a Jupiter analogous orbiting a sun like star at 10 pc would require a flux contrast planet-star below  $10^{-7}$  in the NIR at a inner working angle of  $0.5''$ , but the requirements are even more stringent in the optical band.[72]. Nonetheless , for young giant planets with high temperatures (  $> 1000\text{K}$  ) at big orbital separation the planet star flux contrast in the NIR approaches  $10^{-4}$ , making them observable with today facilities. Even if the number of planet discovered with direct imaging is a lot smaller than transiting exoplanets (78 vs. 4176 with

transit method) , the spectra are typically of a higher resolution and the SNR is bigger. Due to the large aperture ground based facilities with adaptive optics used for this goal. For this reason the method has been successful for obtaining thermal emission spectra of different young giant exoplanets in the NIR. The atmospheric properties that can be obtained with direct imaging are similar to that obtained with the transit method but with crucial differences. A direct imaging spectra is similar with an emission spectra observed for the transiting planets and so it gives us important informations on the temperature profiles and on the atmospheric compositions. However ,differently from transiting exoplanets , the radius, mass and so gravity are not known. This causes degeneracies in the accurate estimate of the actual chemical composition of the spectra since the shapes of the spectral features strongly depend upon gravity. However, the bigger resolution and the SNR of the spectra observed make possible to obtain robust observation of the chemical species in the atmosphere. For example, different observations at high confidence of H<sub>2</sub>O, CO and CH<sub>4</sub> have been reported for different directly imaged exoplanets in the recent years. Given the orbital periods, the spectra of a planet is obtained typically at a single orbital phase that is known, that restricts the constraints on the atmospheric dynamics. However , precise constraints on the globally averaged compositions and profile temperatures at the observed phase are possible using retrieval techniques method. Besides this, given the low radiation regime , the temperature profiles of the atmosphere of directly imaged planets are expected to be really different from those of transiting exoplanets that tend to be highly irradiated.

#### 1.4.4 timing

Besides this 3 method exposed, there are others that are used to find exoplanets, but for now are not useful to do spectroscopic studies: timing and microlensing. The first is based on a concept similar with radial velocity method: If a stellar system has one or more planets, so the radial distance between stars and the Earth changes periodically because of the same reason mentioned in the radial velocity method. So , if the host star has a stable period, if the host star is for example a pulsar, the length of his period changes periodically. Because of the variation of the radial distance between the pulsar and the Earth , every impulse will arrive before or after the moment of arrive predicted (in the absence of the planet), since the

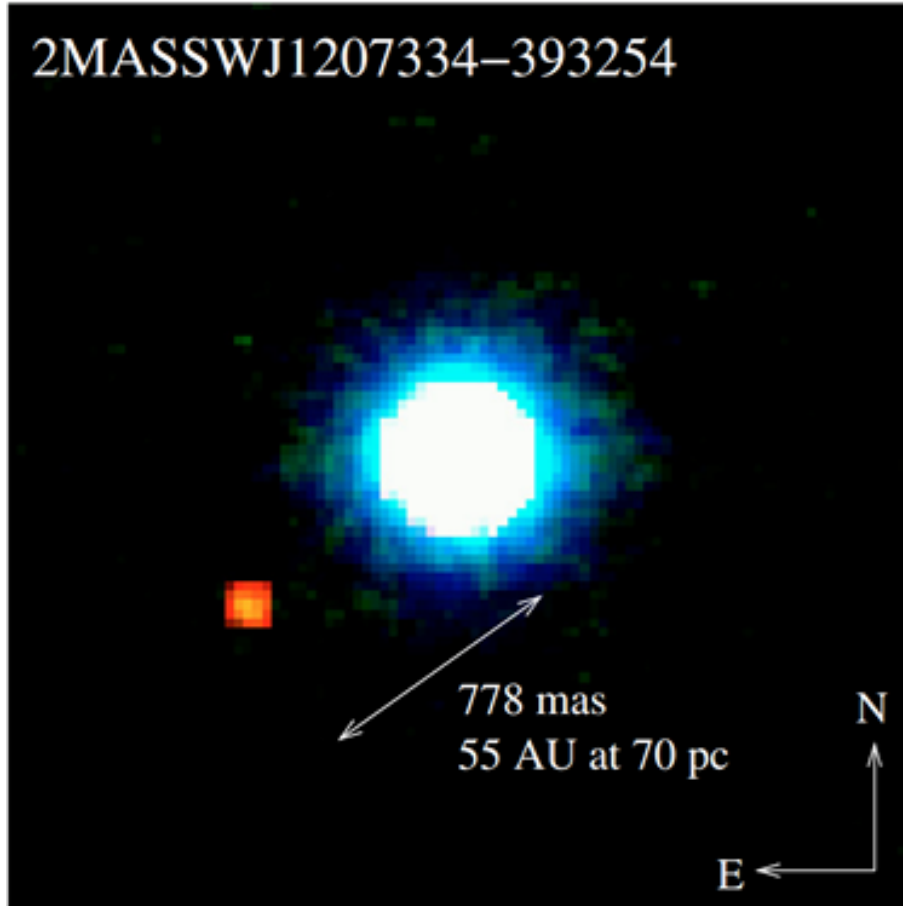


**Figure 1.15:** 2M1207b , the first planet ever detected with the high contrast imaging technique citare (Chauvin et al.2004)

distance variation brings to the variation of the time of arrival of every impulse. The amplitude of every variation of the arrival time,  $\tau_p$ , can be determined. Subsequently it is possible to obtain the minimum mass of the planet  $M_p \sin i$ :

$$\tau_p = \frac{a \sin i M_p}{c M_*} \quad (1.4)$$

Where  $c$  represents the speed of light ,  $M_p$  the mass of the planet,  $i$  represents the orbital inclination,  $M_*$  the mass of the host star , and  $a$  the semi-major axis of the orbit of the exoplanet. Besides Pulsars , there are different celestial bodies that have their period, like the variable pulsing star and the binaries with the eclipse. The exoplanets that orbit around them can even be obtained from the same principle of the pulsar timing. Moreover , if a planetary system has more than a planet, so the gravity between the planets will accelerate or decelerate every one of them. However in a planetary system with multiple planets , the speed of every planet keeps changing due to the gravitational interaction with the other planets. So the transit



period of a planet will not be constant. When the observers will find variations in the transit period of a discovered planet, it is possible to predict that other planet exist in that system. This method is called TTV( transiting timing variation), and can determine the maximum potential mass of an exoplanet.

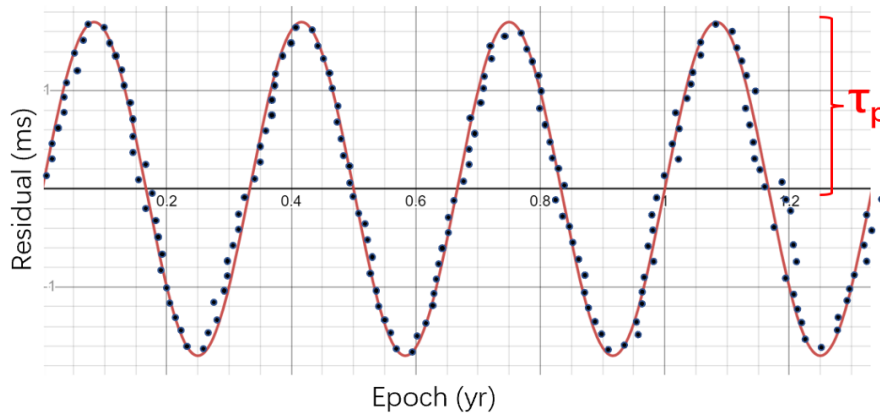


**Figure 1.16:** schematic diagram of the timing method: each black dot represents a pulse emitted by the pulsar. The y axis shows a residual between the actual moment for each pulse arriving at the Earth, and the predicted value of arriving moment if the pulsar has no planet. The red curve is a sin that fits the dots. from [4]

### 1.4.5 microlensing

From the theory of general relativity it is known that a star is able to curve the light rays that pass nearby. When 2 stars and the Earth find them self on a straight line, the star between the Earth and another star bends the light emitted by the star behind and acts like a convex lens that focus the light from the source behind on the Earth. So the luminosity of the star behind will increase drastically. However , when the star has a planet , the gravity of the planet will cause a microlensing effect. With this method it is possible to estimate the mass of the planet. Thanks to this method more than 200 planets have been found. Depending on how the source, lens and observer are aligned , a distorted image of the source is generated. the robust lensing , observable at the level of individual object , is then classified in macro and microlensing. Where instead the microlensing has to do with discrete, unresolved sources, macrolensing generates multiple resolved images , or "archs". The weak lensing is a different regime that is statistically achieved without a clear resolution of the individual objects. [?] Nevertheless the observation is not replicable and this raises the big problem of the lack of falsifiability of the results.

**Table 3.** Comparative analysis of methods

Detection method	Principle	Measurements	Advantages	speciality	Drawbacks	Equipment
Radial velocity	Gravitational Wobble	$m_p, T, a$	large amount of planets can be observe at once, precision	large planets, small cool stars	its for only planets closer to observer	Spectrometer
Transit photometry	Light Dip	$r_p, T, a$	High sensitivity, Large sample	precise evaluation of properties, short period planets	False positives, intersecting and sort period planets	Photometer, TESS, Kepler, CoRoT
Direct Imaging	Visual Observation	$m_p, T, a$	characterization, atmospheres	large size and a hot, planet close to observer	needed stability, glare	comograph and infrared telescope
Gravitational Microlensing	Gravitational Lensing	$m_p$	Distant planets, galactic scale	background towards center of galaxy, large a precise	doubtful alignment, single trial	Warsaw telescope, OGLE
Astrometry	Stellar Wobble	RA, Dec...	High precision, Long baselines		extremely hard	Gaia, keck

**Figure 1.17:** comparison of different analysis method ,from [?] ]

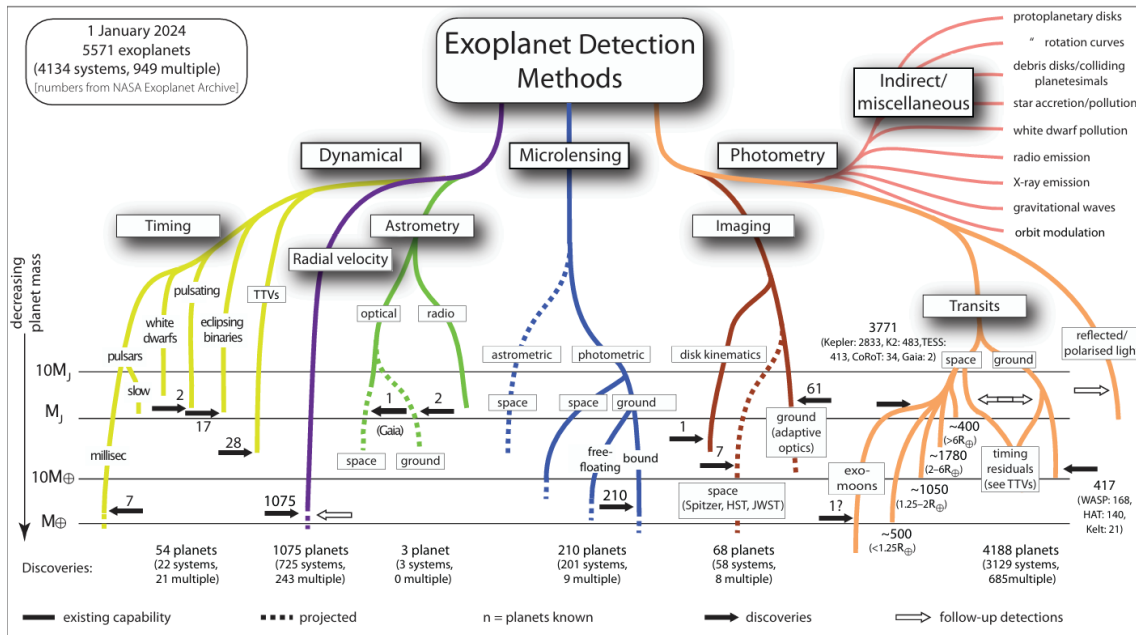


**Figure 1.18:** Perryman Tree 2024

### 1.4.6 comparison of the different methods

As outlined before, it is necessary to distinguish between the detection methods that can help us to study the atmosphere of an exoplanet spectroscopically and those that by now are useful just to find exoplanets and to estimate the bulk parameters. For what concerns the first 3 methods, which are those mostly used for spectroscopic studies, the transit method remains the most successful one, more than a 100 exoplanet's atmosphere have been studied and more than 4000 discovered as it is possible to see in the Perryman tree in figure 1.18.

The advantages of the different methods are the following [72]:

1. Transit spectroscopy allows observations of transmission spectra of day-night terminator, thermal emission spectra of dayside, and phase curves over the orbit.
2. Direct imaging provides high S/N thermal emission spectra at a single phase.
3. High-resolution Doppler spectroscopy allows detection of chemical signatures in planetary spectra Doppler shifted due to radial velocity of the planet.

Most of the planets discovered with the transit method have very short periods, this shows that this method is particularly useful to find planets that are closer to the host star, because shorter is the radius and shorter is the period. The parameters that is possible to find with this method are: radius, orbital radius, radius of the host star, mass of the host star, eccentricity and inclination angle. Beside this , as has been seen from the Kepler telescope and TESS , the transit method allows to find thousands of exoplanets in a small area of the sky simply by continuing to observe the luminosity of the stars in the area. However the transit method can not recognize if the transit is caused by exoplanets or celestial bodies that have the same radius of the planet as for example brown dwarfs.

The radial velocity method is better for exoplanets that have a small orbit radius or a big mass. In other words these exoplanets that can cause bigger impacts on the motion of host stars and the shift of the spectra of the host stars. So it is easier for the observers to see the variations in the spectra. Since the gravity of the exoplanet is directly proportional to the his mass and inversely proportional with the square of the distance between the planet and his host star, it can only help to obtain to identify the minimum mass of the planet, as outlined by [4]. Fortunately if the exoplanet can also be detected with the transit method , substituting the values  $i$  in  $M_p \sin i$ , it is possible to calculate the exact mass of the planet. The microlensing instead can help us to measure the mass of very distant exoplanets, the main problem is that it is not possible to observe again the microlensing event. And this unfortunately undermines the necessary requirement of replicability of the method.

the direct imaging work better with planets that are extremely far away from their host star. Differently from the other methods, that detect the planet indirectly , this method directly "sees" the planet in infrared. If a star is a pulsar, a pulsating star, or part of an eclipsing binary system , the transit method cannot be applied due

to the constant variations in its luminosity. Additionally, the radial velocity method is ineffective since these types of star have highly unusual and complex spectra. As a result, the timing method is the most suitable for detecting exoplanets orbiting such stars. Finally, transiting timing variations (TTV) can help identify additional planets in a system where one has already been detected using the transit method. However, TTV is only useful for specific types of stars or systems where at least one planet can be observed transitin from Earth.

### 1.4.7 Summary

## 1.5 The modelling of the exoplanetary atmospheres

Besides the detection methods explained, that are useful to discover a planet and then analyze the data that we acquire regarding the atmosphere, it is necessary to use atmospheric modelling techniques to understand better the data and estimate the plausibility of a certain detection. In [72] these techniques are classified in 3 different types:

- Forward spectral modelling
- Retrieval methods
- Atmospheric theory

The forward spectral modelling has to do with the study that is done a priori about an observation for being able to estimate the feasibility of this and try to understand a priori what it is possible to find, as chemical abundance, chemical equilibrium and/or radiative convective equilibrium. For the interpretation of the spectra we rely on the retrieval techniques or the inverse techniques, that have to do with the derivation of statistical constraints of the atmospheric properties of a planet from the spectral data using methods for estimating the parameters. In addition to these, there exists many studies that use theoretical atmospheric models to investigate different chemical processes and physical in act in the exoplanetary atmospheres as for example non equilibrium chemistry, atmospheric circulation, clouds/hazes, atmospheric escape, thermal inversion.



## Chapter 2

# Addressing the Challenge of Defining Reliable Biomarkers in Exoplanetary Atmosphere Studies

### 2.1 The search for gaseous biomarkers

One of the most important aspects of the study of exoplanetary atmosphere is the identification of biomarkers. Currently there are dozens of rocky exoplanets discovered in the habitable zone. However the most significant aspect of this kind of studies is being able to establish which conditions and biosignatures constitutes a robust evidence of the presence of life, which means  $p(Life|B) \gg p(abiotic|B)$ , where  $p(life|B)$  is the probability of life given a certain biosignature B, which is the core question of all the thesis. Currently there have been discovered dozens of terrestrial rocky exoplanets terrestrial sized, that have equilibrium temperature that allow the existence of liquid water on surface. We could classify these planets as habitable, but the extension of a given habitable zone depends strongly on the internal properties of the planet, the atmospherical properties and from the astrophysical conditions. [72] Some reference article regarding habitability are: [62] [33]

It is not the goal of this thesis to outline all the aspects regarding habitability since it is a vast topic that would require a work focused on that. It is however important to recall some important aspects. The factors that influence the habitability are: atmospherical and geophysical conditions of the planet, orbital parameters and

evolution, nature and evolution of the host star and his environment, the magnetospheric protection, the history of formation of the planet and other factors.

From an observational standpoint , planets orbiting late-type stars present an excellent opportunity for atmospheric characterization. Due to the smaller size of these stars , there is a bigger planet-to-star contrast in both radius and luminosity, making these systems particularly well-suited for transit spectroscopy. Many planets have been discovered around late-type K and M stars, suggesting that their environmental condition could be significantly different from those on Earth. Recent Observations of planets in the habitable zone of stars like TRAPPIST-1 and Proxima Centauri further encourage ongoing research in this field.

As previously said , for this planetary system it is necessary to being able to establish which could be a biosignature that is a robust evidence of the presence of life. From [43], an ideal biomarker should satisfy the following requirements:

1. it should not have any false positives,i.e. should not be a product of a non biological mechanism
2. it should have strong enough spectral features to be detectable
3. it should be abundant enough to be detectable.

Based on the Earth's atmosphere , the main biomarkers traditionally have been considered to be:  $O_2$ ,  $O_3$ ,  $N_2O$  and  $CH_4$ . Until recently the most promising biomarkers have been considered to be  $O_2$  and  $O_3$ , recent studies however have shown the possibility of abiotic genesis for  $O_2$  , that would produce detectable quantities. [38] It is important to outline that currently there is no molecule that can be considered alone as a robust biomarker,and so to asses the presence of a biosphere it could be important to assess the presence of multiple biosignature that can increase the confidence on the inference. Like The simultaneous presence of  $O_2,CH_4$  and/or  $N_2O$  alongside liquid  $H_2O$ , located in the habitable zone could be indicative of the presence of a biosphere,

Furthermore , for every exoplanets , different properties of the planet and the host star must be taken into account to better constrain the probability of biogenic activity.

As outlined by [13] , the only thing that will be probably possible will be to define probabilistic estimates on the presence of life in a given planetary system with respect to a binary inference.

As we will see later, it is the combination of multiple biomarkers that may eventually help the inference of the presence of biological activity on a planet. For instance, the simultaneous detection of O<sub>2</sub>, CH<sub>4</sub>, and/or N<sub>2</sub>O alongside liquid H<sub>2</sub>O on a planet within the habitable zone could suggest a perfect Earth analog.

However, it is important to remain open-minded regarding biological activity in this field, since our theory of life is far to be complete and consequently our knowledge of gaseous biomarkers.

In 2.1 I have outlined the different definition proposed for biosignatures and i added my proposal.

<b>Author</b>	<b>Definition</b>
Thomas-Keprta et al. 2002 [31]	A physical and/or chemical marker of life that does not occur through random, stochastic interactions or through directed human intervention
Des Marais et al. 2008	Object, substance and/or pattern whose origin specifically requires a biological agent
Catling et al. 2018 [13]	Any substance, group of substances, or phenomenon that provides evidence of life
Pohorille and Sokolowska 2020 [78]	Chemical species, features, or processes that provide evidence for the presence of life
<b>proposed definition</b>	<b>Any phenomenon, substance, or group of substances <math>A</math> that provides a conditional probability <math>P(\text{life} A) \gg P(\text{non-life} A)</math></b>

**Table 2.1:** Different definitions of biosignature throughout the time

In [31], they were analysing the possible biogenity of some presumed Magneto-fossil on the Martian meteorite ALH84001.

The second definition , presented in [19], is the definition considered by the NASA astrobiology roadmap of 2008.

In [13] , The Bayesian framework is considered and simulations of potential biosignature in spectra or photometry are considered to derive the likelihood of the bayesian model.

Finally , in [78], Conceptual frameworks are developed for evaluating the ability of different biosignatures to provide evidence for the presence of life in planned missions or observational studies. They have focused on intrinsic characteristics of biosignatures in space environments rather than on their detection.



## 2.1.1 potential biosignature gases

An atmospheric biosignature is a volatile molecule that is either direct product of life or a secondary product from the environmental processing of biogenic compound. A biogenic gas emission can include those directly related to the primary energy-yielding metabolism or incidental products from other cellular processes. The best targets for the search of biosignature gasses are volatile molecules, with a reasonable chance of accumulating to detectable concentrations. The detailed description of the different gaseous biosignature can be found in [79]. Here I take Phosphine  $\text{PH}_3$  as an example to outline the most important aspects to understand in order to analyze a gaseous biomarker.

Biosignature	Production Environment	Concentration on Earth	False Positives and Secondary Outcomes	Main Spectral Features ( $\mu\text{m}$ ) (strongest <b>bolded</b> ) Via HITRAN and NIST	Citation (see references therein)
Oxygen ( $\text{O}_2$ )	Photic terrestrial and marine environments, produced by cyanobacteria, algae, and plants	20.95%	<ul style="list-style-type: none"> <li>• Low noncondensable inventories (Wordsworth and Pierrehumbert 2014)</li> <li>• Ocean Loss (Luger and Barnes 2015; Tian 2015)</li> <li>• <math>\text{CO}_2</math> photolysis (Domagal-Goldman et al. 2014; Gao et al. 2015; Harman et al. 2015)</li> <li>• High <math>\text{CO}_2/\text{H}_2\text{O}</math> inventories or extremely low initial <math>\text{H}_2\text{O}</math> inventories (Krissansen-Totton et al. 2021)</li> <li>• Atmospheric Exchange/Exogenous Delivery (Felton et al. 2022)</li> </ul>	$\text{O}_2$ at 0.63, 0.69, <b>0.76</b> , 1.27 $\text{CIA}/\text{O}_2$ at 0.445, 0.475, 0.53, 0.57, 0.63, 1.06, <b>1.27</b> , <b>6.4</b>	Meadows 2017; Meadows et al. 2018b
Ozone ( $\text{O}_3$ )	Photochemical product of $\text{O}_2$ , $\text{H}_2\text{O}$ , $\text{SO}_2$ , $\text{CO}_2$	0.07 ppm	<ul style="list-style-type: none"> <li>• Abiotic <math>\text{O}_2</math> or <math>\text{CO}_2</math> can produce <math>\text{O}_3</math> features (Domagal-Goldman et al. 2014; Gao et al. 2015; Harman et al. 2015)</li> </ul>	0.25 (Hartley), 0.4-0.7 (Chappuis), 2.6, 4.7, <b>9.65</b> , 14.6	Meadows et al. 2018b; Kozakis et al. 2022
Methane ( $\text{CH}_4$ )	Wetlands, rice paddies, livestock emissions, biomass burning & decomposition	1.90 ppm	<ul style="list-style-type: none"> <li>• Serpentinization</li> <li>• Fischer-Troph reactions</li> <li>• high-temperature mantle reactions</li> <li>• equilibrium reactions in high-T regions of gas giants</li> </ul>	1.65, 2.4, 3.3, <b>7.7</b> (broad)	Etiopie and Sherwood-Lollar 2013; Thompson et al. 2022
Nitrous Oxide ( $\text{N}_2\text{O}$ )	Marine settings, some soils	0.33 ppm	<ul style="list-style-type: none"> <li>• Production by StEPs</li> <li>• Chemodenitrification</li> <li>• trace production by lightning and <math>\text{NO}</math>, reactions</li> </ul>	1.5, 1.6, 1.7, 1.8, 2.3, 2.6, 2.9, 3.7, <b>4.0</b> , <b>4.5</b> , <b>7.8</b> , <b>8.5</b> , 17	Schwieterman et al. 2022

**Figure 2.1:** prominent biosignature gases on Earth , from [79]

Biosignature	Production Environment	Concentration on Earth	False positives and Secondary Outcomes	Main Spectral Features ( $\mu\text{m}$ ) (strongest <b>bolded</b> ) Via HITRAN and NIST	Citation (see references therein)
Organic sulfur gases e.g. DMS ((CH <sub>3</sub> ) <sub>2</sub> S) DMS ((CH <sub>3</sub> ) <sub>2</sub> S <sub>2</sub> )	marine/lacustrine settings	~100 ppt	Secondary ethane signature may be produced abiotically, if sulfur gases do not reach detectable levels	2.3, 3.4, ~7 (DMS, DMS), ~9 (DMS), ~10 (DMS, CH <sub>3</sub> SH), 14 (DMS, CH <sub>3</sub> SH), 18 (DMS)	Pilcher 2003; Domagal-Goldman et al. 2011
Halomethanes: Methyl Chloride (CH <sub>3</sub> Cl) Methyl Bromide (CH <sub>3</sub> Br)	Marine algae, terrestrial and marine algae; salt marches and wetlands	~500 ppt (CH <sub>3</sub> Cl) ~9 ppt (CH <sub>3</sub> Br)	High T perchlorate pyrolysis (limited in planetary context), Exogenous delivery, Limited hydrothermal/high T processes	3.3, 7.0, <b>9.9</b> , <b>13.7</b> (Cl) 3.5, 6.9, <b>10.2</b> , <b>16.4</b> (Br)	Segura et al. 2005; Leung et al. 2022
Organic Haze	Photochemical product of CH <sub>4</sub> , CH <sub>3</sub> X species	Not present at high altitude on modern Earth due to oxidizing conditions	Abiotic methane can lead to haze production	NIR spectral slope, ~6	Arney et al. 2018
Phosphine (PH <sub>3</sub> )	Strictly anoxic environments including paddy fields, lakes/streams, wetlands/marshes	Ppq-ppb levels, spatially and temporally variable	Phosphite & Phosphate degradation, lightning, volcanism, exogenous delivery	2.9, 3.4, 4.4, 5.0, 8.9, <b>9.5</b> (broad)	Sousa-Silva et al. 2020
Isoprene (C <sub>5</sub> H <sub>8</sub> )	Deciduous trees and land plants	~1-5 ppb localized and time-varying	No known (energetically unfavorable)	3.4, 5.6, 6.3, 9.4, <b>10.2</b> , <b>11.4</b>	Zhan et al. 2021
Methanol (CH <sub>3</sub> OH)	Plants via demethylation of pectin	10 ppb (surface)	Abiotic photochemistry, comets & primitive material	2.9, 3.3, 4.6, 7.5, <b>9.7</b>	Huang et al. 2022b
Carbonyls e.g. Formaldehyde (CH <sub>2</sub> O)	80% of all biological compounds contain carbonyls	~0.4 ppb (CDC)	Detectable signature is CO, which can be produced abiotically (see Schwieterman et al., 2019; Wogan & Catling 2020)	(CO) 1.18, 1.57, 2.35, <b>4.6</b>	Zhan et al. 2022
Ammonia (NH <sub>3</sub> )	Anerobic nitrogen fixing organisms, ammonification and nitrate reduction	Spatially and temporally variable on Earth	Volcanism, photochemistry, high temperature synthesis, equilibrium thermochemistry	1.2, 1.3, 1.5, 2.0, 2.3, 3, 3.9, 6.1, <b>10.5</b> (broad)	Seager et al. 2013a; Huang et al. 2022a

Figure 2.2: alternative biosignature gases , from [79]

## 2.2 Phosphine PH<sub>3</sub>

### 2.2.1 Phosphine as a biomarker in spectroscopic observations

Phosphine has been described in many works as a very promising biomarker. [82]. That's because on Earth it is only associated with anaerobic ecosystems industrial environment, and as such it a promising biosignature gas in anoxic exoplanets [82]. Currently there are no known abiotic false positives that could generate the high fluxes required for detection. Also it has 3 strong spectral features such that at least 1 could be easily recognized even in the presence of other dominant spectroscopic molecules.

Currently the only weakness is his high reactivity , that requires high outgassing rates for detectability. The abiotic production in the planets of the solar systems occurs where there are regions that reach temperatures  $\geq 800K$ , for example in Jupiter and Saturn where the molecule production is thermodynamically favored.

Even if there is robust evidence for the production of Phosphine by biological activity , the exact mechanism of production is still debated.

However, the synthetic pathways for many of life's natural compounds remains

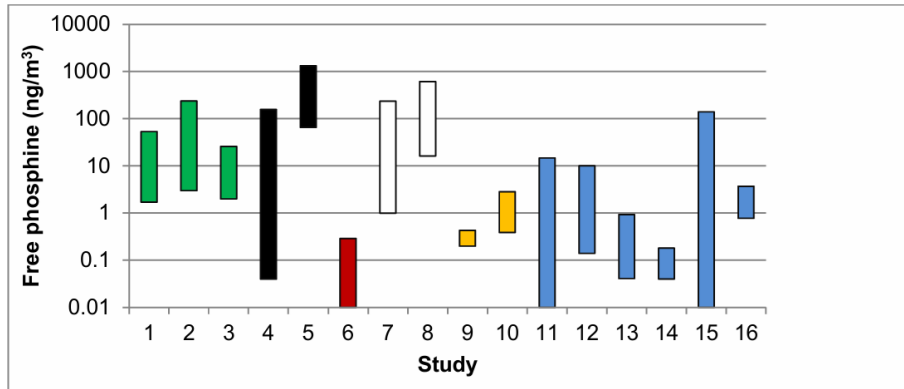


**Figure 2.3:** Measurements of Phosphine concentrations in the Earth’s atmosphere: Green bars- marshlands and paddy fields , black bars-industrial environments , red bars-Namibia(rural environment), White bars-arctic and Antarctic environments, Yellow bars-Upper troposphere, blue bars-oceanic samples(coastal and open ocean. From [82]

unknown. Despite this , their origin is generally considered to be biological due to the improbability of abiotic synthesis , their strong association with living organism , and their resemblance to other biological substances.

There are two proposed explanations for the production of  $\text{PH}_3$  in anoxic ecosystems:

1.  $\text{PH}_3$  is directly produced by anaerobic bacteria from environmental phosphorus
2.  $\text{PH}_3$  is indirectly produced by anaerobic bacteria. Anoxic fermentation of organic matter by anaerobic bacteria results in acid products; these acid products , in turn could react with organic metal phosphides , like those present as a trace elements in scrap metal , resulting in phosphine generation

## 2.2.2 spectral properties of of Phosphine

With photochemical modelling and spectral simulations the team has reached these results on the spectral properties of Phosphine as a biomarker [82]:

- $\text{PH}_3$  is able to reach detectable levels in an exoplanet atmosphere, provided it has high production rate at the planet surface
- $\text{PH}_3$  has unique spectral features , namely strong bands around 2.7-3.6 microns, 4.0 -4.8 microns and 7.8-11.5 microns , that allow it to be distinguishable from other dominant atmosphere molecules

- based on the abundances and surface fluxes needed to produce detectable levels of  $\text{PH}_3$ , it has no known false positives provided that the planet's surface temperature is below 800K
- At surface fluxes near the minimum flux necessary to allow for  $\text{PH}_3$  detection, a "runaway" effect for  $\text{PH}_3$  occurs, where the production increases dramatically.

### 2.2.3 phosphine Surface fluxes required for detection

The surface flux necessary for phosphine to assemble to detectable abundance levels in anoxic atmospheres, so the biological production rate, is critical to assess to determine the efficacy of  $\text{PH}_3$  as a biosignature. The surface flux that a biosphere can plausibly generate must be within the range of the detectable levels of  $\text{PH}_3$ .

Up in the atmosphere the destruction rate and consequent mixing ratio changes, due to the different levels of radical concentrations and radiation at different altitudes. The dominant  $\text{PH}_3$  reaction in  $\text{H}_2$  dominated atmospheres is  $\text{PH}_3 + \text{H}$ . The dominant reaction in  $\text{H}_2$  dominated atmospheres is  $\text{PH}_3 + \text{O}$ . In the high regions of the atmosphere, H produced from the  $\text{PH}_3$  photolysis becomes an increasingly important sink for  $\text{PH}_3$ , even in  $\text{CO}_2$  dominated atmospheres. The team of [82] has used a photochemical model to estimate the minimum surface production flux,  $P_{\text{PH}_3}$ , for the detectability of Phosphine in transmission and emission for a range of planetary scenarios. The results are shown in figure 2.4.

Atmospheric Scenario	Required Mixing Ratio for Detection (in transmission and emission)	$P_{\text{PH}_3}$ [ $\text{cm}^{-2} \text{s}^{-1}$ ]
H <sub>2</sub> -rich planet, Sun-like star	780 ppm (transmission)	$1 \times 10^{14}$
<b>H<sub>2</sub>-rich planet, active M-dwarf</b>	<b>5 ppb (transmission)</b>	<b><math>1 \times 10^{10}</math></b>
H <sub>2</sub> -rich planet, active M-dwarf	220 ppb (emission)	$1 \times 10^{11}$
H <sub>2</sub> -rich planet, active M-dwarf (PH <sub>3</sub> runaway)	0.28% (transmission)	$9 \times 10^{11}$
<b>CO<sub>2</sub>-rich planet, active M-dwarf</b>	<b>310 ppm (transmission)</b>	<b><math>3 \times 10^{11}</math></b>
CO <sub>2</sub> -rich planet, active M-dwarf	15 ppm (emission)	$1 \times 10^{11}$
CO <sub>2</sub> -rich planet, active M-dwarf (PH <sub>3</sub> runaway)	7.6% (transmission)	$1 \times 10^{12}$

**Figure 2.4:** Phosphine mixing ratios needed for detection in transmission and emission for different atmospheric and stellar scenarios, as well as associated surface flux requirements ( $PP_{\text{PH}_3}$  [ $\text{cm}^{-2} \text{s}^{-1}$ ]). The values in red represent surface fluxes and associated atmospheric abundances where PH<sub>3</sub> would be able to approach detection but would require longer than 200 hours of observation (which is longer than our allowed limit for detectability). Taken from [82].

The team [82] found the existence of a critical Phosphine surface production flux, past which PH<sub>3</sub> accumulation is efficient and the atmosphere transitions to a PH<sub>3</sub> rich state. The effect is analogous to the CO runaway effect identified in the early Earth. Once the critical point is passed, the PH<sub>3</sub> production outpaces the ability of stellar NUV photons to destroy PH<sub>3</sub>, whether via direct photolysis or via generation of radical species.

## 2.2.4 Sensitivity to temperature and radiation levels

Since different surface temperature can allow a planet to be habitable, we have to consider the effect of temperature on the concentrations of Phosphine. It can affect the reaction rates of PH<sub>3</sub> with radicals, and the concentrations of H<sub>2</sub>O in the atmosphere from which the radical species are largely derived.

Besides temperature, there is another factor to consider, UV irradiation, since it limits Phosphine concentrations through direct photolysis and radical production, H<sub>2</sub>O or OH. The hypothesis is that PH<sub>3</sub> would build to higher concentrations on a planet orbiting a star with low UV output, such as quiet M-dwarf. The team of [82] has found that, for the equivalent surface production rates, Phosphine concentrations are two orders of magnitude higher on planets in the quiet M-dwarf cases compared to the active M-dwarf cases. Low UV emission favors buildup of PH<sub>3</sub> due

to lower radical concentrations and photolysis rates. So the team concludes that as with other proposed biosignature gases, planets orbiting quiet M-dwarfs are the best targets for detecting biogenic  $\text{PH}_3$ . Also they found that, in planets orbiting a quiet M-dwarf,  $\text{PH}_3$  is able to enter a runaway phase with two orders of magnitude lower surface fluxes than those required in more active stars.

## 2.2.5 Phosphine spectral distinguishability

Phosphine’s spectral signature is distinct from other gases that are expected to be present in the atmospheres of rocky exoplanets, such as water vapor, methane, carbon dioxide, carbon monoxide, ammonia, and hydrogen sulfide. Its spectra in the infrared region contain three key features at:  $2.7 - 3.6\mu\text{m}$ ,  $4 - 4.8\mu\text{m}$  and  $7.8 - 11\mu\text{m}$ . In the table 2.2 I have summarized the different properties of the different spectral regions, given the informations provided in [82].

Spectral Region	Description
$2.7 - 3.6\mu\text{m}$	Dominated by a combination of a hot band and an overtone band, both corresponding to the symmetric bending motion of $\text{PH}_3$ . Additionally, six other combination bands are present in this region.
$4 - 4.8\mu\text{m}$	The most prominent spectral feature of $\text{PH}_3$ , primarily due to the fundamental symmetric and asymmetric stretching vibrations of the $\text{PH}_3$ molecule. Several weaker overtone and combination bands also contribute to this feature, which is the strongest part of $\text{PH}_3$ ’s spectrum and clearly distinguishes it from methane, ammonia, and hydrogen sulfide. Some spectral overlap with $\text{CO}_2$ is noted.
$7.8 - 11\mu\text{m}$	The symmetric and asymmetric bending fundamental bands, along with hot bands, combine to create a broad and strong absorption feature. While there is some overlap with the ammonia spectrum in this region, Phosphine can still be distinguished from other molecules.

**Table 2.2:** Spectral regions and corresponding features of  $\text{PH}_3$ .

( figures 2.6 is preliminary since in 2020, when was written the article, out of the 534 molecules for which there are available spectra, only a few dozen have been adequately measured or calculated, and consequently their spectra should be considered preliminary. There are also thousands of volatile molecules which could contribute to an atmospheric spectra [43] for which there is no available spectra, so

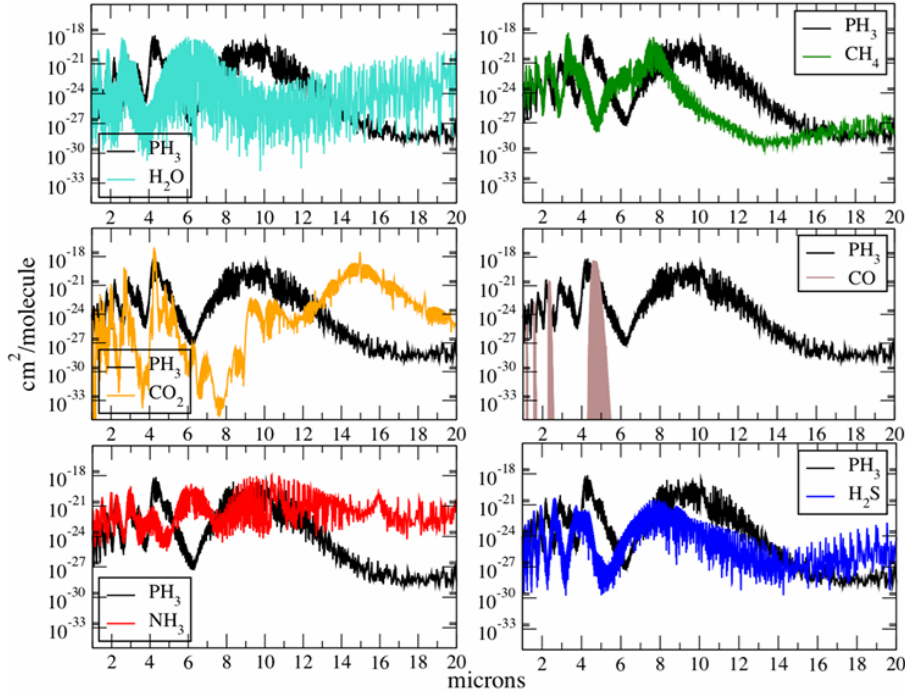


**Figure 2.5:** Comparison of the spectral cross-sections of Phosphine with other molecular gases at room temperature. PH<sub>3</sub>, shown in black, is distinguishable from all compared molecules due to its strong bands in the 2.7–3.6 μm, 4 – 4.8 μm and 7.8 – 11 μm regions. image taken from [82]

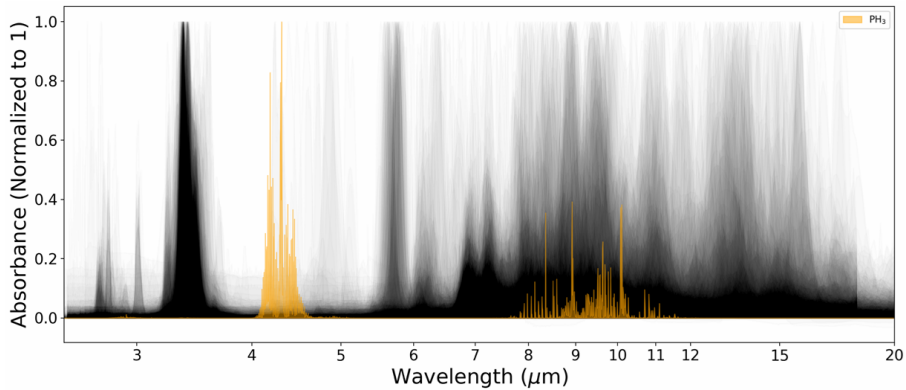


**Figure 2.6:** Comparison of the spectral cross section of Phosphine (orange) with all the available cross-sections for molecules that are volatile at room temperature. Intensity on y-axis in a linear scale representing absorbance (normalized to 1) and wavelength represented on the x-axis in microns, with the spectral range constrained to 2.5 – 18.5 microns for fair comparison (many molecules have incomplete spectra beyond this region). Opacity for all molecules is plotted at 1% so that heavily populated regions are highlighted. all cross sections are calculated with SEAS, using molecular inputs from NIST and EXoMol. The strongest band of PH<sub>3</sub> (4.0–4.8 microns) is easily distinguishable from all other gases, but the broad band at 10 microns can become obscured by other molecules image taken from [82]

further studies are required to reveal the full extent of the spectra comparison in the figure.)

## 2.2.6 Phosphine false positives

As said before, on Earth Phosphine is produced only anthropologically or biologically. As outlined by [82] the formation of  $\text{PH}_3$  on temperature, rocky planets is thermodynamically disfavored, even in the high reducing environments. In thermodynamic equilibrium, phosphorus can be conservatively expected to be found in the form of  $\text{PH}_3$ , only at  $T > 800\text{K}$  and at  $P > 0.1$  bar. Since the critical temperature of water is  $647\text{K}$  there are no surface conditions that allow both  $\text{PH}_3$  production and the presence of liquid water. So in a temperate, rocky planet, it's implausible that  $\text{PH}_3$  can be produced without biological intervention. However the team [82] has considered many false positive that can influence the global concentrations of  $\text{PH}_3$ :

- Phosphite and Phosphate disproportionation: Phosphine could form geochemically by reduction of phosphate or phosphite to  $\text{PH}_3$ , however the team concludes that the formation of  $\text{PH}_3$  from phosphate or phosphite is unlikely in the absence of a biological catalyst.
- Lightning: Lightning discharges even in highly reducing atmospheres produce only negligible amount of reduced phosphorous species, including  $\text{PH}_3$ , and are very unlikely to provide high flux sources of  $\text{PH}_3$  globally.
- Volcanism: Phosphine is not known to be produced by volcanoes on Earth. The team [82] estimated that the maximum production of  $\text{PH}_3$  by volcanoes in any planetary scenario, even  $\text{H}_2$ -rich atmospheres, is at least seven orders of magnitude lower than the surface fluxes required for detections
- meteoric delivery: as a source of reduced phosphorus species that could lead to the abiotic production of phosphine. The team concludes that the contribution from meteoric sources to the global average  $\text{PH}_3$  production rates is still negligible.

From the study of [82] it is clear that non-biological  $\text{PH}_3$  formation is not favored on temperate rocky worlds and no abiotic pathways can produce  $\text{PH}_3$  with production rates necessary for its detection on habitable exoplanets. So they conclude that



unlike ammonia and methane , a detection of  $\text{PH}_3$  on a temperate exoplanet is likely to only be explained by the presence of life.

## 2.2.7 conclusion:phosphine as a biosignature gas

As previously outlined the perfect biosignature has three characteristics:

1. Lacks of (currently known) abiotic false positives
2. has uniquely identifiable spectral features
3. Is unreactive enough to build up to detectable concentrations in exoplanet atmospheres.

$\text{PH}_3$  fulfills the two criteria. As we have seen the geochemical false positives for  $\text{PH}_3$  generation are highly unlikely , it possesses three strong features in the 2.7-3.6 microns , 4-4.8 microns and 7.8-11 microns regions that are distinguishable from common outgassed species that may be present in terrestrial exoplanets atmospheres, such as  $\text{CO}_2$ ,  $\text{H}_2\text{O}$ ,  $\text{CO}$ ,  $\text{CH}_4$ ,  $\text{NH}_3$  and  $\text{H}_2\text{S}$ . The biggest challenge in the detectability of Phosphine at low surface fluxes is its reactivity to radicals, and its vulnerability to UV photolysis. The study of [82] suggests that at high but plausible surface fluxes ( $10^{12} - 10^{14} \text{cm}^{-2} \text{s}^{-1}$  ) ,  $\text{PH}_3$  is able to exhaust the supply of M-dwarf NUV photons and enter a "runaway" phase. This will make  $\text{PH}_3$  easily detectable, it also protects other trace gases from destruction by radicals and rapidly changes the overall composition of the planetary atmosphere. [82]

## 2.3 chemical imbalance as a biomarker

The chemical disequilibrium, i.e. the long-term coexistence of two or more chemically incompatible species that is maintained in the Earth's environment by biogenic fluxes, has also been proposed as a biosignature. Due to oxygenic photosynthesis Earth has a much larger chemical disequilibrium than other solar system planets with atmosphere. As we have seen  $\text{O}_2$  has many problems as a biosignature , since even if it is relatively easy to detect , and is generated in large quantities by relatively few abiotic processes, it has been detectable in the Earth's history for only the past 1/8 of the earth inhabited history. Also , oxygenic photosynthesis is a complex

metabolism that only evolved once on Earth and it is unknown whether its origin on an exoplanet is likely. The coexistence of  $\text{CH}_4$  and  $\text{O}_2$  is an example and indicates continuous replenishment of these gases by biogenic fluxes. But under certain circumstances it can also be an anti signature. In particular it has been showed from [59], that the prebiotic earth likely had a relatively large atmosphere-ocean disequilibrium due to the coexistence of water vapour and volcanic  $\text{H}_2$ ,  $\text{CO}_2$  and  $\text{CO}$ . The subsequent chemotrophic life probably destroyed nearly all of the prebiotic disequilibrium through its metabolism, leaving a likely smaller disequilibrium between  $\text{N}_2$ ,  $\text{CO}_2$ ,  $\text{CH}_4$ , and liquid water. The disequilibrium fell with the rise of chemotrophic life then later rose with atmospheric oxygenation due to oxygenic photosynthesis. The study concludes that big prebiotic disequilibrium between  $\text{H}_2$  and  $\text{CO}_2$  or  $\text{CO}$  and water is an anti-biosignature because these easily metabolized species can be eaten due to redox reactions with low activation energy barriers. They suggest that a large chemical disequilibrium can also be a biosignature when the disequilibrium arises from a chemical mixture with biologically insurmountable activation energy barriers and clearly identifiable biogenic gases. The Earth modern disequilibrium between  $\text{O}_2$ ,  $\text{N}_2$ , and liquid water along with minor  $\text{CH}_4$  is such a case. As with mostly all the biosignatures, chemical disequilibrium can be used to infer the dead or living worlds only analyzing carefully the context.

In the study of [34] they found that Earth's atmosphere-ocean system has more than an order of magnitude disequilibrium (in joules per mole of atmosphere) than any other planet due to biogenic fluxes. As pointed out in [59], the interpretation of disequilibrium as a sign of life is unclear. If a planet has no life it still might have a large disequilibrium of untapped free energy because life is not consuming it, so disequilibrium in that case becomes an antisignature. The study of [59] helps to distinguish the general cases when disequilibrium indicates life versus when it is an anti-biosignatures. In the table 2.7 there have been outlined different types of disequilibrium biosignature gasses.

Pairing	Indication of	Observational Strategy ( $\mu\text{m}$ ) (e.g.)	Citations:
$\text{O}_2/\text{O}_3 + \text{CH}_4$ (oxic atmospheres)	“redox disequilibrium”, since oxidation to $\text{CO}_2$ and $\text{H}_2\text{O}$ does not occur, sources of $\text{O}_2$ and $\text{CH}_4$ must be present	Combined detections of $\text{O}_2$ : 0.76, $\text{O}_3$ : 9.65, $\text{CH}_4$ : 1.65, 3.3, 7.7	Lovelock 1965; Hitchcock and Lovelock 1967; Sagan et al. 1993
$\text{CO}_2 + \text{CH}_4$ (anoxic/Archean-like atmospheres)	non-volcanic source of $\text{CH}_4$ if observed without significant $\text{CO}$	Combined detections of $\text{CH}_4$ : 1.65, 3.3, 7.7 $\text{CO}_2$ : 1.6, 2.0, 4.3, 15	Krissansen-Totton et al. 2018a,b
$\text{N}_2 + \text{O}_2 + \text{H}_2\text{O}$	largest thermodynamic equilibrium on the modern Earth	Combined detections of oceans (via glint or polarimetry), $\text{N}_2$ (via $\text{N}_2$ - $\text{N}_2$ CIA centered at 4.3 $\mu\text{m}$ or scattering), $\text{O}_2$ : 0.76	Krissansen-Totton et al. 2016
$\text{N}_2\text{O} + \text{O}_2/\text{O}_3$ and/or $\text{CH}_4$	“redox disequilibrium,” since oxidation states differ between $\text{N}_2\text{O}$ , $\text{O}_2$ , and $\text{CH}_4$	Combined IR detection of $\text{N}_2\text{O}$ : 7.8, 8.5, $\text{O}_3$ : 9.65, and $\text{CH}_4$ : 7.7	Kaltenegger 2017; Schwieterman et al. 2022

**Figure 2.7:** example of disequilibrium biosignature gases , from [79]

## 2.4 critical aspects of the concept of biosignature

In the study of [17] many critical aspects about the field have been outlined. Since in my thesis I focus on gaseous biosignatures I will outline the problems concerning the definition of this type of biosignature. Regarding a gaseous biosignature, for example oxygen, the concept may refer to the gaseous substance (oxygen) directly produced by biological entities , to the gaseous substance ozone, resulting from the transformation of primary products (intermediaries), to specific properties of either substances, such as their specific absorption spectra or their abundance (“observable features”), or to the end-observations that are made , for instance the full spectrum resulting from a measurement procedure (“observations”). As noted by [80] it is difficult to say whether a biosignature is the measured spectral signal or the inferred presence of the gas based on the signal, or even the inferred presence of biological entities at the origin of that gas.

The problem that they have found to be the most crucial are the following:

1. The terms “Biomarkers” or “biosignature” are generally poorly defined , so there is the need of a more formal and rigorous definition, especially because

of the big number of missions that include the topics of life detection in their mission strategy, and because the term biosignature implies implicitly a certain proof of the presence of life, which is impossible to obtain due to the high number of false positives.

2. The inference from observations of a certain signal all the way back to the assertion of the presence of biological entities somewhere at the origin of that signal is actually a chain of interwoven abductive backward inferences mediated by several layers of theories, models and particular conditions. Furthermore, since each of these theories, models and particular conditions only receive a certain degree of confirmation, the overarching inference of the presence of biological entities can only be confirmed up to the compounded degrees of confirmation of all the ingredients used in the chain of backward inferences. In practice, this confirmation ought to be even lower than that since alternative, less favorable models cannot be ruled out for sure, which is a general issue for any abductive reasoning.[80]
3. Depending on context, the concept of biosignature may apply to different types of elements intervening along the way in the causal chain. Yet, depending on the position of these elements in the chain of backward inferences, corresponding biosignatures will be subject to varying degrees of confirmation. [80]
4. it is necessary to answer 3 question regarding the signal: 1) is the signal real? 2)does the signal correspond to what we think it corresponds to? 3) Is the thing you think the signal corresponds to actually indicative of life?
5. Since there is always a non zero probability that a biosignature is not produced by life , the claims of a biosignature discover should always be used together with a confidence level specifically addressing the uncertainty.

It is impossible to deny from what we have seen that the concept of biosignature is intrinsically fraught with ambiguities. Nevertheless , as pointed out in [17] , many scientific concepts are vague but nevertheless useful , for example: information, gene, evolution and probability. In some ways they are useful because they are vague: flexible or "fuzzy" definitions may guard against inflexible thinking and promote interdisciplinary. [17] have suggested a series of question for those interpreting biosignature concepts and terms in the work of others.

- If several similar concepts are used in a publication, are they used as synonyms or with specific differences?
- Are terms such as “biomarker” being used in a sub-discipline-specific way?
- What does the word “biosignature” (or similar) refer to? Is it being used to refer to an observation (e.g., signal from a spectrograph), an observable feature (a transmission spectrum), an observable object or substance (ozone), or an intermediary object or substance (oxygen that is transformed into ozone), or a plurality of any of these?
- Upon which models and assumptions do the backward abductive inferences from observations to the presence of life rely?
- Is the context of the signature well-described and is this context fully considered in the assessment of biogenicity?
- If the detection is presented with error bars/caveats/less than total confidence, is this because of uncertainty about the association of the phenomenon with life, the identification of the phenomenon in the data, or the quality of the data themselves? Is an abiotic hypothesis tested? Has enough science been done to explore the possibility of abiotic “mimics” in the relevant environment?
- Does the concept of biosignature that is used correspond to a stronger (binary) or weaker (probabilistic) inference to the presence of life?
- What implicit conceptualization of life do the authors have in mind?

Another work that has brought attention on many critical aspects regarding the field of biosignature is [63]. Here I make a summary of the main critical aspects that have been covered.

1. The search for life outside the solar system seems more a study of the Earth 2.0 biosphere in the galaxy , instead of the search for life , Since the discovery of an exoplanet with an atmosphere similar to Earth’s would not teach us anything new about life, it would only help us better understand the distribution of exoplanets with a Earth 2.0 biosphere.
2. It is not possible to detect life with features that are shared between non-living and living system since there is no underlying theory of life, we should better

ask ourselves what kinds of exploration are needed to help us formalize such a theory.

3. Building bigger telescopes that can resolve more data , have more spatial resolution, won't resolve the problem since we are limited by the theories developed to assign cause to the observations we are making. the question is "how useful is the detection of a very high confidence biosignature if it doesn't teach us anything new about life, or even change our approach to learning about life.

They propose that the community should focus on identifying unambiguous features of life via four areas of active research: understanding the principles of life on Earth, building life in the lab, detecting life in the solar system and searching for techno signatures.

Regarding the third critical aspect it is not true that in fact it doesn't change our approach , since as we will see later , the observation can help us to constrain better the parameters of the Bayesian approach and so help us to better decide which strategy to focus on when searching for biospheres.



## Chapter 3

# Application of the Bayesian statistics to the inference of gaseous biomarkers

### 3.1 The use of a Bayesian approach

#### 3.1.1 The different ways of seeing probability

Probability can be defined as the quantification of the level of randomness of an event, where something is termed random if it is not known or cannot be predicted with absolute certainty. The various interpretations of probability fundamentally arise from its dual meaning: epistemic, that is, as uncertainty related to (limited) human knowledge, and empirical, that is, as intrinsic uncertainty of phenomena. Let's see the different interpretation of the concept of probability:

- **classic interpretation** ( De Moivre, Laplace): the probability of an event is the ratio between the number of positive results and those possible, supposed that every event has the same probability , so  $P_A = \frac{N_A}{N}$ , where N is the number of possible cases and  $N_A$  is the number of positive cases for the event A. This definition of probability is based on discrete events of finite number and it is hard to extend it to the case of continuous variable. Another problem is that every event has the same probability.
- **Frequentist** (Von Mises): The probability of an event is the limit towards which the relative frequency of the event tends, as the number of trials ap-



proaches infinity.  $P_A = \lim_{N \rightarrow \infty} \frac{N_a(N)}{N}$ . Such a definition can also be applied without knowing the sample space a priori and without assuming the condition of equiprobability of the elementary events. However, it is assumed that the experiment can be repeated multiple times, ideally infinitely, under the same conditions. The rigorous definition is :

$$\lim_{n \rightarrow \infty} \Pr \left( \left| \frac{N_a(N)}{N} - P_a \right| > \epsilon \right) = 0$$

. This definition, however, contains a circularity issue related to deciding how small the approximation should be (i.e., how large N should be). Additionally, not all experiments are repeatable or can be repeated under the same conditions, and probability applies exclusively to phenomena that occur on a large scale, while it is not possible to talk about the probability of single events (or never-occurred events). An important advancement from the classical conception, where probability is established a priori before looking at the data, is that in the frequentist view, probability is derived a posteriori from the examination of data. However, both views are objective probabilities. The frequentist perspective is not about epistemic uncertainty but rather tied to an empirical view of probability.

- **Bayesian** In the Bayesian approach, probability is a measure of the degree of plausibility of a proposition. This definition is applicable to every event. Bayesian probability is an inverse probability, it consists of going from the observed frequencies to probability. In the Bayesian approach "personal consideration" are used to assign probability to a given event before doing the experiment. So the prior probability is connected to the degree of credibility of the event, chosen in a subjective way. The Bayes theorem allows, using the observed frequencies, to "adjust" the prior probability, calculate the posterior probability. Thus, through this approach, a prior estimate of the degree of credibility of a given hypothesis is used before observing the data, in order to assign a numerical value to the degree of credibility of that same hypothesis after observing the data. Being based on prior information, it is not an absolute probability but always conditioned (on prior knowledge). In the frequentist approach you calculate how many times the observation falls in a certain interval, instead in the Bayesian approach you choose directly a probability of truth

for the interval. In Bayesian terms, there is no distinction regarding the origin of uncertainty, i.e., between statistical uncertainty (due to the finite precision of the measurement instrument) and systematic uncertainty (related to deterministic effects that are only partially known, such as calibration effects). In both cases, the issues are related to a lack of information, and the random nature of statistical uncertainty is simply due to the unknown exact conditions of the system. Bayesian statistics only considers the data actually observed, whereas in the frequentist approach, assumptions must be made about the distribution of possible unobserved data.

So in Bayesian analysis probabilities do not represent the frequency of specific outcomes after repeated observation or experiment. Instead they represent the confidence in that outcome being an accurate model of reality. This is a subtle difference and in many application it doesn't matter in which way you see probability. For example if you consider the flipping of a fair coin , you know that there is a 50% chance of landing heads up, and it doesn't matter whether you chose for a frequentist observation or a Bayesian interpretation. However if we are considering life detection, if we claim that there is a 50% probability a planet hosts alien life, we are not saying that out of many observations of that planet half of the time it has no life- instead we are quantifying our uncertainty about a presumably objective, observational feature of that planet. That's why the Bayesian approach to probability is the most suitable for the application to biosignature studies.

### 3.1.2 General properties of probability

let's recall the basic axioms of probability theory as formulated by Kolmogorov in the XX century. If we call  $S$  the space of events, so the set of all the possible results in the experiment, and we consider an event  $A$  , so a subset of the set  $S$ ,  $A \subseteq S$ . The probability  $P_A$  associated with  $A$  is a real number that has the following characteristics:

1.  $P_S = 1$
2.  $P_A \geq 0, \forall A$
3.  $P(A \cup B) = P(A) + P(B)$  for every  $B$  such that  $A \cap B = \emptyset$

From these axioms, it is possible to demonstrate that  $P(\neg A) = 1 - P(A)$ , where  $\neg A$  is the complement of  $A$ . Additionally,  $P(B) \leq P(A)$  if  $B \subseteq A$  and  $P(A \cup B) = P(A) + P(B) - P(A \cap B)$ .

These are the axioms of probability but they don't say anything about how it should be interpreted. The conditional probability  $P(A|B)$ , which is the probability of  $A$  given  $B$ , is given by:

$$P(A|B) = \frac{P(A \cap B)}{P(B)} \quad (3.1)$$

Two subsets  $A$  and  $B$  are independent if  $P(A \cap B) = P(A)P(B)$ .  $P(A, B) = P(A \cap B)$  is called joint probabilities, instead  $P(A \cup B)$  is called disjoint probability. It can be demonstrated that  $\sum_B P(A, B) = P(A)$  where here  $P(A)$  is called marginal probability.

### 3.1.3 What is the Bayesian approach to probability theory

The Bayesian approach to probability theory allows us to make inferences from the data using Bayes' theorem and formula. The Oxford Dictionary of Statistics (2014) describes it as: "an approach concerned with the consequences of modifying our previous beliefs as a result of receiving new data." Bayes' theorem states that the posterior conditional probability of  $A$  given  $B$  can be written as:

$$P(A|B) = \frac{P(B|A)P(A)}{P(B)} \quad (3.2)$$

where:

- $P(B|A)$  is called the likelihood
- $P(A), P(B)$  are called the prior probabilities

Let's see an easy derivation of this expression. The formula to calculate a conditional probability is:

$$P(A|B) = \frac{P(A \cap B)}{P(B)} \quad (3.3)$$

Thus, we have:

$$P(A \cap B) = P(A|B) \cdot P(B) \quad (3.4)$$

Similarly, for the reverse conditional probability, we have:

$$P(B|A) = \frac{P(B \cap A)}{P(A)} \quad (3.5)$$

And therefore:

$$P(B \cap A) = P(B|A) \cdot P(A) \quad (3.6)$$

From the equations above, we can write:

$$P(B|A) \cdot P(A) = P(A|B) \cdot P(B) \quad (3.7)$$

By dividing both sides by  $P(B)$ , we obtain Bayes' theorem:

$$P(A|B) = \frac{P(B|A) \cdot P(A)}{P(B)} \quad (3.8)$$

As noted in [74], there are essentially two ways of thinking about Bayes' theorem:

- It describes the relationship between  $P(A|B)$  and  $P(B|A)$
- It describes how a subjective degree of belief should rationally change considering the evidence

It is possible to use Bayes' theorem every time we have a conditional probability  $P(A|B)$  but we are asked to find the inverse, so  $P(B|A)$ . The theorem is helpful because it is often easier to estimate one of these conditional probabilities instead of the other, as outlined in [74].

The expanded version of Bayes' theorem focuses on inference and has the form:

$$P(A|B) = \frac{P(B|A) \cdot P(A)}{P(B|A) \cdot P(A) + P(B|\neg A) \cdot P(\neg A)} \quad (3.9)$$

Where:

- $P(A|B)$  is the probability of  $A$  given  $B$
- $P(B|A)$  is the probability of  $B$  given  $A$
- $P(A)$  is the probability of  $A$
- $P(\neg A)$  is the probability of not  $A$

- $P(B|\neg A)$  is the probability of  $B$  given not  $A$

and it is the one that we will use in the model. The denominator is still the sum of two joint probabilities that equals the marginal probability  $P(B)$ . Bayesian inference can be defined as: “The use of Bayes’ Theorem to draw conclusions about a set of mutually exclusive, exhaustive, alternative hypotheses by linking prior knowledge about each hypothesis with new data. The result is updated probabilities for each hypothesis of interest.”

As pointed out in [74], Bayes’ greatest insight was that when we use Bayes’ theorem in this way, the equation itself can be used to draw inferences regarding competing hypotheses and thus is directly tied to the scientific method.

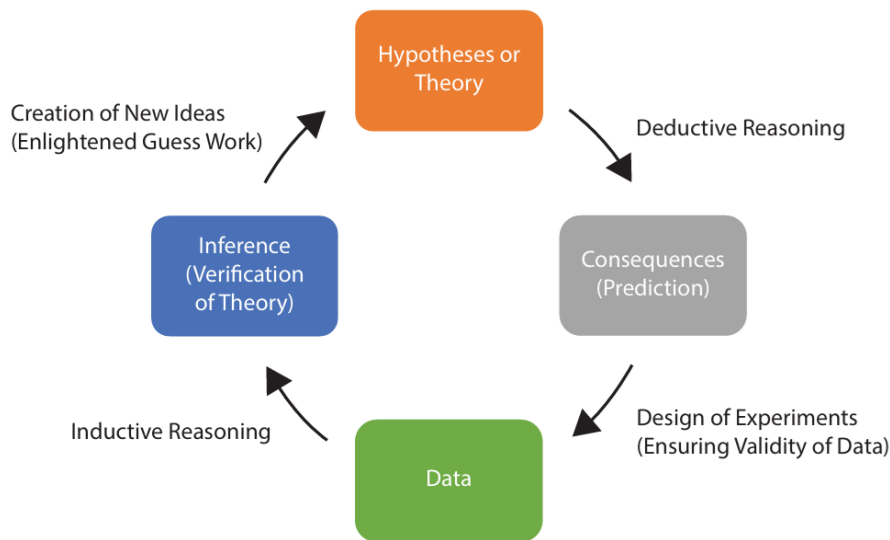


**Figure 3.1:** Schematising the scientific method, Bayesian inference begins with the notion of multiple hypotheses, taken from [74].

Regarding Figure 3.1, we can say that the hypotheses has to do with the prior probabilities, the consequences box has to do with the likelihood. Regarding the likelihood, the definition given in [74] is: ”likelihood involves the collection of data, and we look retrospectively at the probability of collecting those data.” In fact, likelihood can be seen as another way of saying probability. There is a subtle difference in the way the word is used in statistics: here the likelihood describes the probability of observing data that have already been acquired. The likelihood and the probability can also be differentiated in this way: likelihood is the hypothetical probability that an event that has already happened will give us a specific outcome.

Probability instead has to do with future events, the likelihood instead refers to past events with known results.

In Bayesian analysis, the sum of the prior probabilities around the hypothesis, as the sum of the posterior probabilities on the hypothesis, must be 1. This is in general not true for the likelihoods of observing the data under every hypothesis.

In the frequentist notion of Bayes' theorem, priors are only the marginal probabilities. But in Bayesian inference, priors represent a prior probability that every alternative hypothesis is correct, where a priori means: "before collecting data". It is not possible to do a Bayesian analysis without using a priori distribution, and also it is necessary to take data to estimate the likelihood of the data itself, considering the hypothesis true.

The problem that arises when considering a flat distribution for  $P(H_i)$ , which is what is done in the frequentist approach, is that in this case  $P(H|E)$  is proportional to  $P(E|H)$  which is not true in Bayesian statistics.

All the significance testing in the frequentist approach is based only on  $P(E|H)$ , which is the likelihood of observing the data, given that the hypothesis is true.

One of the hardest things to do in Bayesian analysis is the estimation of the prior. This can be differentiated between non-informative prior and informative prior. The first is a distribution that adds almost no information to the Bayesian inference. If we choose to use a non-informative prior it is because our goal is to obtain a posterior distribution that is shaped primarily from the likelihood of the data. When we do analysis based on the frequentist approach we are in fact considering a flat distribution of the priors, where every hypothesis has the same prior.

### 3.1.4 Bayesian approach applied to astrobiology

As outlined by [64]: "Bayesian methods are founded on the explicit use of judgment, expressed as prior beliefs, and provide a natural means of revising opinions in the light of new evidence". For this reason, Bayesian statistics can be very flexible. In principle, it can be applied to every problem where we can calculate the likelihood under every hypothesis. This is not always easy and can often lead to computations that cannot be done analytically, but once it is done, we can apply this kind of analysis. The Bayesian framework can help us make claims for the detection of

life and estimate the prior probability of finding a certain biosignature. It permits evaluating the probability of a hypothesis, like the presence of life, given a set of observed data. The posterior probability quantifies the probability of a hypothesis once the evidence has been taken into account. As previously stated, the definitions of biosignatures are the following:

<b>Author</b>	<b>Definition</b>
Thomas-Keprta et al. 2002	A physical and/or chemical marker of life that does not occur through random, stochastic interactions or through directed human intervention
Des Marais et al., 2003, 2008	Object, substance and/or pattern whose origin specifically requires a biological agent
Catling et al. 2018	Any substance, group of substances, or phenomenon that provides evidence of life
Pohorille and Sokolowska 2020	Chemical species, features, or processes that provide evidence for the presence of life
<b>Proposed Definition</b>	<b>Any phenomenon, substance, or group of substances <math>A</math> that provides a conditional probability <math>P(\text{life}   A) \gg P(\text{non-life}   A)</math></b>

**Table 3.1:** Different definitions of biosignature throughout the time

The problem with the first and second definition is that in most cases it is difficult, if not impossible, to rule out an abiotic origin when we talk about chemical signatures. The problem with the third is that the word "evidence" may suggest that the probability of the biosignature being biogenic is 100%, which again is almost always impossible. The definition that I propose relies on on the quantitative framework of the Bayesian statistics. Thus, the problem shifts to being able to calculate the various terms of the Bayes inference formula, and so to calculate the posterior probability. as we will see later in the chapter.

As pointed out in [54], a Bayesian claim of detection of life requires quantifying the following:

- The likelihood of the signal arising due to living processes

- The likelihood of the signal arising due to abiotic processes
- The prior probability of the living process

The terms used are conditional probabilities: the likelihood of observing an event  $A$ , given another event  $B$  has already occurred,  $P(A|B)$ . For example, on Earth, the probability of phosphine arising by biotic production is much higher than by abiotic origin:  $P(\text{PH}_3|\text{biotic}) \gg P(\text{PH}_3|\text{abiotic})$ . The same can be said for  $\text{O}_2$ , since on Earth the likelihood of it arising due to life,  $P(\text{O}_2|\text{oxygenic photosynthesis}) \gg P(\text{O}_2|\text{abiotic})$ . Thanks to Bayes' theorem, we can calculate the posterior probability of life for a given set of observational data:

$$P(\text{life}|\text{data}) = \frac{P(\text{data}|\text{life})P(\text{life})}{P(\text{data})} \quad (3.10)$$

where data refers to every observable indicative of life, for example: the statistics from the planet surveys, the context of a particular planetary system, or the observation of the planet itself. So the conditional probability will be a function of the system parameters:  $P(\text{data}|\text{life}) = f(M, \rho, o, c)$  and  $P(\text{data}|\text{abiotic}) = g(M, \rho, o, c)$  are both functions of the planetary observables. The denominator of Eq. 2.1 is the total likelihood of observing a given data set and can be expanded further with:

$$P(\text{life}|\text{data}) = \frac{P(\text{data}|\text{life})P(\text{life})}{P(\text{data}|\text{life})P(\text{life}) + P(\text{data}|\text{no life})(1 - P(\text{life}))} \quad (3.11)$$

What we would like to know is  $P(\text{life}|\text{data})$ , the posterior probability of life, given a set of observational data. But first we have to tightly constrain  $P(\text{data}|\text{life})$ , the probability of the observational data given life is present, and  $P(\text{data}|\text{no life})$ , the probability of the observations arising if life is not present. In addition, knowledge of  $P(\text{life})$ , the prior probability of living processes, is required to assess the likelihood of life, as outlined in [54]. One of the main positive aspects of the Bayesian approach is that it permits separating the calculation of the prior probability of life,  $P(\text{life})$ , from the likelihood of observational data if life is present  $P(\text{data}|\text{life})$  or if life is not present  $P(\text{data}|\text{abiotic})$ . So it allows us to quantify the detectability of life from a specific type of data and provides a tool for identifying promising targets in our search for life without necessarily knowing the prior probability of life itself, which is currently unconstrained, as outlined in [54]. In the Bayesian framework,



detectability can be quantified as:

$$D = \frac{P(\text{data}|\text{life})}{P(\text{data}|\text{abiotic}) + P(\text{data}|\text{noise})} \quad (3.12)$$

In the limit of no experimental noise, we have:

$$D_{\text{noise} \rightarrow 0} = \frac{P(\text{data}|\text{life})}{P(\text{data}|\text{abiotic})} \quad (3.13)$$

This equation gives us an operational definition of detectability, providing a guide for our search for the best targets for observing life in terms of both what to look for and where to look [54]. In other words, detectability provides a quantitative means to answer the question: if we detect a candidate biosignature, can we be confident life produced it? Detectability is distinct from habitability: a world might be habitable but could host life that is not detectable.  $D > 1$  is a quantitative threshold for the definition of a detectable biosignature. A given signal may be a biosignature but not be evidence for life if  $D \leq 1$ . To link observations to biosignatures, the surface chemistry, atmospheric mass, temperature profile, outgassing rate, and photochemistry of a planet must all be modeled, along with any putative biological processes that could be occurring on its surface. The modeled atmospheres can then be compared with observed spectral features, and the plausibility of the biogenicity of the observations evaluated [54]. If no plausible abiotic model can reproduce the atmospheric context for the gas at the same level of detection, but a model including life processes can, then we could conclude that the gas is biogenic. In this case, we should expect  $D \gg 1$ .

Nevertheless it should always be applied the Bayesian model to calculate the posterior probability and assign a threshold to assess the high confidence for biogenicity, which I consider  $P > \mathbf{0.95}$  but there is not a currently universally accepted value.

The hardest parameter to constrain is  $P(\text{life})$ . This is due to the fact that we don't have a theory for life's origin, so we don't know how to calculate this probability yet. The studies [73] [83] that have tried to constrain  $P(\text{life})$  in a Bayesian framework, have concluded that  $P(\text{life})$  could be close to 1 or 0 based on our current state of knowledge, which means there are basically no constraints at all. As pointed out by [54], the goal of the Bayesian framework is to answer the question: How can we develop the most effective strategies for searching for life, faced with the challenge that we have only trivial bounds on its prior occurrence? In the next section I will

offer some answers that come from the strenght and limitation of the model. In table 3.2, we can see how the different term in the field of astrobiology can be quantified in terms of the bayesian framework, where I've also added my proposal definition for biosignature. Instead In 3.2 there are listed all the different aspects that have an influence on the Bayesian parameters, as presented in [54].

**Table 3.2:** Exoplanet Biosignature terminology quantified in a Bayesian framework. Adapted from [54]

<b>Biosignature</b>	<b>Any phenomenon, substance, or group of substances <math>A</math> that provides a conditional probability:</b> $P(\text{life}   A) \gg P(\text{non-life}   A)$
<b>Detectability (D)</b>	Confidence in biological origins for an observed biosignature signal. In the Bayesian framework, $D = \frac{P(\text{data} \text{life})}{P(\text{data} \text{abiotic})}$ (in the absence of noise).
<b>Habitable</b>	Conditions suitable for life where the expectation of the prior probability of life is nonzero, $P(\text{life}) > 0$ .
<b>False positive</b>	Abiotic observations that mimic biologically produced observables, occurring when $P(\text{data}   \text{abiotic})$ is large, such that $D \leq 1$ .
<b>False negative</b>	Biosignatures that are not detectable, occurring when $P(\text{data}   \text{life})$ is small, such that $D \leq 1$ , even in cases where life may be present.
<b>Antibiosignature</b>	An object, substance, and/or pattern that diminishes the likelihood that the signal is generated by life, such that $P(\text{data}   \text{life})$ is less than its absence. A given piece of contextual information $C$ is an antibiosignature if $P(\text{data}   \text{life}, C) < P(\text{data}   \text{life})$ .

### 3.1.5 Statistical approaches to characterizing atmospheres of non-Earth like worlds

The statistical approaches that can be used to better constrain atmospheres of non-Earth like worlds proposed by [54] are:

- The first approach eludes the need to either define the biosignature produced

	P(data abiotic)	P(data life)	P(life)
<b>Stellar context</b>			
Stellar observations	✓	✓	✓
Statistical constraints on age, $T_{eff}$ , composition, irradiance, etc.			
Stellar impact on atmospheres	✓	✓	
Models of stellar activity on atmospheric observables, e.g., lifetime exposure to UV			
<b>Planetary context</b>			
Planets without life	✓		
Observational data of planets without life to constrain abiotic models			
Atmosphere observations	✓		✓
Statistical data on frequency of biosignature gases in exoplanet atmospheres			
Global climate models of exoplanets	✓	✓	
Identify favorable/unfavorable conditions for life and generate statistical data sets of likelihood of observations			
Geochemical modeling	✓	✓	
Model physical contexts more relevant for exoplanets than that of Earth			
Catalog small molecules	✓	✓	
Expand available data on kinetic and thermodynamic properties of small molecules that may be present in exoplanet atmospheres			
<b>Living processes</b>			
Coevolution of life and Earth		✓	✓
Statistical data and models for past biogeochemical states in the history of Earth			
Frequency of major transitions			✓
Constraints on the likelihood of major evolutionary innovation			
Origins of life			✓
Theory and experiments to constrain probability for life to emerge			
Thresholds in chemical complexity		✓	
Identify cases where observable much more likely to be produced by life than not			
Universal biology		✓	✓
Identify network and other properties of life on Earth likely to be universal			

**Figure 3.2:** Summary of Observational, Theoretical, and Empirical Research Necessary to Constrain Variables in a Bayesian Framework for Life Detection [54].

by life or the processes that produce them and has to do with searching for any signal that is unexpected from an abiological model of a planet. Looking at equation 3.13 we can maximize detectability by either maximizing the numerator,  $P(data|life)$ , or minimizing the denominator,  $P(data|abiotic)$ . Even if there is an extremely small probability that a signal is consistent with life, we can still identify it as a biosignature if we can demonstrate there is yet a smaller probability for the signal to be consistent with an abiotic origin.

- it is important however to develop strategies to avoid Earth-centric approach if we are to determine  $P(data|abiotic)$  and  $P(data|life)$  for many words that are not considered Earth-like. The approach should follow [43], which focused on identifying volatile molecules as atmospheric signatures and determining all gases that can stably accumulate in any atmosphere. A size limit was set for molecules with no more than six non-hydrogen atoms stable in the presence of water. The project's goals are to create a database for biosignature research and to explore potential molecules for probing biochemical "laws" in other worlds. Major challenges include a lack of kinetic and thermodynamic data, solubility in water, and atmospheric reaction chemistry for many biosignature molecules. Additionally, measuring kinetic data for gas reactions at various

temperatures and pressures is complex and time-consuming, but not often rewarded with high-profile publications. As noted by [54], future research should focus on new technologies to expedite the measurement of gas kinetics and thermodynamics, making data collection more efficient and less time-consuming.

### 3.1.6 $P(\text{data}|\text{abiotic})$

Constraining  $P(\text{data}|\text{abiotic})$ , means studying all the possible false positives, and involves enhancing our understanding of lifeless worlds and their observational characteristics. But Merely observing planets outside the habitable zone is not enough to ensure the absence of life since those planets might still harbor life and not accurately represent those within the habitable zone. This is evident in the contrasts between present-day Earth and Venus. Our current knowledge about likely uninhabited worlds is undoubtedly incomplete. Additionally, it is crucial to recognize that planets within the habitable zone that do not exhibit obvious biosignatures could still be inhabited. The early Earth in fact possessed a photosynthetically active biosphere, but the biosignatures were challenging to detect. To better constrain  $P(\text{data}|\text{abiotic})$  it will be important to develop strategy and models to study and constrain observational signatures of planets without life. This could be done in the future by a combination of detailed understanding of abiotic processes, and observational surveys that constrain with care likely uninhabited worlds for observation to constrain  $P(\text{data}|\text{abiotic})$ . As outlined in [54]: "By better constraining the observables of strictly abiotic planets, it will become easier to disentangle true-positives biosignatures from false-positive biosignatures and to understand cases where life might be present, but not detectable". Many aspects have an effect on  $P(\text{data}|\text{abiotic})$ , like stellar environment, climate and geochemistry. a detailed treatment can be found in [54].

As correctly outlined by [45], the history of life detection is a history of false positives. Given the high number of false positive explanation for current most used biosignatures, there is a common assumption that biosignatures with false positives are unavoidable. This problem also arises from the fact that we don't have a theory of life that is able to quantify rigorously and separate life from non life. Even if biological matter follows the same physical and chemical rules of abiotic matter,

nevertheless it has great differences and if it is so, and these differences are objective there must be a method to measure them [45]. If they are not objective, we cannot expect to ever detect life, as the distinction between life and non-life would not be a naturally defined category. This pushes us to study them but also to focus our attention to the signature that have no false positives, like technosignatures. As we will see later this is also suggested by the analysis of the Bayesian approach.

Assembly theory is an example of a theoretical framework that tries to quantify the difference between abiotic and biotic matter [49].

The Assembly index (AI) gives the number of operations needed to construct a molecular graph, representing the minimum steps required to create a molecular structure. This index captures the molecule's specificity within the set of all possible alternatives. The core assertion of the theory is that complex, multi-step assembled objects cannot arise without life, which means that they will not be created in significant quantities through abiotic processes.

The theory has been empirically validated: molecules with a high assembly index in detectable quantities have only been observed in living systems. Therefore, finding such molecules on another planet would serve as strong biosignature, which lacks of false positives. What assembly theory suggests is that, while abiotic processes can create molecules, they cannot replicate identical, non-trivial structures without the information processing found in living organisms.

Most importantly, this biosignature can be tested experimentally on Earth, without the need to simulate an entire planetary environment or biosphere, so it is a falsifiable theory.

Life detection based on molecular assembly avoids false positives associated with traditional biosignatures. It directly detects phenomena dependent on an evolutionary process, making the probability  $P(life|obs)$ , certain. Unlike biosignatures, which need environmental context for validation, molecular assembly detection only requires confirmation of the signal, offering direct insights into the underlying evolutionary process and life itself.

The assembly index is defined as "the total amount of selection necessary to produce an ensemble of observed objects". With  $N_T$  total objects in the ensemble,  $N$  of which are unique, the assembly index is defined as:

$$A = \sum_{i=1}^N \exp(a_i) \cdot \left( \frac{n_i - 1}{N_t} \right) \quad (3.14)$$

where  $n_i$  denotes the copy number , the number of objects of type  $i = (1, 2, \dots, N)$  having assembly index  $a_i$ .

### 3.1.7 $P(data|life)$

To constrain  $P(data|life)$  , we have to acquire knowledge about the biotic processes that could generate a signal.

As suggested by [48],to study the biosignatures on another planet , it can be used a black box approach , where nothing need to be assumed about the internal workings of life on a planet, it consumes some gases and emits others. So it can be done a classification based on this approach. The biosignatures are then classified by the process that has produced them, with the idea to use this as a guide to view those processes each as a "black box" of unknown mechanism. This classification scheme considers the potential inputs and outputs of the system that could provide energy and mass to the system. Potential biosignature waste products are considered as the output from processes that:

1. capture chemical energy
2. capture biomass
3. other processes

The type classification of [48] provide four classification types for biosignatures, as described in table 3.3.

Type Classification by [48]	
Type	Description
Type I: Energy Capture	Energy capture by life can occur through exploiting chemical gradients and harvesting light, producing biogenic molecules like gases and pigments. Examples include methane from methanogenesis and CO <sub>2</sub> from respiration. Predicting type I biosignature gases requires understanding the chemical environment of life, with ammonia being a potential biosignature on hydrogen-rich planets. The challenge is accounting for Earth’s diverse chemical environments, where methane can be both an oxidized and reduced waste product. Future research should focus on understanding the diversity of environments and their impact on biosignature detection, as highlighted by [48]
Type II: Biomass Capture	On planet-sized bodies with thin atmospheres, carbon is likely mostly oxidized (CO <sub>2</sub> ) or reduced (CH <sub>4</sub> ), the thermodynamic minima. Life converts this carbon into intermediate redox states to build complex molecules, needing to oxidize or reduce environmental materials. This process can be modeled to predict biosignature outputs, informing $P(data life)$ . Photosynthesis exemplifies this, with CO <sub>2</sub> , H <sub>2</sub> O, and light input producing biomass and O <sub>2</sub> , Earth’s most notable biosignature. This ”organism-level black box” approach helps suggest inputs and outputs for biomass capture before understanding the internal mechanisms.
Type III: Other Uses	The production of type III gases is a result of the ecological or physiological demands on the organism, themselves the result of evolutionary contingencies and of relationships with other organisms: data that are not accessible for exoplanets. As a result, in principle we might consider any chemical to be a type III biosignature.
Type IV: Products of Modification of Gases	Gases produced by life can be modified by the environment, providing a source of secondary signatures of life. Examples include ozone (the photolytic product of oxygen) and dimethyl sulfoxide (the oxidation product of dimethyl sulfide—DMS). These could in principle be predicted if the environment and products of life are known, for example, for types I and II biosignature gases, but will not be predictable for type III biosignature gases.

**Table 3.3:** Type Classification by [48]

Another "black box" approach focuses on the complexity of life's chemical products rather than classifying the processes by which they are produced. The ability to produce similar, complex or non-random structures in large quantities could be exploited as a key observable that distinguishes living organisms from inanimate matter. In fact, the distribution of molecules from abiotic sources differs significantly from biotic ones, exhibiting a smooth curve, as shown in 3.3. A biosignature could be the entropy of a molecular distribution, where such distributions are highly improbable to form abiotically. The challenge with this method lies in defining a minimum threshold of complexity, beyond which we can confidently assert that  $P(\text{data}|\text{life}) > P(\text{data}|\text{abiotic})$  for a given molecule.

Assembly theory, as we have seen provides a useful framework that can help to quantify that threshold through the use of assembly index.

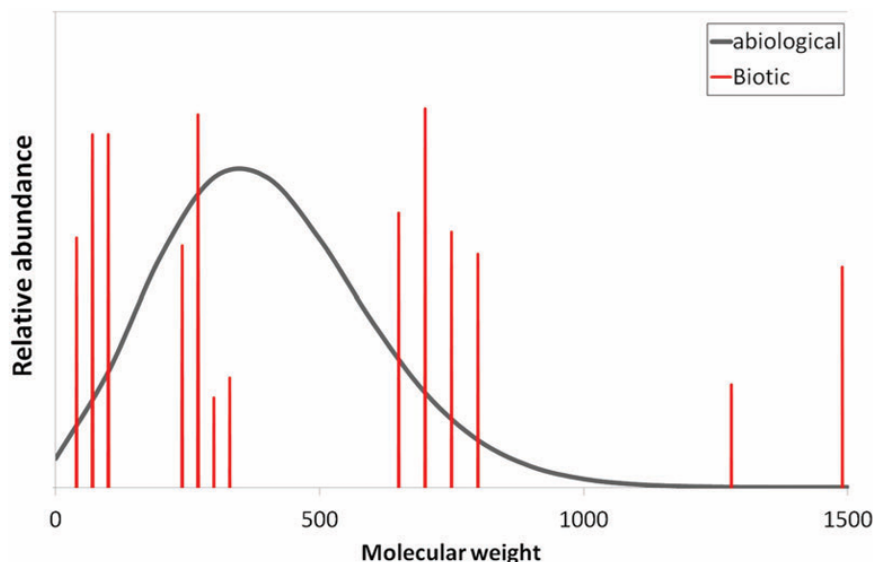


**Figure 3.3:** Schematic illustrating the difference between abiotic (smooth curve) and biological (spikes) distributions of organic molecules. Nonliving systems tend to produce smooth thermodynamic distributions, whereas in living processes, only a subset of molecule species are selected (through natural selection) to form a functional set, from [54]

### 3.1.8 P(life)

The final term to constrain to being able to calculate the posterior likelihood of life (apart from knowledge of experimental noise) is the prior probability for life to exist,  $P(\text{life})$ . As we have seen previously it is the most challenging term to quantify. It is



not sufficient to simply assign a probability that life as we know it exists on another world(which is unknown) ,instead  $P(\text{life})$  should be considered as decomposed into a family of conditional probabilities for the existence of different living processes on other worlds, which may be similar or dissimilar to those on Earth, as pointed out in [54].

The prior probability of any living process ultimately depends on  $p(\text{emerge})$ , the probability that life originated in a given environment. Our ability to constrain  $P(\text{life})$  relies on how accurately we can estimate the probabilities of the candidate living processes that may have produced the signal, along with their evolutionary history, and the origins of life in that specific planetary context.

As we have seen, in the works of [73] and [83] they have tried to constrain  $P(\text{emerge})$  with the conclusion that it can be arbitrarily close to 1 or 0, so it is currently unconstrained. The problem is that right now there are no theoretical framework from which to calculate it. We don't have a definition of life nor a theory of emergence for life. Even if for now it is very hard to calculate  $P(\text{life})$  a priori, there are situations where we can estimate that  $P(\text{life})$  is very low. Since we think that the emergence and evolution of life requires time, knowing the age of the star can tell us where  $P(\text{life})$  might be too low to detect it [54].

As pointed out by [45], there are three sources of new data that could help to constrain  $P(\text{life})$ :

1. New evidence of life earlier in Earth's history
2. New knowledge of the emergence of life from experiments in the lab
3. Detection of another biosphere

the third data accumulation means to do large scale surveys of Earth-like exoplanets in a search for biosphere. In [16] they have demonstrated how this surveys will provide the data most likely to change the shape of the mean of the probability distribution for the likelihood of abiogenesis per unit time, at least on Earth-like planets. This data could be useful in constraining the likelihood of the origin of life even if none of the planets surveyed had detectable biospheres. This strategy however presents a problem , as outlined by [45]; since in the coming years , our ability to gather data from exoplanets will be limited by technological challenges and the lack of clear theories about life. These limitations may prevent us from

accurately interpreting the data, leading to only weak constraints on the probability of life, even considering missions like JWST , LUVOIR, HABex.

Apart from this, [45] has identified some of the aspects that the lab experiments that study the emergence of life should focus on answering and that can help to constrain  $P(\textit{life})$ :

1. Understand the timescales for the emergence of life in different chemical contexts.
2. Understanding the relationship between chemical initial conditions and the observable features of the biochemistry , or the lack of.
3. Understand if we can trade time for space (volume of chemical experiments) in solving the origin of life, or if indeed there is a contingent set of steps , each of finite duration necessary for life to emerge ( in which case we cannot trade time for space)

One of the most recent work that has focused on rigorous estimates of the parameter  $p_{\textit{life}}$  is [69]. Using a Bayesian framework, they showed that, by considering the fact that life has appeared on Earth, it is possible to place lower bounds (at a given confidence level) on the potential value of  $p_{\textit{life}}$ . They also demonstrated that these bounds crucially depend on both the prior presuppositions concerning the probability of abiogenesis and the independent expectation about the number of habitable worlds.

The parameter  $p_{\textit{life}}$  is strictly tied to the parameter  $N_H$ , which represents the number of habitable planets. According to conservative estimates, the number of planets in the Milky Way  $N$  is at least of the same order of magnitude as the number of stars [12], with  $N = 10^{11}$ . The number  $N_H$  of habitable planets is, however, much more difficult to assess. Estimates have ranged from merely a few in models inspired by the "Rare Earth" hypothesis [87] to the upper limit where  $N_H = N$  [86]. Due to the lack of knowledge regarding what makes a planet habitable, we can treat  $N_H$  as a free parameter, as pointed out by [69]. Since the expected number of inhabited planets is  $N_L = p_{\textit{life}}N_H$ , the absence of confirmed estimates of  $p_{\textit{life}}$  translates into the impossibility of calculating this number, even assuming that  $N_H$  is well constrained. As discussed in detail in [69], we cannot rely on the so-called principle of mediocrity to help us constrain the value of  $p_{\textit{life}}$ , which is the assumption that our situation is

not privileged or special, and that it can be considered a random sample drawn from some suitable set. This assumption, in fact, has many limitations and/or flaws.

Finally in [69] using the Bayesian framework they investigate how the number of habitable worlds ( $N_H$ ) in the Milky Way , as well as crucial assumptions concerning the prior likelihood , regulate the bounds that can be placed on the probability of abiogenesis. The expected number of inhabited planets is expressed as  $N_L = p_l N_H$  ,where  $p_l$  stands between 0 and 1. The equation used to calculate  $P(p_l|E)$  where  $E$  is the evidence that at least life has appeared on Earth is:

$$P(p_l | E) = \frac{P(E | p_l) \cdot P(p_l)}{\int P(E | p_l) \cdot P(p_l) dp_l} \quad (3.15)$$

where  $P(p_l)$  is the prior probability of  $p_l$ , which is unknown. So the team has adopted three different priors:

- the prior  $P(p_l)$  constant , that is uniform in  $p_l$  , this choice represent an optimistic or deterministic scenario for abiogenesis
- The prior  $P(p_l) = \frac{1}{(p_l)^2}$  which is uniform in  $(p_l)^{-1}$  and accords more weight to values  $p_l$  close to 0, so it corresponds to a pessimistic scenario for the origin of life.
- Log uniform prior  $P(p_l) = \frac{1}{p_l}$  gives equal weight to all orders of magnitude of  $p_l$  and may consequently be considered neither optimistic nor pessimistic; this prior is usually called uninformative.

The lower bounds they have obtained are listed in 3.4. The findings of the study conclude the following:

- Varying  $N_H$  ostensibly has a minimal effect on  $N_L$  for both the optimist and pessimist; the lower bound for  $p_l$  is mostly independent of  $N_H$  , as seen in 3.4.
- Varying  $N_H$  does indeed exert some influence on the agnostic, but it roughly goes in the opposite direction with respect to the naive surmise that large values of  $N_H$  are tantamount to a higher likelihood of extraterrestrial life. More precisely, as indicated by 3.4, increasing  $N_H$  makes a smaller value of  $p_l$  more compatible, but it does not directly shed light on the frequency of life elsewhere.

- However, it is extremely important to quantify  $N_H$ , since the parameter modulates the plausible lower bound on  $p_L$ . If future studies are able to constrain  $N_H$ , it will be possible to take advantage of a Bayesian approach.
- On account of the approximate inverse correlation between  $N_H$  and the lower bound for  $p_L$  evinced by Table 1, it is conceivable that 'Rare Earth' hypotheses might favor the emergence of life on habitable worlds. The reason is that such hypotheses suggest that truly habitable worlds (akin to Earth) are rare because a number of criteria (e.g., large moon) must be met. A low value of  $N_H$  would, in turn, be compatible with an enhanced lower bound for  $p_L$ .

From this it is possible to understand that the prior has a central role and has the ability to cancel the evidence in certain cases. So the paper highlights that until rigorous theory of living systems and the prior probability distribution  $P(p_L)$  is available, we will not be able to accurately judge the frequency of abiogenesis and the number of inhabited worlds in the universe.

	optimistic	uninformative	pessimistic
prior	$4.9 \times 10^{-2}$	$5.4 \times 10^{-15}$	$1.0 \times 10^{-15}$
post., $N_H = 10$	$1.1 \times 10^{-1}$	$1.5 \times 10^{-2}$	$5.1 \times 10^{-15}$
post., $N_H = 10^4$	$4.9 \times 10^{-2}$	$5.5 \times 10^{-5}$	$3.6 \times 10^{-15}$
post., $N_H = 10^7$	$4.9 \times 10^{-2}$	$1.0 \times 10^{-7}$	$2.5 \times 10^{-15}$

**Figure 3.4:** Lower bound on the probability of abiogenesis ( $p_L$ ) at 95 per cent confidence level, assuming the cut-off  $p_{L,\min} = 10^{-15}$ . The first row corresponds to the bounds derived from the optimistic, uninformative, and pessimistic priors, whereas the remaining rows show the bounds for the posteriors, where the evidence that life exists on Earth is taken into account. The bounds are a function of the number of habitable worlds ( $N_H$ ) in the Milky Way. Taken from [69]

).

### 3.1.9 Bayesian framework example: building a toy model for phosphine detection

To begin with, I try to replicate the results of [54]. The parameter he uses are completely arbitrary so I take  $\text{PH}_3$  as an example from the beginning. Since  $\text{PH}_3$  has been very well characterized recently [82], and seems to be one of the best biosignatures, due to the fact that in many circumstances it lacks of the false positives

and it has some very strong features. The model that I will apply is meant to be conceptual, since the likelihoods and priors are not known. It used the Bayesian inference framework in order to assess the posterior probability of biogenity for a given gaseous biosignature, and allows to add contextual information to better constrain it.

As we have seen the posterior probability of life given a set of observational data is given by:

$$P(\text{life}|\text{PH}_3) = \frac{[P(\text{PH}_3|\text{life}) + P(\text{PH}_3|\text{error})]P(\text{life})}{[P(\text{PH}_3|\text{life}) + P(\text{PH}_3|\text{error})]P(\text{life}) + [P(\text{PH}_3|\text{no life}) + P(\text{PH}_3|\text{error})]P(\text{no life})} \quad (3.16)$$

$P(\text{PH}_3, \text{error})$  is the likelihood of failure in our detection apparatus and captures the possibility of falsely detecting a positive signal of  $\text{PH}_3$ , when there is no  $\text{PH}_3$  present, or could correspond to failure to detect  $\text{PH}_3$  when it is present, and it will be considered in the next section. The goal of the method is to determine  $P(\text{life}|\text{PH}_3)$ . We have to assume a reasonable value for  $P(\text{PH}_3|\text{life})$ , which can be the fraction of Earth life for which it had detectable  $\text{PH}_3$  in the atmosphere. That will be the fraction of planets with life that have detectable  $\text{PH}_3$ . Then we have to assume a value for  $P(\text{PH}_3|\text{no life})$ , the fraction of planets without life that will have detectable  $\text{PH}_3$  in the atmosphere. We want  $P(\text{PH}_3|\text{error}) = e$ , which is the measurement error to be small. As we have seen, the prior probability of life can be considered unconstrained. So it is uniformly distributed between 0 and 1 with a value given by  $P(\text{life}) = p_l$ . As done by [54], I assume  $e = 0$  to start, and then I vary the parameter in the next chapter when I expand the model. As in [54], I assume that our measurements are Bernoulli distributed, the number of positive results will follow a Binomial distribution, with probability mass function:

$$P(\text{data} = X) = \binom{n}{x} p^x (1 - p)^{n-x} \quad (3.17)$$

where  $x$  is our measurement (the number of planets with confirmed  $\text{PH}_3$ ),  $n$  is the number of planets we have taken measurements (the same as  $x$  in this example since we assume every observation yields a positive result for simplicity),  $p$  is the probability of positive measurement.

The first plot, Figure 3.5 simply shows that  $P(\text{life}|\text{PH}_3)$  increases with the increase of  $P(\text{life})$ .

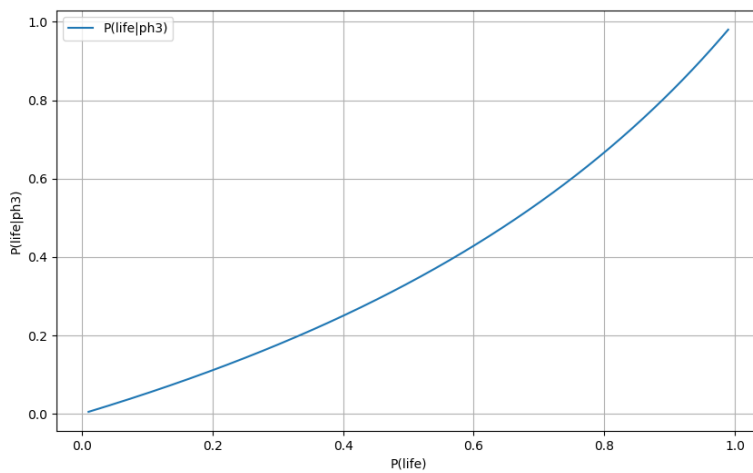
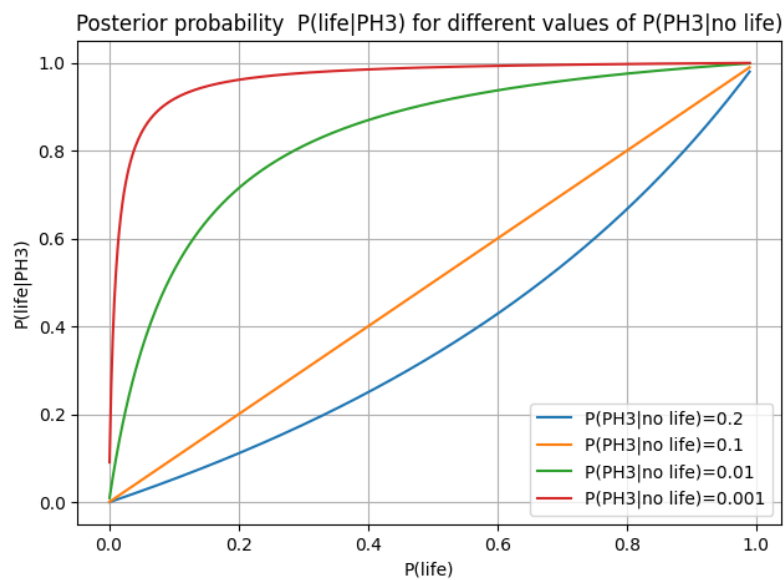


**Figure 3.5:** Posterior probability of life against prior probability  $P(\text{life})$  with no additional context, here the posterior probability simply increases with  $P(\text{life})$ .



htbp

**Figure 3.6:** Posterior probability of life for different values of  $P(\text{molecule}|\text{no life})$

In Figure 3.6 we can see how our posterior probability of life changes, assuming one transit measurement, for different values of  $P(PH_3|nolife)$ . Even in cases where the signal is unlikely to be produced abiotically, where  $P(PH_3|abiotic) = 0.001$ , so a 0.1% probability for an uninhabited world to have detectable levels of atmospheric  $PH_3$ , if life is not common,  $P(life)$ , our posterior probability for life will not be "very likely inhabited". which means that the value is  $< 0.95$ . In this case there is the need for more data.

Then I consider a Bernoulli distributed probability and use the parameter in table 3.4, to make the plot of figure 3.7, just as in [54]. The number here are chosen arbitrarily just to show the trends.

$P(life)$	$P(no\ life)$	$P(PH_3 life)$	$P(PH_3 no\ life)$	$P(PH_3 error)$
$p_l$	$1 - p_l$	0.1	0.2	$e$

**Table 3.4:** First parameters for the model with no additional contextual information, plot shown in Figure 2.7

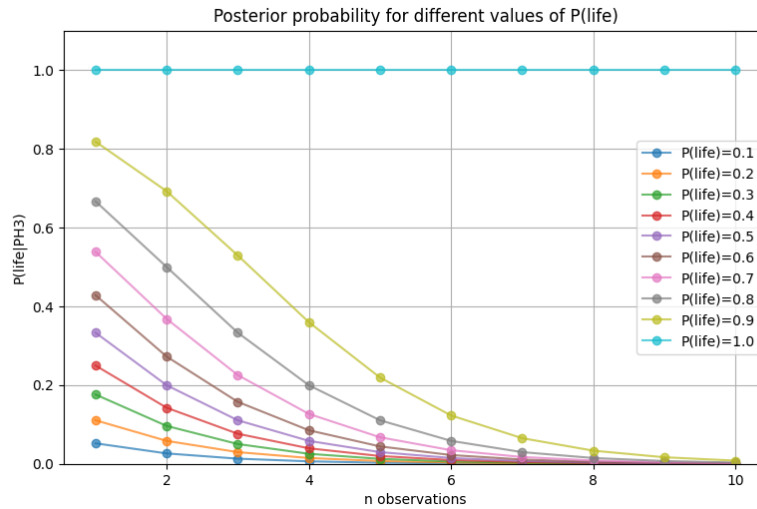


**Figure 3.7:** Posterior probability of life as a function of repeated independent observations of  $PH_3$ . The number of observations is discrete; continuous curves are shown here to better illustrate trends. Model parameters are from Table 2.1 (with  $e = 0$ ), using Eq. 2.16 for the measurement distribution as described in the text. Shown are cases for varying assumptions about the prior probability of life  $P(life)$ .

Since  $P(PH_3|no\ life) > P(PH_3|life)$  in this case, increasing our number of independent measurements decreases our confidence in detection of life, due to the false positives, as we can see from Figure 3.7. That's because nonliving processes are more likely to produce the same signal. Any biosignature that is more likely

to be produced abiotically than biotically will hardly be used to detect life without additional context.

In the Bayesian framework, it is possible to add contextual information. The formula in this case becomes:

$$P(\text{life}|\text{PH}_3) = \sum_{i=1}^n \frac{P(\text{PH}_3|\text{life}, C_i)P(\text{life}, C_i)}{P(\text{PH}_3|\text{life}, C_i)P(\text{life}, C_i) + P(\text{PH}_3|\text{no life}, C_i)P(\text{no life}, C_i)} \quad (3.18)$$

The Bayesian framework allows us to quantify when and how context can permit distinguishing between the hypotheses of biogenic or abiotic sources. In the next section I will choose different contextual information for Phosphine.

## 3.2 Expanding the model

To start let's try to change the parameter in table 3.2 to see how the posterior probability of life changes with  $P(\text{life})$ . If we have  $P(\text{molecule}|\text{life})$  equal to the probability of false positive  $P(\text{molecule}|\text{nonlife})$  this will result in a slightly faster growth of  $P(\text{life}|\text{molecule})$  which happens to be linear as we can see in figure 3.6. In this case i choose a value of 0.1.

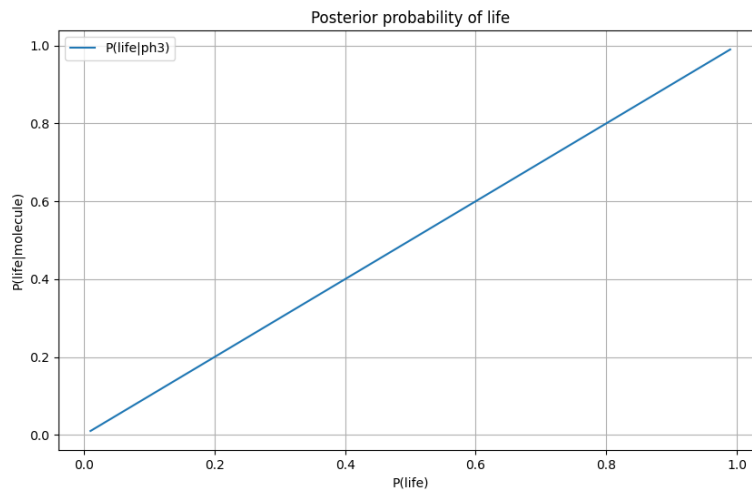


**Figure 3.8:** Posterior probability of life against prior probability  $P(\text{life})$  with no additional context, where now  $P(\text{molecule}|\text{life}) = P(\text{molecule}|\text{nonlife}) = 1$ , we can see that now  $P(\text{life})$  increases linearly with  $P(\text{life})$ .

If now instead we consider the case in which the value of  $P(\text{molecule}|\text{life})$  is bigger than  $P(\text{molecule}|\text{nonlife})$ , choosing for example 0.2 for the former and 0.1



for the latter we obtain a trend that approaches the logarithmic one, as we can see from figure 3.9.

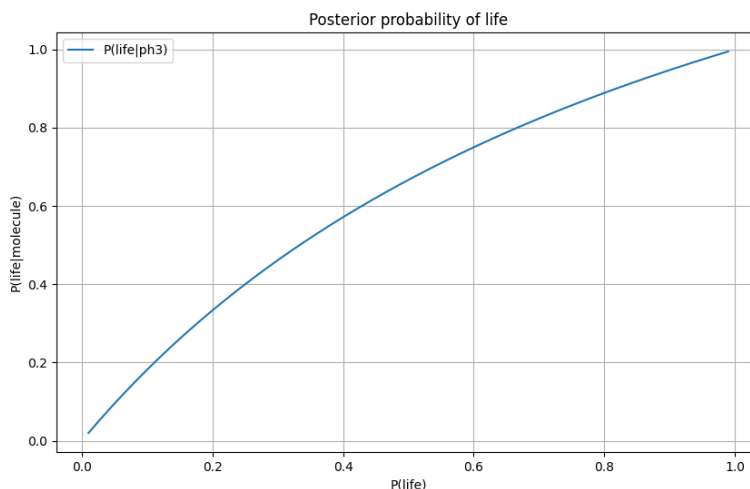


**Figure 3.9:** Posterior probability of life against prior probability  $P(\text{life})$  with no additional context, where now  $P(\text{molecule}|\text{life}) > P(\text{molecule}|\text{nolife})$ , we can see that now  $P(\text{life})$  increases logarithmically with  $P(\text{life})$ .

In both these cases, we reach a high posterior probability only for a very high prior.

As we have previously seen in paragraph 3.1.5, one strategy could be to better constrain all the possible abiotic sources of a molecule, in order to have a very small parameter  $P(\text{molecule}|\text{nolife})$ . In this case we can have a great increase in the posterior probability even if  $P(\text{molecule}|\text{life})$  is low. If we take for example  $P(\text{molecule}|\text{life}) = 0.05$  and  $P(\text{molecule}|\text{nolife}) = 0.001$ , which means that only 1 in 1000 exoplanets will give us a false positive, the posterior probability of life has a much steeper trend as shown in figure 3.10, and is over 0.9 from a prior probability of life of 0.149.

Now let's try again to use the equation 3.18 and a Bernoulli distribution for the likelihood as done in 3.7 and see what happens when we change the parameters. If we try to see the opposite case in respect to 3.4, where now we consider  $P(\text{PH}_3|\text{life}) = 0.2$  and  $P(\text{PH}_3|\text{nolife}) = 0.1$ , so now the likelihood of the presence of life is twice the likelihood of false positive, we can see from 3.11 that the curve all converge towards 1 while approaching observation number 10. If we take  $P(\text{PH}_3|\text{life}) = 0.15$  and  $P(\text{PH}_3|\text{nolife}) = 0.1$  now we can see from fig 3.12 that all the curves except for  $P(\text{life}) = 0.1$  are over 0.9, which means that even with a low prior probability of life

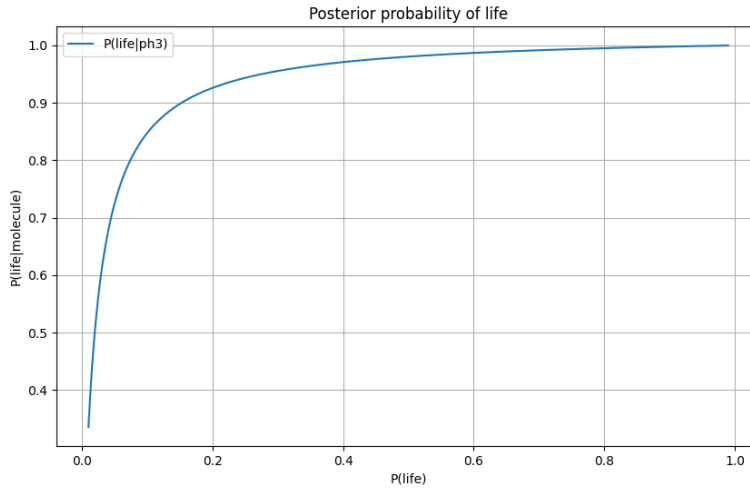


**Figure 3.10:** Posterior probability of life against prior probability  $P(\text{life})$  with no additional context, where now  $P(\text{molecule}|\text{life}) = 0.05$  and  $P(\text{molecule}|\text{no life}) = 0.001$ ,

we can have an high posterior in this case. If now we consider  $P(PH_3|\text{life}) = 0.11$  and  $P(PH_3|\text{no life}) = 0.1$  we can see from figure 3.13 that only the curve with a value of  $P(\text{life}) = 0.9$  and 1 are over **0.95**, which can be consider as The threshold beyond which the presence of life can be considered plausible given the observation of the biomarker. Even if it could be very difficult for a biomarker to have  $P(PH_3|\text{life}) > P(PH_3|\text{no life})$  due to the presence of the always possible unknowns false positives, these cases show that constraining the false positives of a biomarker and/or focusing on developing a theoretical framework that can help us to look for biosignature that lack of false positive should be the optimal strategy for life detection missions.

The situation changes when we consider more observations. As we can see from 3.14 the curves converge to 1 after 70 observation, even in the case of a low prior. This suggests that even with a very pessimistic prior, repeated observations can lead to results that might indicate an high probability of the presence of life.

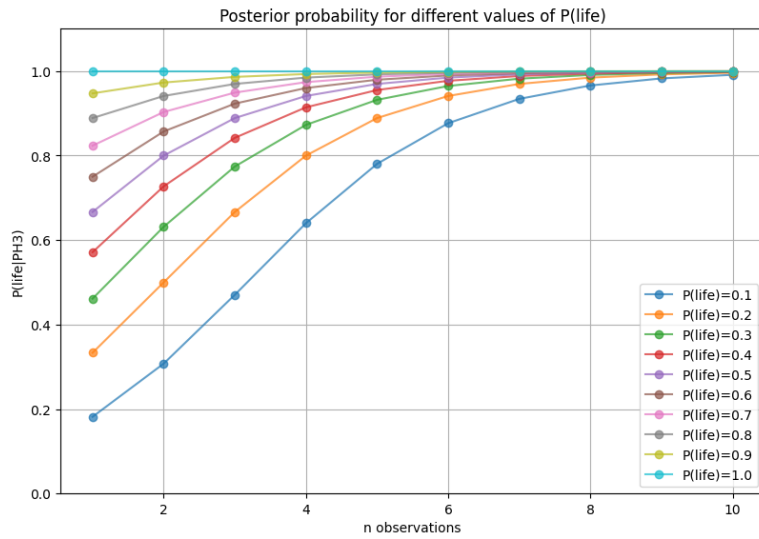


**Figure 3.11:** Posterior probability of life considering a binomial distribution , where now  $P(PH_3|life) = 0.2$  and  $P(PH_3|not\ life) = 0.1$ .

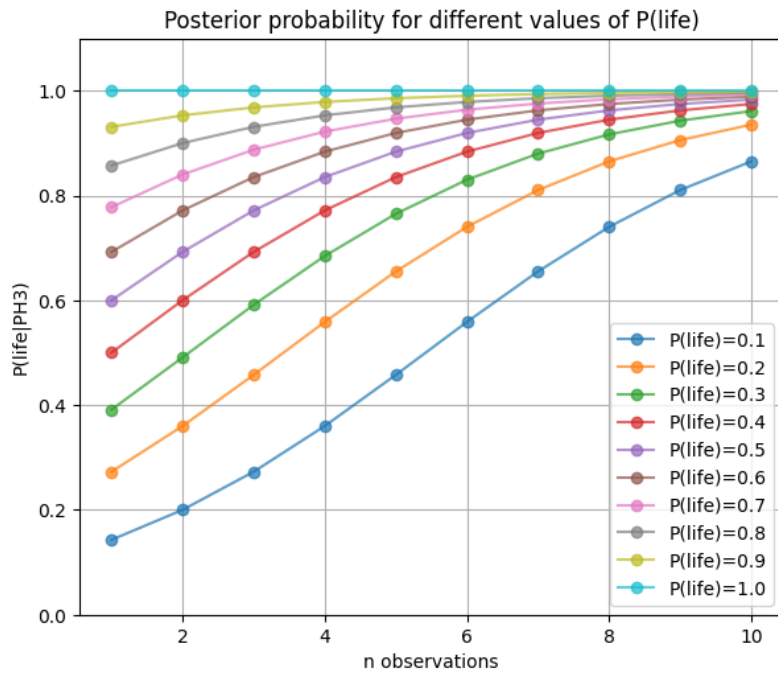


**Figure 3.12:** Posterior probability of life considering a binomial distribution , where now  $P(PH_3|life) = 0.15$  and  $P(PH_3|not\ life) = 0.1$ .

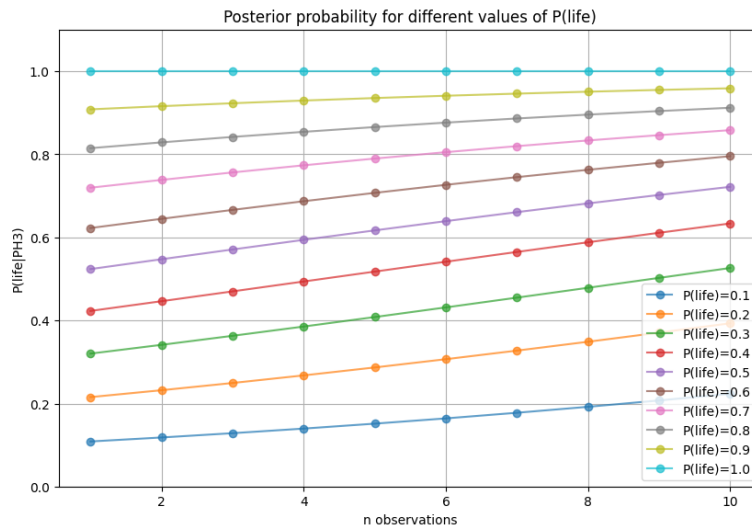


**Figure 3.13:** Posterior probability of life considering a binomial distribution , where now  $P(PH_3|life) = 0.11$  and  $P(PH_3|nolife) = 0.1$ .

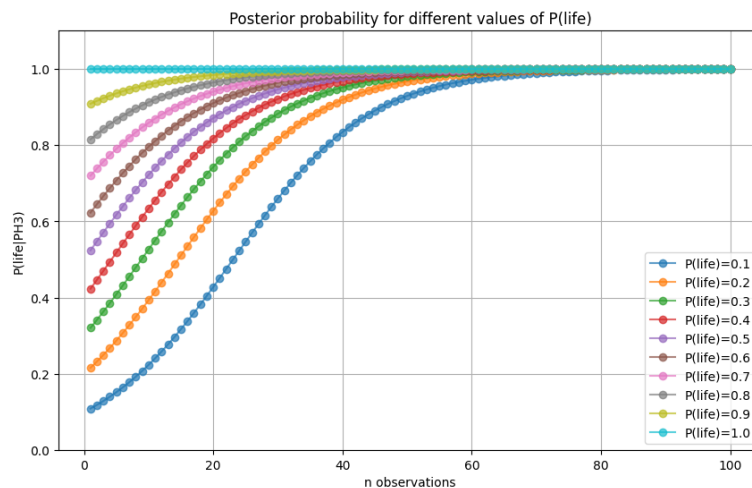


**Figure 3.14:** Posterior probability of life considering a binomial distribution , where now  $P(PH_3|life) = 0.11$  and  $P(PH_3|nolife) = 0.1$  but now we consider 100 observations.

Again all these graph show how the combination of eliminating possible false positives during biomarker discovery , or selecting a biomarker without false positives , along with a large number of observations that build large statistical samples , can lead to obtaining posterior probabilities of high confidence detection.

### 3.2.1 Application to Phosphine case

The goal of this section is to analyze the currents abiotically favored productions of phosphine in Earthly exoplanets to propose the contextual information that can be used to apply the Bayesian model. As we have seen in [82], different possible false positives are considered for phosphine, which are:

1. Phosphine and Phosphate disproportion
2. Lightning
3. Volcanism
4. Exogenous delivery

For what concerns Phosphite and phosphate disproportionation [82] concludes that the formation of  $\text{PH}_3$  is thermodynamically disfavored, and that the formation is unlikely in the absence of a biological catalyst. Nevertheless Phosphine can disproportionate to phosphine at  $T > 323\text{K}$  and acidic pH, raising the possibility that "black smoker" Hydrothermal system ( $T \leq 678\text{K}$   $\text{pH} = 2 - 3$ ) might generate phosphine [82]. Such systems do not dominate volcanic emission on Earth, leading them to propose they would be a negligible contributor on Earth analog worlds. On the other hand, if a world had global, hot, acidic oceans (e.g., due to very high  $\text{pCO}_2$ ), then the theoretical possibility of abiotic phosphine production exists, though likely only in the presence of high  $\text{H}_2$  concentrations, very low pH and within a very hot temperature band [82]. Given that these oceans would be unlikely to have pH values below 4 (carbonic acid has a pH of 3.6) and  $\text{PH}_3$  formation is only favored at pHs closer to 2. From [82] this scenario is considered possible but implausible. So it has to be considered in the model.

For what concerns lightning there are no current kinetically favored reactions that would promote the conversion of the thermodynamically favored phosphate to  $\text{PH}_3$  [82]. So this source can be neglected in the model.

For volcanism, the team [82] has estimated the maximum production of  $\text{PH}_3$  by volcanoes in any planetary scenario; even  $\text{H}_2$  rich atmospheres, is at least seven orders of magnitude lower than the surface fluxes required for detection.

For what concerns exogenous delivery, so the possibility of meteoric delivery as a source of reduces phosphorus species, is also considered negligible from the

calculation of [82]. This calculations are in agreement with previous estimations of the phosphine production through meteoric delivery , which were also found to be negligible [66].

Now let's try to build a model where we apply the contextual information to inference the presence of life given the observation of phosphine. Firstly , since we don't know how life can be possible without the presence of water , let's consider the observation of the presence/absence of it as a contextual information. Secondly let's consider the possibility of presence/absence of hot acid oceans (HAO) that , as we have seen ,could produce abiotically generated phosphine. The parameter of the models are listed in 3.5 and 3.6. The results can be seen in figure 3.15. But we can see that, since we have a case where  $P(\text{molecule} | \text{life}) > P(\text{molecule} | \text{non-life})$ , we obtain slightly increasing results, where, however, only with  $P(\text{life}) = 0.9$  do we reach a posterior probability value higher than **0.95**. As we can see from 3.16, the results stabilise after 10 observations.

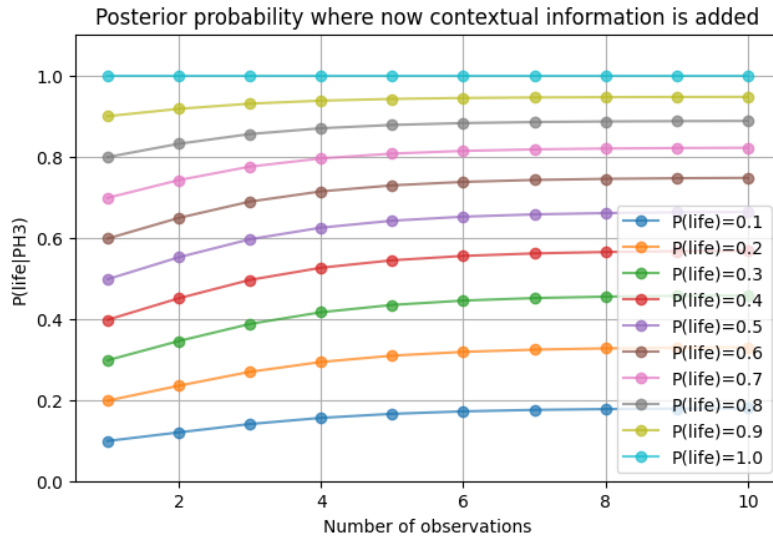
Ci	$P(\text{life}, Ci)$	$P(\text{nolife}, Ci)$
H <sub>2</sub> O, HAO	0.495	$\frac{1-pl}{4}$
no H <sub>2</sub> O, HAO	0.495	$\frac{1-pl}{4}$
H <sub>2</sub> O, no HAO	0.495	$\frac{1-pl}{4}$
no H <sub>2</sub> O, no HAO	0.495	$\frac{1-pl}{4}$

**Table 3.5:** Model parameter, where now contextual information is added.

Ci	$P(\text{PH}_3   \text{life}, Ci)$	$P(\text{PH}_3   \text{nolife}, Ci)$
H <sub>2</sub> O, HAO	0.01	0.09
no H <sub>2</sub> O, HAO	0	0.05
H <sub>2</sub> O, no HAO	0.09	0.01
no H <sub>2</sub> O, no HAO	0	0.05

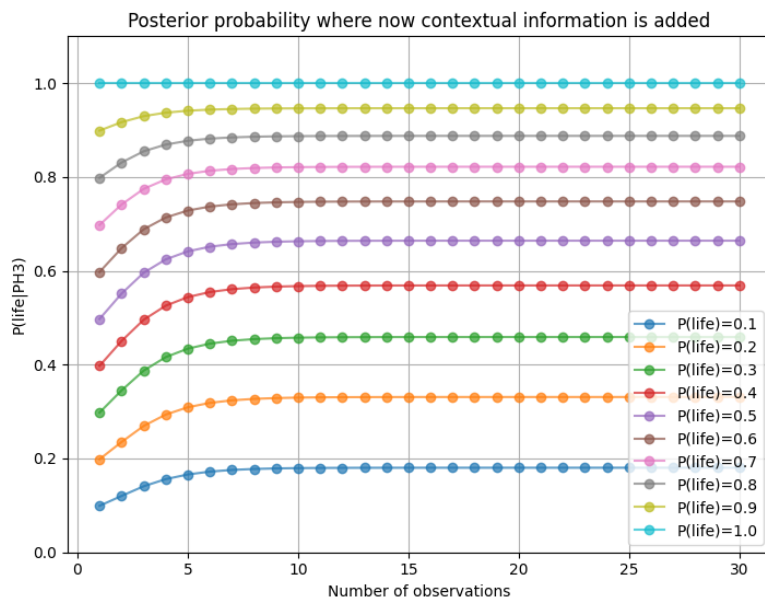
**Table 3.6:** Model parameter, where now contextual information is added.

As outlined by [82] , detection of contextual observables that discriminate between true and false positives will further constrain the posterior probability of life. cases where a given piece of contextual information significantly increases detectability should inform prioritized measurements for future missions. And also any constrain on  $P(\text{life})$  that comes from biology or from statistical analysis of exoplanets data sets can be crucial to narrow the space of probabilities. Knowledge about what environments cannot make life emerge or where it can be sustained is just as important as knowledge about where it can be.



H

**Figure 3.15:** Posterior probability distribution where now contextual information is added.



H

**Figure 3.16:** Posterior probability distribution where now contextual information is added. Where now we considered 30 observations, we can see that the curves stabilise after 10 observations.

This example shows how the knowledge about contextual information added in the Bayesian model can help us to have situations where  $P(\text{molecule}|\text{life}) > P(\text{molecule}|NL)$  and so to have an high confidence detection given by the high posterior probability.

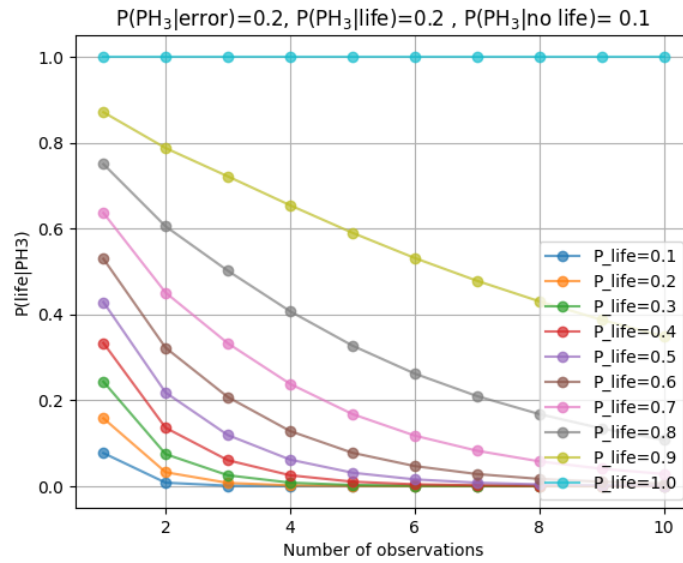
### 3.2.2 Quantifying the error

As we have seen in the previous section , in equation 3.16 , to use a complete model we have to consider and quantify the parameter  $P(PH_3|error)$  which is the likelihood of failure in our detection apparatus and captures the possibility of falsely detecting a positive signal of  $PH_3$  , when there is no  $PH_3$  present, or could correspond to failure to detect  $PH_3$  when it is present. in this section we will see the trend of the plot first considering it as a free parameter and then we will try to see what happens when we try to constrain the value considering the results in [24]. One of the main problem that raised when considering the results of ALMA and JCMT is that there could be a possible contamination by sulphure dioxide  $SO_2$ , and the team calculated that there was a 10% and 2% contamination respectively for JCMT and ALMA observation. This values can be taken for the error when considering the likelihood of failure that captures the possibility of falsely detecting a positive signal of  $PH_3$  when there is no  $PH_3$ . If instead we want to consider the standard deviation  $\sigma$  as as the likelihood of failure , in both cases there is a very robust result: for JCMT and ALMA they claim a  $15\sigma$  confidence interval [24] , which means that the error probability associated with the result is of the order of  $10^{-51}$  which is negligible.

To see how the likelihood of error influences the posterior probability i performed the computation varying the parameters. The results can be seen in 3.17, 3.18, 3.19. As we can see from 3.17 , the situation in very similar with 3.7, that has the same values for the parameter but lacks of the error term. So again, since we have  $P(\text{molecule}|\text{life}) \ll P(\text{molecule}|\text{nonlife})$  the posterior probability decreases rapidly with increasing observations and the likelihood of error doesn't change much the results.

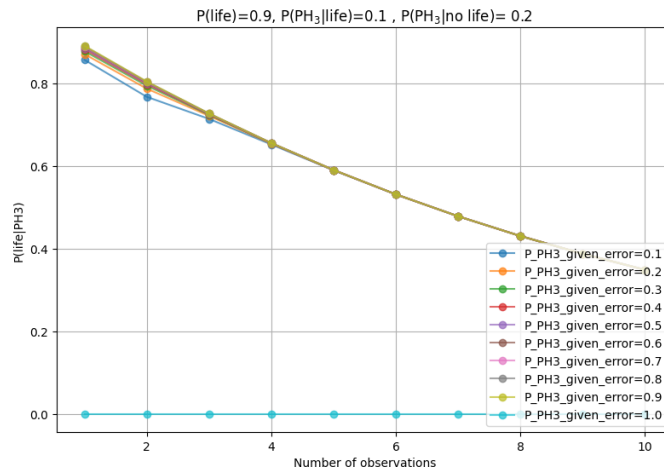
In 3.18 and 3.19, the fact that the plots with different values of likelihood error shows almost overlapping curves indicates that the likelihood error parameter has little influence on the final result, and this in consistent with the sensitivity analysis performed later in the text.





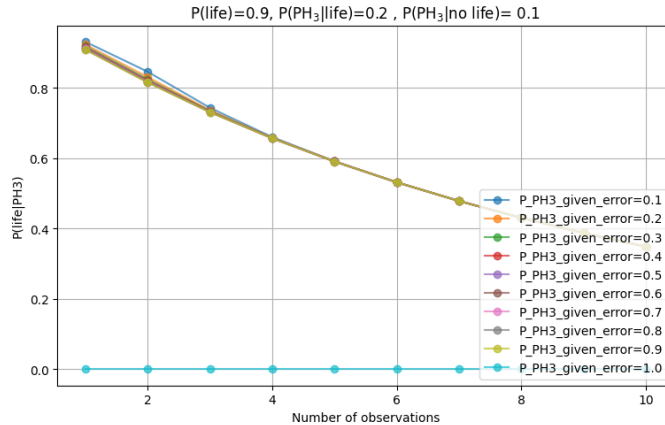
H

**Figure 3.17:** Posterior probability of life , with  $P(PH_3|error) = 0.2$  for different values of the prior.



H

**Figure 3.18:** Posterior probability of life , with different values for  $P(PH_3|error)$  and  $P(life) = 0.9$



H

**Figure 3.19:** Posterior probability of life , with different values for  $P(PH_3|error)$  and  $P(life) = 0.9$

### 3.3 Sensitivity analysis

The aim of sensitivity analysis in general is to determine how sensitive the output of a model is, with respect to the elements of the model which are subject to uncertainty or variability. As outlined by [75] , this is useful as a guiding tool when the model is under development as well as to understand model behaviour when it is used for prediction or for decision support. In [64] It has been performed an sensitivity analysis on the bayesian model in order to provide a first quantitative framework that evaluates the uncertainty of in situ biogenic assessments using recursive Bayesian statistics. Their results show that detecting more than seven potential biosignatures does not increase the reliability of biogenic assessments unless the probability of detection of biosignatures in the sample and the probability of the biosignature being false positive are well constrained. So their work focus on the need for quantitative support of biogenic assessments and astrobiology strategies in general. Even if their analyses is applied to in situ biogenic assessment , the model can be modified to apply the same to the biogenic assessment for gaseous biomarkers. The team also postulates that the potential biosignatures may be ranked according to three criteria:

1. Reliability (the probability of a biosignature to be produced by life)
2. their detectability (the likelihood that a biosignature can be observed or measured)
3. Their survivability(their ability to be preserved in the geological record)

For the case of gaseous biomarkers detected from a telescope on Earth, we can not of course consider the third one, but we can still use the other 2 to classify them. In the study [64] they have done a sensitivity analysis on the recursive Bayesian equation , which is:

$$P(\text{biogenic} \mid \text{signature}, C)_n = \frac{P(\text{signature} \mid C, \text{biogenic})_i \cdot P(\text{biogenic} \mid C)_{n-1}}{P(\text{signature} \mid C, \text{biogenic})_i \cdot P(\text{biogenic} \mid C)_{n-1} + P(\text{signature} \mid C, \text{abiogenic})_i \cdot (1 - P(\text{biogenic} \mid C)_{n-1})} \quad (3.19)$$

Where  $n \geq 1$  is the number of signatures detected in the sample, and  $i$  ( $1 \leq i \leq n$ ) is the  $i$ th signature. As outlined by [64], the sensitivity analysis may have various objectives, and this should be specified beforehand. these can include:

1. Identify and prioritise the most influential inputs
2. Identify non-influential inputs in order to simplify a model
3. calibrate model inputs using the information that is known on the model

In my case , as in [64], it is to identify and prioritise the most influential inputs. Since in the model considered by them there are only three different parameters , it is possible to choose a sensitivity analysis method that has an high computational cost, so they choose the Sobol indices. The Sobol indices ,also called variance-based sensitivity analysis , decompose the variance of a model output into fractions that can be attributed to the variance of the model inputs. There are different types of Sobol indices, in this study they use the first. The first order Sobol sensitivity index accounts for the proportion of variance of a model output explained by changing each variable alone while marginalizing over the rest , and are computed as follows:

$$S_i = V \left[ \frac{\varepsilon[Y|Q_i]}{V(Y)} \right] \quad (3.20)$$

where  $S_i$  is the first order Sobol index for the  $i$ th parameter ,  $V[\varepsilon[Y|Q_i]]$  is the conditional variance of the expected model output  $Y$  when the parameter  $Q_i$  is fixed, and  $V(Y)$  is the total variance of the response. The higher the first order index is, the more influential the variable is. The Sobol method allocate the output variance to each inputs variance, but it also evaluates the interactions between the model inputs. Performing the Sobol method requires the model inputs to be independent and non-correlated, and the model to be deterministic.[64] In [64] the first order

method has been computed following the Monte Carlo method described in (monod et al.2006) and implemented in the 'sobolSalt' function of the R 'sensitivity package. The indices were computed along fifteen biosignatures ( $n = 15$ ) as beyond fifteen Bayesian inferences the results from the sensitivity analysis stabilises. Following the (monod et al. 2006) procedure , the indices were estimated using  $m = 1.000000$  combinations of  $p = 3$  variables uniformly and randomly distributed on  $[0;1]$  and for a total cost of  $m * (2p^2 + 2) = 15.000000$  model evaluations.The results of the analysis is showed in 3.20.

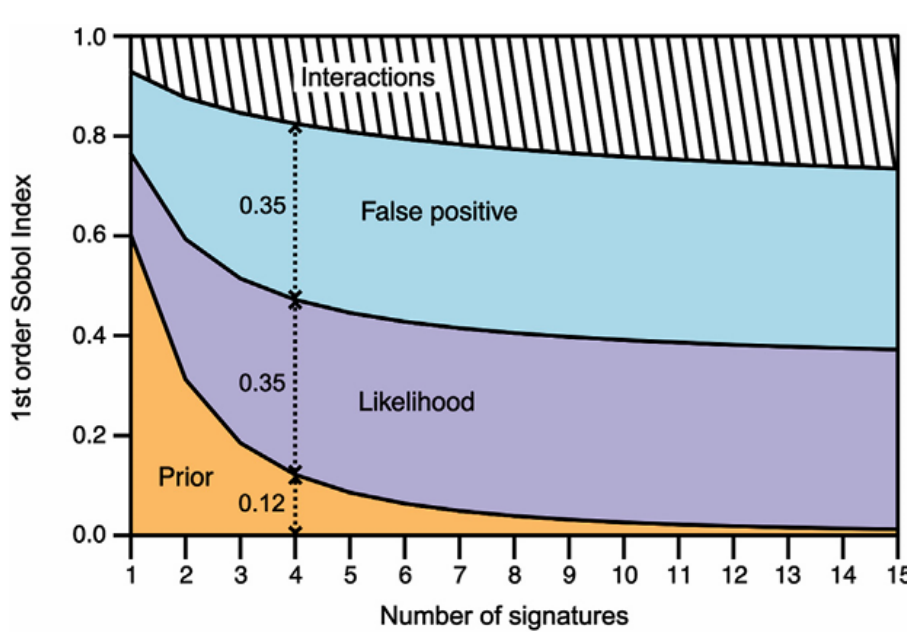


**Figure 3.20:** The Sobol' index values of each variable are given by the vertical extent of the colored fields. For example, for  $n = 4$ , the prior probability has a first Sobol' index value of 0.12, whereas the likelihood and false positive variables have first Sobol' index values of 0.35 each. In other words,when detecting four potential biosignatures, the uncertainty of the prior is responsible for 12% the uncertainty of the biogenic assessment, whereas the uncertainty of the likelihood and false positive are distinctively responsible for 35% of the final assessment's uncertainty

### 3.3.1 application of the sensitivity analysis to the model

to begin with , i performed the sensitivity analysis on equation , 3.19, as did by [64]. Nevertheless I followed a slightly different approach. I used the Salib module in python ,and applied the procedure used by [64]. Salib is and open source library for performing sensitivity analyses. It provides a decoupled workflow, meaning it

does not directly interface with the mathematical or computational model. Instead, Salib is responsible for generating the model inputs, using the **sample** functions, and computing the sensitivity indices from the model outputs, using one of the **analyze** functions. A typical sensitivity analysis using Salib follows 4 steps:

1. Determine the model inputs and their sample range
2. Run the **sample** function to generate the model inputs
3. Evaluate the model using the generated inputs, saving the model inputs
4. Run the **analyze** function on the outputs to compute the sensitivity indices

The program uses the application of the Bayesian model as used in [13] and the application of the Monte Carlo simulation for the computation of the Sobol indices used in [75]. The structure of the program used to perform the analysis is the following:

- The program generates 2 matrix N rows and 3 columns, with N number of sampling.
- the Bayes recursive formula is written using a method used by [13]
- Computes the Sobol indices using the formulas reported in [75]

I've chosen a number of samples of  $m = 2^{17} = 131072$  and  $p = 3$  so it has a total cost of  $m * (2p^2 + 2) = 2621440$ . My result is showed in 3.21. I used this value of m because Salib uses only sampling values that can be written as  $2^N$ .

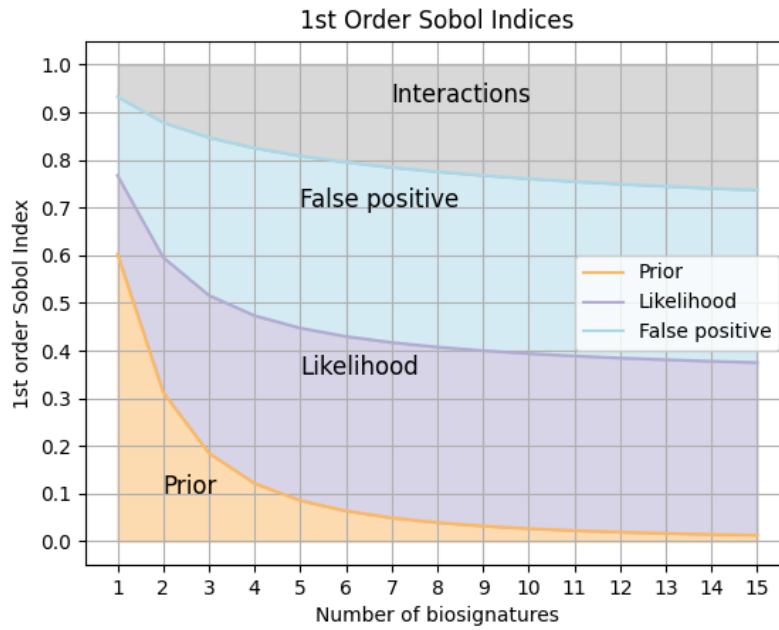


**Figure 3.21:** Sobol indices of recursive Bayes model using SALib.

What I have obtained is showed in 3.7.

number of biosignatures	$P(\text{signature} \text{biogenic})$	$P(\text{signature} \text{abiogenic})$	$P(\text{life})$
n=1	0.16	0.16	0.60
n=4	0.35	0.35	0.12
n=7	0.37	0.37	0.05

**Table 3.7:** Results for sensitivity analysis of the recursive Bayes formula with  $m = 2^{17} = 131072$  and  $p = 3$ , at different number of biosignatures.

The I applied the same sensitivity analysis to the Bayesian equation that includes the likelihood of the error, eq. 3.16. This help us to see the influence on adding the error term in the Bayesian model.

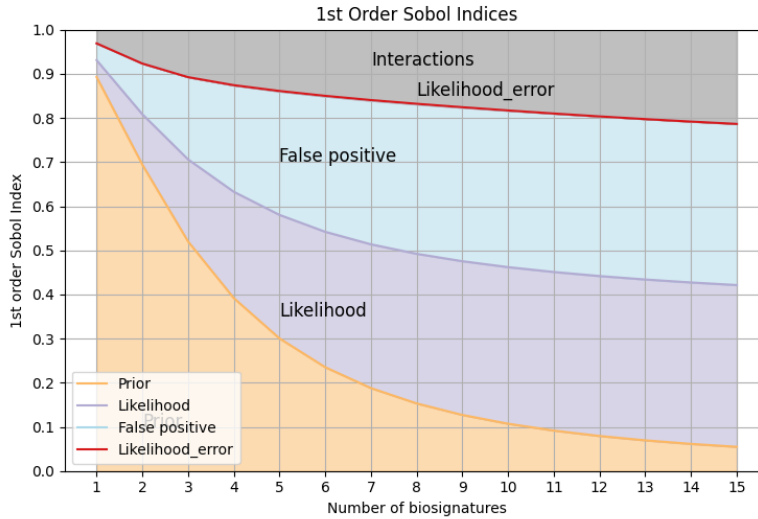


**Figure 3.22:** Sobol indices of Bayes formula including the error, using SALib.

Number of Biosignatures	$P(\text{signature} \text{biogenic})$	$P(\text{signature} \text{abiogenic})$	$P(\text{life})$	$P(\text{molecule} \text{error})$
$n = 1$	0.38	0.38	0.89	0.0001
$n = 4$	0.24	0.24	0.39	-0.0005
$n = 7$	0.32	0.32	0.18	$9.7 \times 10^{-5}$
$n = 15$	0.37	0.37	0.05	0.0007

**Table 3.8:** Results for sensitivity analysis of the recursive Bayes formula, considering the likelihood of error, with  $m = 2^{17} = 131072$  and  $p = 4$ , at different numbers of biosignatures.

As we can see when we are considering eq.3.19 the results show that 60% of the uncertainty of biogenic assessment based on a single potential biosignature is due to the uncertainty of the prior. With the detection of new biosignatures we can see that the effect of the prior decreases, from 12% at 4 biosignatures to 5% at 7 biosignatures. So we can conclude, as done in [64] that after 7 detected biosignatures, the effect of the prior on the final biogenic assessment becomes negligible. These findings align with recursive Bayesian inference, which aims to update the prior belief in a hypothesis as new data is collected, reducing its influence on the final outcome. Therefore, this result indicates that the Sobol' method is consistent with the model expressed by the equation 3.19. As we can see, for four biosignatures detected the likelihoods are equally responsible for the 35% of the biogenic assessment's uncertainty. So knowing the exact probability of a potential biosignature to occur in a biogenic sample and to be a false positive would increase the reliability of biogenic assessment's by nearly 70%. When considering the equation where now the error term is added, as we can see from 3.8 the influence of the prior on the uncertainty

becomes negligible only after 15 biosignatures detected. This can make difficult the analysis where the likelihood of an error is not negligible. Nevertheless, as we can see from the figure 3.22 the likelihood of the error has no influence on the uncertainty of the results even for only 1 biosignature detected.

Since in the analysis we are considering a uniform prior, which is uninformative, future investigations may perform a sensitivity analysis on the prior in order to choose a prior that is more informative and closer to realistic situations when looking for extra terrestrial life, as noted by [64].

### 3.3.2 Search Strategies Based on Bayesian Approach

As we have seen, the fact that  $P(life)$  is poorly constrained can become less important if we are able to detect more than 15 biosignatures. As outlined by [54], there are two strategies that can be employed in the development of future missions to search for life:

- to maximize our confidence in  $P(data|life)$
- the second is to maximize our confidence in  $P(data|abiotic)$

Having confidence in these terms, together with knowledge of  $P(life)$ , can inform mission design. This is, in fact, the strongest advantage of a well-developed Bayesian framework: it can quantitatively inform observational strategies.

Clearly, the best way to constrain  $P(data|abiotic)$  is to conduct large statistical surveys of uninhabited worlds. The advantage of a statistical approach to life detection is that it allows for the combination of a range of observations, including integrating over time and sampling large statistical datasets. This can help to constrain the three parameters of the Bayesian framework, as outlined in [54].

In [54], another toy model has been developed that shows important statistical aspects of the Bayesian approach.

In this case, it has been assumed that the number of inhabited worlds is Poisson distributed, rather than uniformly distributed as in the previous toy model. For a sample of exoplanets of size  $N$ , the probability of life arising  $k$  times is:

$$P_{\text{Poisson}}(k, \lambda, N) = \exp(-\lambda N) \times \frac{(\lambda N)^k}{k!} \quad (3.21)$$



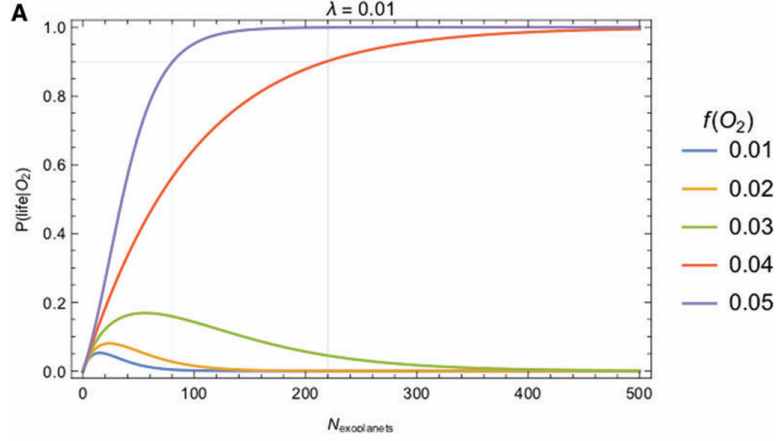


**Figure 3.23:** The posterior probability of life assuming a fraction  $f(O_2)$  of the  $N_{exoplanets}$  observed have detectable levels of atmospheric  $O_2$ . Plot from [54]

where  $\lambda$  is the probability per planet of life developing. The probability to have no life in a sample of  $N$  worlds is then:

$$P(\text{no life}) = P_{\text{Poisson}}(0, \lambda, N) = \exp(-\lambda N) \quad (3.22)$$

with:

$$P(\text{life}) = 1 - \exp(-\lambda N) \quad (3.23)$$

In [54], they assume life is detectable when  $O_2$  is observed, but also that life is rare.  $P(O_2|\text{life}) > P(O_2|\text{no life})$ , with  $P(O_2|\text{life}) = 0.1$  and  $P(O_2|\text{no life}) = 0.01$ . Let's consider two different cases:

1. Life occurs on 1 in 100 worlds ( $\lambda = 0.01$ )
2. Life occurs on 1 in 1000 worlds ( $\lambda = 0.001$ )

For both, they calculate the posterior probability of life assuming the fraction  $f(O_2)$  of the total number of exoplanets observed ( $N_{exoplanets}$ ) have detectable  $O_2$ . In the figure, the trend for  $P(\text{life}|PH_3)$  is shown for different measurement distributions with different percentages of worlds having detectable atmospheric  $PH_3$ .

When the percentage of observed planets with  $PH_3$  is low, 1%, our posterior probability for life approaches zero as additional data are accumulated. However, if the percentage of observed planets with  $PH_3$  is much higher than our expectation for an ensemble of exoplanets with no life, then our confidence in the hypothesis of

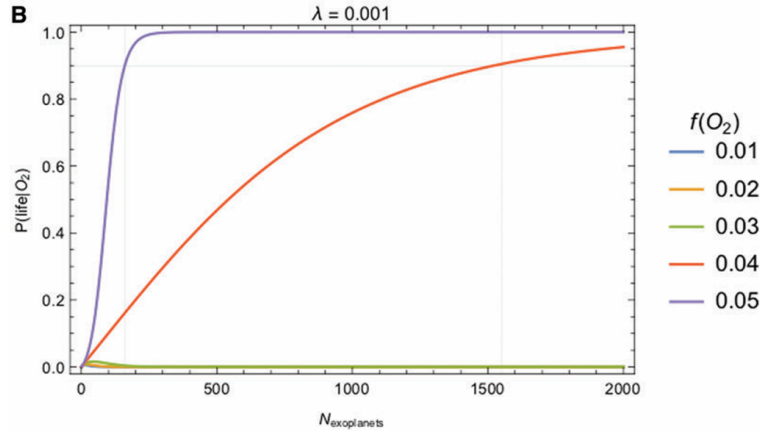


**Figure 3.24:** The posterior probability of life assuming a fraction  $f(O_2)$  of the  $N_{exoplanets}$  observed have detectable levels of atmospheric  $O_2$ . Plot from [54]

life as the correct explanation for the data increases with our number of samples at a rate determined by the rarity of our prior.

As the sample size increases, it becomes increasingly unlikely that the abiotic distribution of uninhabited worlds with  $PH_3$  atmospheres will deviate significantly from the expected value of 1%. In large samples of observations, deviations from the expected abiotic value, therefore, lend support to the hypothesis that life is generating  $PH_3$  on a fraction of the worlds.

This model shows how the unknown value  $P(\text{life})$  can be critical to determining the most effective search strategy. Depending on the value of  $P(\text{life})$ , different strategies could be followed. If  $P(\text{life}) \gg 0$ , it may make sense to target individual worlds and obtain high-resolution spectra. If instead  $P(\text{life})$  is very low, it could be better to take more lower-resolution spectra of more worlds to generate better statistics, as outlined in [54].

### 3.4 critical aspects of the Bayesian approach to astrobiology

In [63] many critical aspects regarding various topics of biosignature are analyzed, and also the Bayesian approach to life detection. To understand the reasoning made by Smith and Mathis, I present the example they gave:

### The two observers example

Suppose Observer A claims to have detected  $O_2$  and  $CH_4$  in an Earth-like atmosphere and, for this reason, argues that their posterior probability  $P(L|D)$  is sufficiently high to justify the hypothesis that life is present on that planet. Observer B, on the other hand, has observed a random spectral signature from a random planet and also claims to have a  $P(L|D)$  that justifies the hypothesis of the presence of life. Observer A criticizes B's results, arguing that there is no model to justify the correspondence between the spectral signature detected and the possible presence of life. B responds that they can simply invent a new alien metabolism that produces what they have observed and create a new geological cycling that allows for that metabolism. A replies that this metabolism and cycling are not based on any known metabolism or cycling, so their model will surely have a lower value of  $P(L|D)$ . B counters that there is no parameter in the Bayesian framework that would lower the probability based on this argument. They argue that it is included in the parameter  $P(L)$ , which is not constrained at present, and therefore, their  $P(L|D)$  will not be lower due to the lack of an existing metabolism that justifies their observations with the presence of life.

The problem that arises from this example is that  $P(D|L)$  is completely determined by whatever model you choose to use to represent your abiotic scenario and your biotic scenario, with no way to account for how "realistic" those are. So the greatest problem seems to be that the only factor really determining  $P(L|D)$  would be  $P(L)$ , which is unconstrained and strictly depends on our theory of life which is based only on 1 example. When comparing the model A and B we recognize only intuitively that A is "more likely" but in fact there is no way to rigorously assign any different certainty to either. The author criticizes the fact that without a complete theory of the living systems, the prior probability of life in any particular environment remains unconstrained both numerically and conceptually. It seems that the probability of a biological explanation given the data is completely dependent on an unconstrained variable. While this is in fact true, as we have seen the study of the Bayesian framework can help us to understand how the different parameters influence our posterior probability of life and so it can help us to decide the strategy to follow in order to maximize the probability to find biospheres. As we have seen,

when Kepler started the observatory campaign , it has been decided to focus on scanning many stellar systems since the probability  $P(\text{planet})$  was not constrained, so it was not known if and how many star systems had planets.

Now let's examine another important example that comes from [45]:

#### the biased coin example

suppose we have two coins. One is a fair coin with a side for heads and a side for tails, while the other is a biased coin where both sides are tails. We pick one of the coin without knowing which one we have chosen. So we want to know it by flipping it and reveal which one we picked. The results can be head or tails , but because we are uncertain about which coin we have , the probabilities are conditional on the likelihood you have selected either coin: a tail result from the fair coin with chance  $P(T|F)$  , a heads result from the fair coin  $P(H|F)$  , a tails result from the biased coin  $P(T|B)$  , and a heads result from the biased coin  $P(H|B)$ . Let's say we observe tails when we flip it. What can we infer from this? to find the answer we use the Bayes theorem,  $P(F|T) = \frac{P(T|F)P(F)}{P(T)}$ . By definition  $P(T|F) = 0.5$ ,  $P(F) = 0.5$ . The denominator can be decomposed in conditional probabilities for getting tails from either coin:  $P(T) = P(T|B)P(B) + P(T|F)P(F)$ ,  $P(T) = (1 * 0.5) + (0.5 * 0.5) = 0.75$  , using the Bayesian equation you get  $P(F|T) = 0.5 * 0.5 / 0.75 = 0.33$  , which means that if you flip a coin and observe tails , you can have a confidence of approximately 33% chance you have picked up the fair coin. Nevertheless , if you had observed heads you know with 100% confidence you have the fair coin in hand

The problem of discerning between the fact that we have in hand a fair coin or a biased coin , as suggested by [45] can be analogized to the problem of detecting life, where we want to determine whether we have observed a planet that has a biosphere or does not. All the ambiguity arise because we don't have enough data to assign a higher likelihood to one of our hypotheses over the other.

The major issue with biosignature susceptible to false positives is that they are not based on a robust theory distinguishing life from non-life, making it impossible to determine if all potential abiotic mechanism have been accounted for. Every time we detect a potential biosignature on a planet , we must first understand the abiotic formation pathways before we can assess the likelihood of a biological origin. As

we've seen, for most current biosignature candidates, conducting an exhaustive search for all possible abiotic formation mechanisms is not feasible, either because these mechanisms are not fully understood, or because there is insufficient knowledge about the planetary environment to constrain them completely.

As suggested by [45], the example with biosignatures is in direct analogy to the "tails" result, where the inhabited planets is analog to the biased coin (always produces tail is analogous to always produces an atmosphere containing the gaseous biosignature), and uninhabited worlds to the unbiased coin (sometimes produces tails is analogous to sometimes produces the atmosphere containing the biosignature). So if, instead of testing the hypothesis "I have the biased coin", we want to test the hypothesis that "this planet has a biosphere".

The equation now can be written as:

$$P(\text{life}|\text{obs}) = \frac{P(\text{obs}|\text{life})P(\text{life})}{P(\text{obs}|\text{life})P(\text{life}) + P(\text{obs}|NL)P(NL)} \quad (3.24)$$

which is the same considered in the previous sections. If  $P(\text{Obs}|NL)$ , the probability of false positive is zero, then the posterior probability is one, independent of the prior probability of life,  $P(\text{life})$ . This aspect is the key point of the example.

If there are any false positives associated with our biosignature, we need strong priors that life is responsible for producing the signature. Nevertheless, if we know with certainty that a specific observation can only arise from living systems, regardless of the context, we do not need to consider the prior probability of life emerging in an alien environment, since the observation would suffice to claim life detection.

The coin analogy teaches us an important lesson: when we have false positives it is required a well supported prior hypothesis explaining why life should be expected in a particular environment. This holds true even when contextual information reduces the likelihood of false positives to a minimal value. If false positives are not entirely ruled out, this problem persists. The alternative is that life detection should rely on biosignatures that are not susceptible to false positives (similar to the coin always landing on heads).

So this example shows us that the high confidence in detection claims using the Bayesian hypothesis testing requires:

1. A strong prior hypothesis on the existence of life in a given alien environment when we have false positives for the observation

2. Biosignatures that lack of false positives

### 3.5 Signal detection theory

In this chapter i present the results and equation as shown in [78]. Signal detection theory is a conceptual framework which provides a precise language for decision making under certain conditions. It come from psychology and the military, since it was applied in the world war 2 to interpret radar signals. It has been applied in many fields like: medicine , telecommunications and artificial intelligence. In signal detection theory it is assumed that there is a stimulus that , if present , elicits response. For life detection , the presence of life (L) is the stimulus and the presence of a biosignature (B) is a response to this stimulus. Each outcome is summarized in table 1.

TABLE 1. RELATION BETWEEN STIMULUS (LIFE) AND RESPONSE (BIOSIGNATURE) IN SIGNAL DETECTION THEORY

	<i>Stimulus (Life) present</i>	<i>Stimulus absent (no Life)</i>
Reaction (biosignature) present	True positive Biosignature present if there is life Probability $P(B L)$	False positive (error I) Biosignature present if no life Probability $P(B \sim L)$
Reaction (biosignature) absent	False Negative (error II) No biosignature if there is life Probability $P(\sim B L)$	True negative No biosignature if no life Probability $P(\sim B \sim L)$

Figure 3.25: taken from [78]

$P(B|L)$  is the probability of the biosignatures being present, given that life is present.  $P(\neg B|L)$  is the probability of B being absent if life is present. These two are not independent. Therefore their sum must be equal to 1. [78] In the same way  $P(B|\neg L)$  and  $P(\neg B|\neg L)$  are complementary event. Different pair of conditional probabilities can be chosen to characterize outcomes. If we are looking for true and

false discovery rates ,  $P(B|L)$  and  $P(B|\neg L)$  should be considered. The former can be interpreted as the signal and the latter as the noise. If we want to understand errors due to false positives and false negatives , the appropriate pair of probabilities is  $P(\neg B|L)$  and  $P(B|\neg L)$ . A perfect ideal biosignature has the probabilities of both false positives and false negatives equal to zero. All other biosignature can be evaluated with respect to this ideal. An index used for this purpose is the Youden's J statistics. J is defined as:

$$J = P(B|L) + P(\neg B|\neg L) - 1 \quad (3.25)$$

the equation can be rewritten in terms of true and false positives:

$$J = P(B|L) - P(B|\neg L) \quad (3.26)$$

it changes in the range between -1 and 1. In general J is a measure of the distance from perfect biosignatures. The closer the index is to 1 the more likely it is that finding B means that life is present. [78] The equation can also be expressed in terms of false positives and false negatives.

$$J = 1 - [P(B|\neg L) + P(\neg B|L)] \quad (3.27)$$

it is also possible to place more emphasis on either false positive or false negatives , introducing a parameter  $\alpha$  and redefine J:

$$J = 1 - [\alpha P(B | \neg L) + (1 - \alpha)P(\neg B | L)] \quad (3.28)$$

large value of  $\alpha$  (close to 1) correspond to avoiding false positives and small values are used if the goal is to avoid false negatives. So this parameter can be considered the "mission objectives parameter". If several missions to a given target are considered, the goal of the initial mission might be to establish whether this target is worth further exploration in search for life. Then, it might be desirable to set  $\alpha$  to a small value, not to overlook possible, though not definitive, signs of life. Along with J there is another parameter that can be used: a measure of signal/noise ratio ,  $K(B)$  , defined as:

$$K(B) = \frac{P(B|L)}{P(B|\neg L)} \quad (3.29)$$

used together with  $J$  it can be used to ascertain utility of a biosignature for detecting life. Even if  $J$  and  $K(B)$  are different, they are monotonically related, which means that they will give the same ranking of biosignatures. This parameter also connects SDT with Bayesian hypothesis testing formalism.

### 3.5.1 Bayesian Hypothesis testing

As we have seen, in the Bayesian framework we are interested in the conditional probability  $P(L|B)$  that life is present if biosignature  $B$  is present and has been found. This is a posterior probability. Instead, in SDT we are interested in  $P(B|L)$ , which is a likelihood. As shown in [78], the two methods don't lead to different evaluations of biosignature. As we have seen before, Bayes' theorem tells us that:

$$P(L|B) = \frac{P(B|L)P(L)}{P(B)} \quad (3.30)$$

In an analogous way, this probability can be expressed as:

$$P(\neg L|B) = \frac{P(B|\neg L)P(\neg L)}{P(B)} \quad (3.31)$$

$P(\neg L)$  is the prior probability that there is no life. We can now consider the ratio  $R_{LB}$  of the posterior probabilities:

$$R_{LB} = \frac{P(L|B)}{P(\neg L|B)} = \frac{P(B|L)P(L)}{P(B|\neg L)P(\neg L)} = K(B) \frac{P(L)}{P(\neg L)} \quad (3.32)$$

This is the relative probability of the hypothesis that life is present compared to the hypothesis that life is absent, both evaluated assuming the presence of biosignature  $B$ . If  $R_{LB}$  is less than 1, it means that the presence of  $B$  does not give us high confidence in the presence of life, as  $B$  is likely to be of abiotic origin. If  $R_{LB}$  is larger than 1, it is more likely than not that life is present if  $B$  is present. In statistics, it is usually required that  $R_{LB} \geq 20$ . The problem with this equation is that it depends also on prior belief about the probability that life is present at the target, and this is not constrained at all so it can vary widely. If we were able to obtain a big variety of data,  $P(B|L)$  would be sufficiently big to overcome prior belief, even if it disagreed with evidence. In life detection, obtaining such data could be impossible. If we instead compare two biosignatures, there are no more problems regarding the



influence of the prior. As shown in [78], considering another biosignature  $B'$ , one can define the ratio  $R_{LB}$  for  $B'$ :

$$R_{LB'} = K(B') \frac{P(L)}{P(\neg L)} \quad (3.33)$$

Then the ratio

$$\frac{R_{LB}}{R_{LB'}} = \frac{K(B)}{K(B')} \quad (3.34)$$

is independent of the prior and depends only on the Bayes factors for  $B$  and  $B'$ . If  $K(B)$  is larger than  $K(B')$ ,  $B$  can be considered a better diagnostic biosignature than  $B'$ . As pointed out in [78], we would reach the same conclusion if we used the equation for  $K(B)$  derived with SDT, so the ranking of biosignatures obtained from SDT and Bayesian hypothesis testing should be the same.

### 3.5.2 possible application of SDT and BHT to gaseous biomarkers

As we have seen we can use the signal detection theory method combined with the Bayesian hypothesis testing in order to build a framework that can guide our biomarkers detection, i.e. our inference on the probability of life, and also to guide our observation strategy when we have to confront different the quality of different biomarkers. In practice i propose to use the following equations to classify the biomarkers and to confront them:

$$J = P(B|L) - P(B|\neg L) \quad (3.35)$$

$$K(B) = \frac{P(B|L)}{P(B|\neg L)} \quad (3.36)$$

$$R_{LB'} = K(B') \frac{P(L)}{P(\neg L)} \quad (3.37)$$

$$\frac{R_{LB}}{R_{LB'}} = \frac{K(B)}{K(B')} \quad (3.38)$$

Here i propose a method to classify the biomarkers considering equation 3.35 and 3.36: When studying a given habitable exoplanet, considering the information we have acquired, we will consider the number of possible biotic productions that can occur, referring to the existing knowledge regarding the biomarker in question and the number of known false positives that can generate the molecule. Through these, we will construct our  $P(B|L)$  and  $P(B|\neg L)$ . Using these two values, we classify the biomarker based on the indices  $J$  and  $K(B)$ .

## 3.6 Ladders for life detection

Since we don't have an universal accepted method for reporting high detection findings about life detection, every claim of finding of exolife will always remain ambiguous. One tempting of a standardized method has come in the forms of ladders.

One such scale is the Confidence of Life Detection (CoLD) scale [25]. This scale, illustrated in 3.9, is structured around a sequence of evidence thresholds that must be met before a life detection claim can be substantiated. Another framework, developed through a community-wide effort, is the 3.10. This scale proposes five criteria for assessing life detection claims, categorized into two groups.

The level 1 criteria are common to every field of planetary science and not just astrobiology. Even if these ladders can be useful, they present some problems, as pointed out by [45]:

- These scale based approaches separate assessment of the life hypothesis from the assessment of abiotic explanations, but as we have seen they are not independent. Assessing a signal that is known to be produced by both living and non-living systems also depends on the prior probability of life existing in a given environment. This poses a challenge because evaluating the strength of a biosignature requires robust theoretical support, which is not explicitly addressed in the scale format. Consequently, any assessment of the prior probability of life will be largely theoretical rather than empirical.
- they make an explicit assumption that any life detection will always be subject to false positives.

The main problems when considering the advancements in the theory of life connected to astrobiology, such as the "life detection knowledge database" (LDK), is that the works that are used to motivate each argument are themselves not translated into probabilistic statements. As pointed out in [45], the LKD could serve as a point of organization in aggregating the data and models needed to quantitatively evaluate biosignatures, which can provide estimates for  $P(data|life)$  and  $P(data|NL)$ . So what is needed in the field right now is a connected work between the field of life sciences, and biosignature science, to construct a common framework, based on Bayesian methodology, for Life detection in astrobiology.

CoLD scale level	Corresponding Measurement Indicator
Level 1	Detection of a signal known to result from a biological activity
Level 2	Contamination ruled out
Level 3	Demonstration or prediction of biological production of signal in the environment of detection
Level 4	All known non-biological sources of signal shown to be implausible in that environment
Level 5	Additional, independent signal from biology detected
Level 6	Future observations that rule out alternative hypotheses proposed after original announcement
Level 7	Independent, follow-up observations of predicted biological behavior in the environment

**Table 3.9:** CoLD, Confidence of Life Detection scale proposed by [25]

Level	Standards of Evidence Criteria	Question
Level 1	1	Have you identified the signal of interest?
	2	What confidence do you have in the source, strengths, and possible confounding factors in the data analysis?
Level 2	3	Have you ruled out abiotic explanations?
	4	Can you rule in biological explanations?
	5	Can you identify alternative lines of evidence?

**Table 3.10:** Standards of Evidence Life Detection scale, produced by a community-wide effort

## Chapter 4

# The case of detecting Phosphine in the atmosphere of Venus

### 4.1 Venus properties and habitability

Venus is often defined as the twin of the Earth, due to the great similarities in their bulk properties. Since there are great differences between the two in terms of Atmospheric composition, pressure and temperature, it is important to understand what brought the planets to differentiate each other so much. This can give us important insights about the evolution of habitability of rocky planets outside the solar system.

Despite the great similarities in mass and radius, there are important differences in terms of: rotation rate, obliquity and magnetic field. In 4.2 we can see a comparison between different astronomical data of Venus and Earth. because of this it is not possible to explain the differences in temperature and chemical atmospheric composition only considering the smaller distance from the Sun of Venus. For this reason the precise contribution of the solar flux to the global evolution of Venus, remains unconstrained. In this sense Venus offers a key point to start with to discuss about the habitability of a planet, since its evolution history represents an alternative development from Earth despite the similar origins. In the Astro2020 Decadal Survey of 4th of November 2021 3 priority area have been identified for the future development of astrophysics. One of this is the "Pathways to Habitable worlds". What has been proposed as strategy has to do , beside the observation and characterization of exoplanets, The necessity of accurately interpreting the solar system data , so the close collaboration of astronomy and planetary sciences. Un-

Understanding the evolution of the Properties of Venus will be important in the future to have a much more clear comprehension of habitability in the context of geological evolution. In Astro2020 it has been reported: “Venus provided context for loss of habitability, with relevance for Venus-analogue extrasolar planets, and studies of stellar wind/planetary atmosphere interactions at Mars discovered and informed planetary atmospheric loss processes” and also : “Combination of measurements and theory of the nature and processes that drove Earth’s early habitability, and the loss of habitability on Venus and Mars can inform our understanding of exoplanet habitability”. The possibility that we have with Venus, to understand with in situ missions a rocky terrestrial planet that has extremely different climatic conditions won’t be given from the exoplanetary studies. Studying Venus will help us to understand the conditions that allow long-term habitability and to better interpret the exoplanetary data, as pointed out in [84].

As previously said, despite the similar bulk properties, there are great differences in the planets: The insolation of Venus is twice the one on Earth, it has a retrograde period of rotation of 243 days and its atmosphere is composed mainly of CO<sub>2</sub>, with a little amount of N<sub>2</sub>, traces of other gases as SO<sub>2</sub>, Ar and water vapour. Besides this the planet is surrounded of a layer of clouds of H<sub>2</sub>SO<sub>4</sub> that give the planet an albedo that is twice the one of the Earth. All this contributes to make the planet extremely hot and with a pressure that is the one at 900m below the terrestrial ocean. The surface temperature expected is 735K. The high surface temperature can not be attributed only to heating , but due to the high pressure. The atmosphere is opaque , with an optical depth  $\gg 1$  due to the predominance of green house gases.

Below the clouds and down to the surface, the temperature profile of Venus’s atmosphere is primarily regulated by convection and follows a dry adiabatic. The lapse rate , which can be calculated using thermodynamic principles , is approximately 10 K km<sup>-1</sup>. The diagram of the mean vertical temperature is shown in 4.1

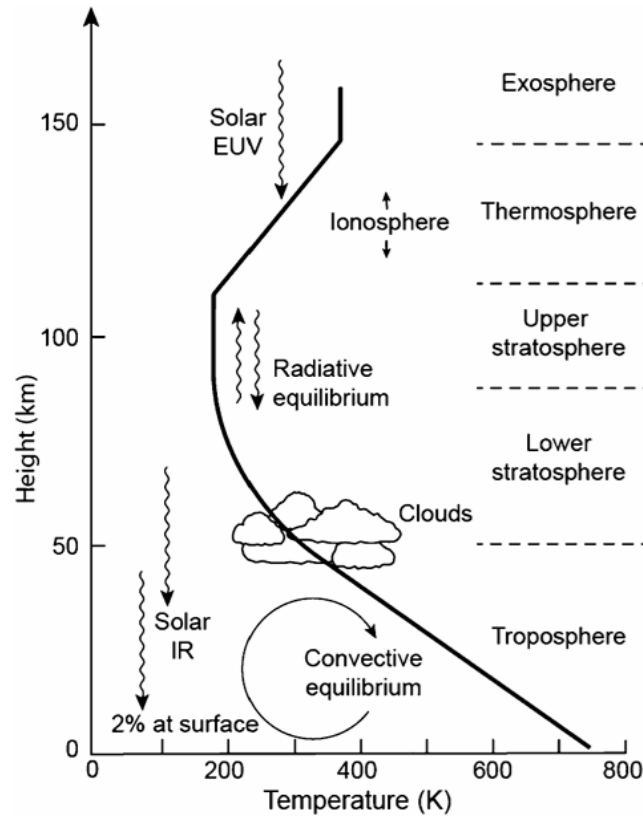


**Figure 4.1:** A diagram of the mean vertical temperature profile in Venus's atmosphere, showing the major processes at work, and the approximate locations of the main cloud layers. From [51]

Beside this Venus lacks an intrinsic magnetic field. The measurement of the deuterium hydrogen rate made by the pioneer probe in the 70s have showed that Venus lost a big amount of water. One of the hypothesis made to reconcile the observations with what is known about the planet today is that the planet has formed with an atmosphere rich in water vapour, over a magma ocean and it would have been too close to the Sun for being able to disperse heat in space with another method other than the atmospheric escape of water , as pointed out in [36]. For this reason the planet would have acquired his conditions in the initial phases of his evolution and wasn't habitable ever since.

In [70] It has been noted how the lost of oceans or of an atmosphere rich of Water vapour through a runaway greenhouse can bring to a temporary increase of atmospheric  $O_2$ . In particular, in addition to undergoing potential desiccation, planets with inefficient oxygen sinks at the surface may build up hundreds to thousands of bars of abiotically produced  $O_2$ , resulting in potential false positives for life[70].

Astronomical data	Venus	Earth
Mean distance from Sun ( $10^8$ kilometres)	1.082	1.496
Comparative solar distances	0.723	1
Orbital period	0.615	1
Rotational period (hours)	5832.24	23.9345
Comparative rotational periods	243	1
Comparative length of solar day	117	1
Comparative length of year	0.615	1
Orbital eccentricity	0.0068	0.0167
Comparative eccentricities	0.412	1
Obliquity (deg)	177	23.45
Comparative obliquities	7.548	1
Equatorial radius (kilometres)	6052	6378
Relative radius	0.95	1
Mass ( $10^{24}$ kg)	4.87	5.97
Relative mass	0.816	1
Mean density ( $\text{kg/m}^3$ )	5240	5500
Relative density	0.950	1
Acceleration of gravity ( $\text{m s}^{-2}$ )	8.89	9.79
Comparative surface gravity	0.877	1
Escape velocity	0.929	1
Solar Constant ( $\text{kW m}^{-2}$ )	2.62	1.38
Bond albedo	0.76	0.4
Net heat input ( $\text{kW m}^{-2}$ )	0.367	0.842

**Figure 4.2:** Data comparison between Venus and Earth. From [51]

Despite the fact that there are not enough data to choose for a particular model of the history of Venus it is possible to make measurements that give us important constraints. For example to understand the atmospherical composition of elemental gasses and isotopes could give important insight on the initial composition of Venus and his history of water loss [30]. In the same way understanding the history and the rate of volcanic activity on Venus could allow us to do estimates on the entire planet and the degassing rate [76]. Besides giving useful insights to understand the atmospheric evolution of Venus, such a comprehension could allow us to obtain critical informations regarding the heat loss mechanism on the habitability of Venus to generate and to maintain a magnetic field and the effects that we expect on his atmosphere, as outlined in [40]. One of the main methods with whom a planet regulates his climate is through the cycle of carbons-silicates, in which the carbons is stripped away from the atmosphere and brought inside the planet. On the Earth this happens mainly thanks to tectonics plates. If this is ever happened on Venus is not completely clear, although at least some spatially limited subduction has been documented on the planet [18]. An important aspect of this is that water plays an important role in the development and operation of plate tectonics.

In [84] it is defined the Venus Zone(VZ) as a reference target to identify rocky

terrestrial planets where the atmosphere could have potentially gone towards a runaway greenhouse that could bring to similar conditions to those on the surface of Venus.

The external boundary of the VZ is the "runaway Greenhouse" line, that is calculated with the terrestrial atmosphere models.

The internal boundary is estimated on where the radiation of the star would cause a complete atmospheric erosion. [29] has calculated an occurrence rate of VZ terrestrial planet of 32 % for low mass star, and 45 % for a Sun-like stars. The team has calculated the occurrence rate of VZ planets for GKM stellar spectral types , using the data from dressing and Charonneau 2013 (for M dwarfs) and [41] (for K and G dwarfs). In these studies the occurrence rate has been calculated based on the following equation:

$$f(R_p, P) = \sum_{i=1}^{N_p} \frac{a_i}{R_{*,i} N_{*,i}} \quad (4.1)$$

where  $a_i$  is the semi-major axis of planet  $i$ ,  $R_{*,i}$  is the host star's radius of planet  $i$ ,  $N_{*,i}$  is the number of stars around which planet  $i$  could have been detected and  $N_p(R_p, P)$  is the number of planets with the radius  $R_p$  and period  $P$ . The ratio  $a_i/R_{*,i}$  is the inverse of the probability of transit orientation , which is considered to take non transiting geometries into the estimation of occurrence rate. The extent of the VZ and HZ boundaries are shown in figure 4.3.

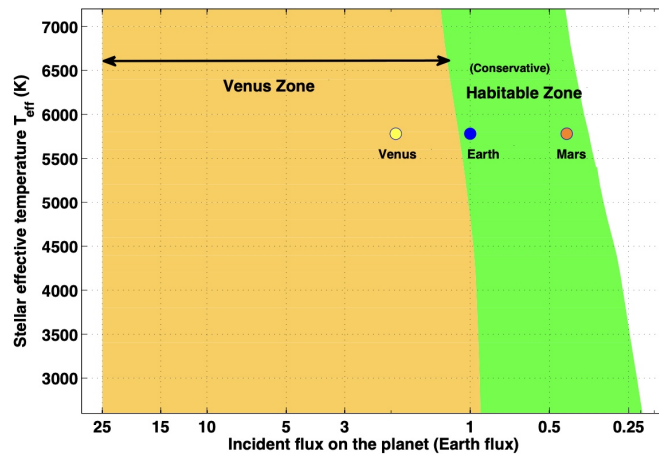


**Figure 4.3:** incident stellar flux on a planet versus stellar effective temperature, showing the extent of Venus zone and habitable zone



As noted in [29], it is important to remember that the boundaries of the habitable zone (HZ) and the Venus zone (VZ), are hypotheses subject to testing, as the runaway greenhouse effect could occur beyond the calculated limits. Additionally, while the insolation flux of a planet is a significant factor, it is not the sole determinant of a planet's climate. Other factors also play a crucial role in influencing whether a planet might enter greenhouse phases during the early stages of its evolution. The future missions included the VERITAS NASA's mission, and DAVINCI, and ESA's ENvision spacecraft will allow us to understand better the evolution history of Venus.

## 4.2 venus and the search for life

The recent debated discovery of Phosphine in his atmospheres has raised the question of whether there might be niches of microbiological activity in his clouds, where the condition might not be so hostile and this raises questions about the past life on Venus. Since it has been suggested that in the past Venus might not have had such a hostile environment and life that has emerged in the past might persist today in the dense clouds above its surface [?]. Phosphine is a molecule suggested as a potential biosignature since on Earth it is only associated with anaerobic ecosystems and with human industrial chemistry as we have seen in chapter 2. Even if it is clearly associated with anaerobic biology the specific biochemical pathway for Phosphine production in anaerobic systems remains unclear. As discussed, while Venus's surface is currently an extremely hostile environment, there is a potential niche for biological processes within the planet's clouds. There are region in the clouds that are cool enough to allow for the presence of liquid water, with atmospheric pressures comparable to those at Earth's sea level.

### 4.2.1 The alleged discovery of Phosphine in the atmosphere of Venus

Since Venus is the best rocky planet candidate to search for Phosphine in the solar system, in 2016 it has been put together a proposal, from a team of astronomers led

by Prof Jane Greaves , to the JCMT to conduct observations to look for the J=1-0 rotational transition of Phosphine, which would produce an absorption line at 1.123 mm(267 GHz). Even if there are other transitions of Phosphine in other wavelenght in farIR and midIR, this one has several advantages.First of all observations can be conducted from the ground. The next highest rotational transition , J=2-1, would require observation from the stratosphere. It is also possible to conduct Mid-IR observations of other transitions from the ground , but the team could not have easy access to mid IR facilities. The first observational idea was to acquire a few hours of data to better understand the observational issues with looking for a weak absorption line against the very bright continuum source which is Venus with the eventual intent to propose a longer series of observation to set a stringer upper limit, since phosphine was not expected to be found.

### 4.2.2 JCMT and ALMA observations

Venus was observed by the JCMT using RxA3 in search of Phosphine on five mornings in June 2017. These dates were chosen so that Venus appeared large enough to fill the telescope beam, minimising any effects due to errors in pointing the telescope.Venus is a strong continuum emitter at millimetre wavelengths , so phosphine would be detected as a weak absorption line against this strong continuum. This continuum can cause a number of issues regarding the quality of the data. Many effects can influence them, like the reflections from the floor or roof of the telescope dome, or in the receiver cabin itself, entering the beam, lead to strong, time varying baselines in the output spectra. It was important to detect this errors and remove them.These effects were removed using the fitting of polynomial functions to the data, and then exclude regions of the spectrum where Phosphine might lie. This method was applied to the 140 spectra that made the observation and an absorption line attributed to Phosphine was detected, and it did correspond to an abundance of 20-25 parts per billion (ppb), as shown in figure 4.4.

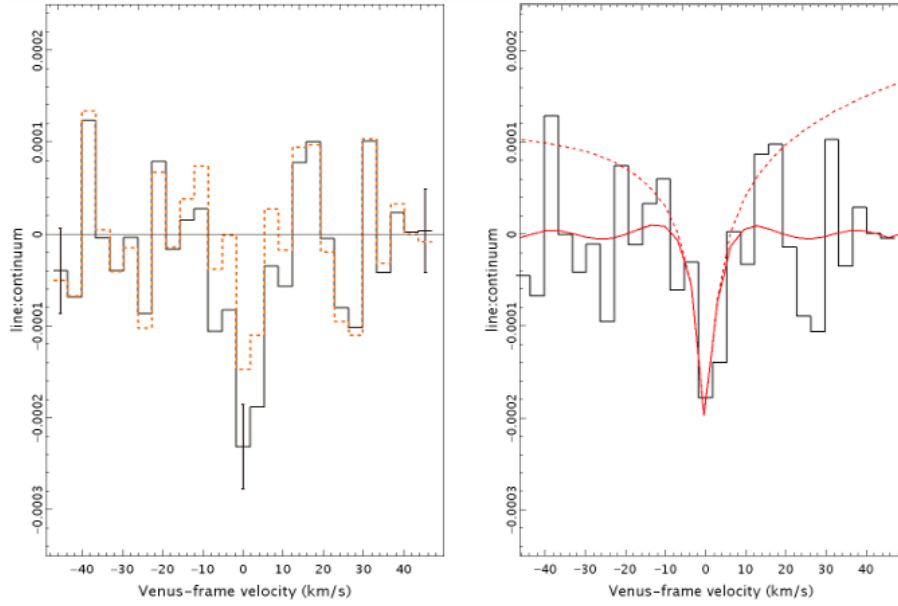


**Figure 4.4:** Panels show spectra of PH3 1-0 in Venus' atmosphere as observed with the JCMT. Axes are line to-continuum ratio against Doppler-shifted velocity referenced to the Phosphine wavelength. Left: the least and most conservative solutions after fitting and removing spectral ripple. from [22]

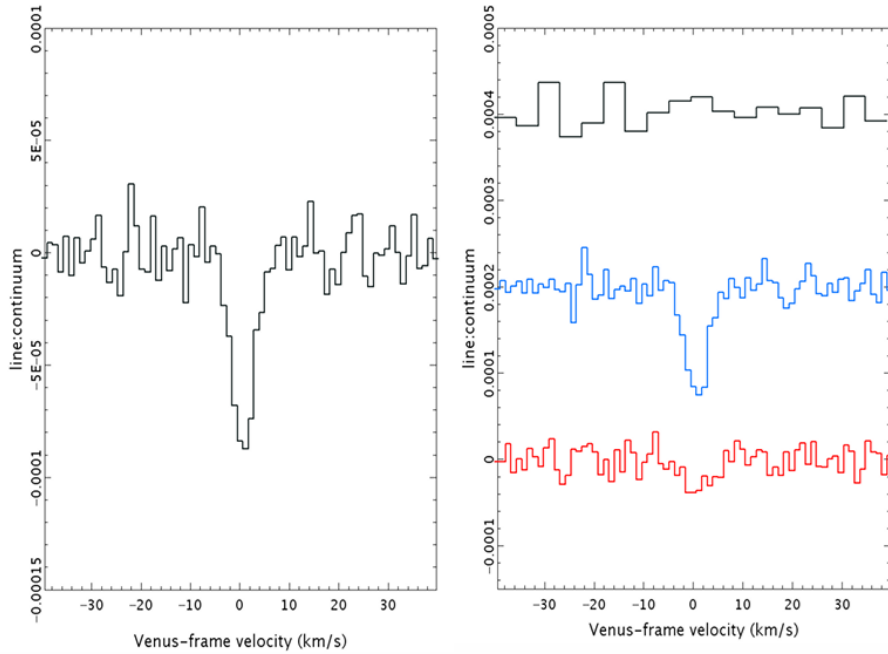


**Figure 4.5:** Spectra of Venus obtained with ALMA. Left panel shows the PH3 1-0 spectrum of the whole planet, with  $1\sigma$  errors (here channel-to-channel) of  $0.11 \cdot 10^{-4}$  per  $1.1 \text{ km/s}$  spectral bin. Right panel shows spectra of the polar (histogram in black), mid-latitude (in blue) and equatorial (in red) zones. From [22]

As soon as the surprising detection of Phosphine from JCMT was claimed there

was a urgent need of and independent confirmation. This was done using the ALMA observatory in March 2019. A very diffent facilities since it is an interferometer, made up of 66 separate antennas , 12m in diameter , and the signals are combined together to produce the final result.Only 43 of the antennas were used. The signals are treated in a similar way with the RxA3 on the JCMT, with a heterodyne SIS mixer and local oscillator in the receiver. But then they are cross correlated with those from each of the other antennae in the array(each pair of antennae is a baseline) and this produce as a result the interferometric map of the target. The angular resolution that is possible to achieve with an interferometer correspond with the one achievable with a telescope whose diameter equals the longest baseline in the array. The process of cross correlation of the signals produces the so called visibilities, that consist of a measure of the 2D Fourier transform of the sky distribution of brightness. These are then Fourier transformed to produce a series of images at successive frequencies, a spectral cube.Since there is a finite number of antennas in the array , the Fourier space is never covered completely as happens with a telescope that uses only one big mirror. That's why to derive the image from the under sampled Fourier space it is necessary to use an algorithm called CLEAN , to do the cleaning process. The use of an interferometer to observe Venus leads to different challenges in respect to JCMT. One of this was that that angular size of Venus was so great that even the shortest ALMA baseline could not provide good images on the scale of the whole disc and the imperfect sampling led to strong ripples so the data from the affected short baselines, all less than 33m in length , were removed.There were also found some errors in the standard reduction script used. Once all the possible error and effects were taken into account , a good detection of phosphine absorption of 20ppb that matches what was seen by the JCMT but with somewhat an higher SNR.

### 4.2.3 further analysis from the ground

After the detection paper by [22] the data from ALMA were reanalyzed by a separate group [53], they did not find the detection claimed by [22], and found instead an upper limit to the Phosphine abundance of about 1 ppb. They identified some processes used in the standard ALMA calibration scripts which were not adequate

for a very bright, time varying, beam-filling target or indeed for the correspondingly bright calibrator sources used, as pointed out in [?]. After this the staff of the ESO reprocessed the raw data from ALMA independently. This process simplified the basic removal of instrument bandpass ripples using the moon callisto as a calibrator, and also avoided the chance of spectral averaging producing sharp edges which could mimic an absorption line. The new script also accounted for the non linear instrumental response to the high intensity of Venus (that is the brightest source in the sky after the Sun at these wavelengths) and its large angular size, although, since this exceeds the extent of accurate models of the response of individual ALMA dishes, this is thought to be a source of residual error. The response by [22] to this reanalysis can be found in [23] using the new scripts and exploiting three different independent methods to obtain the final images and spectra. The steps after the observatory calibration are the following: removing the shortest baselines, and make a linear spectral fit to the visibility data to remove the contribution of Venus. Next, residual spectral ripples can be corrected either in the visibility data or after the Fourier transforming to make an image cube, and before or after cleaning. Spectra were extracted over different portions of the planet; small residuals errors meant that only those spectra extracted from regions symmetric about the planet centre were considered reliable. The Phosphine signal was obtained using all the updated methods. The team of [22] attributed the negative result of the team of [53] as caused by including baselines shorter than 33m in most of their analyses, and including parts of the image of the planet that had significant spectral artifacts that raise the noise in the final combined spectrum, as outlined by [?]. Greaves team concluded that the Phosphine detection in the ALMA data remained robust.

#### 4.2.4 The debate around the line

Many authors suggested that the use of high order polynomials to allow the removal of varying baselines caused the generations of fake lines in both the ALMA and JCMT Phosphine detection. In fact, when using this method you have to mask out the region of the spectrum around a suspected line otherwise the polynomial fitting method might fit and remove a real line, recognizing it as a small scale baseline

ripple. however, as pointed out by [?] the detection of Phosphine did not rely solely on measuring the depth of an absorption line at a random position. It also relied on the wavelength of the line seen coinciding with that of the line being searched for , Phosphine. This reduces a lot the chances of a noise spike or residual masquerading as a Phosphine detection. In [21] it is shown how adding the additional constraint that a fake line must be at a specific frequency reduces the chance of a false positive to  $< 1.5\%$ . besides this the chances that a fake line appears exactly at the same wavelength both in ALMA and JCMT are very low. Both these reasons improve the probability that the line of Phosphine detected is not a a statistical artefact but real.

Even if , given the mentioned reasons , the line is unlikely fake, there still is the possibility that the absorption feature is indicative of some other molecule and not Phosphine. For example  $\text{SO}_2$ , that is a constituent in the Venus atmosphere , has a transition at 266.9443329 GHz (  $J = 30_{9,21} - 31_{8,24}$  ) , it is at a frequency shift from  $\text{PH}_3$   $J=1-0$  at 266.944513 GHz that corresponds to a velocity difference of just 1.3 km/s. By [?] have been pointed out many problems with this interpretation:

- while the two line centres of these two transition are close, they are still 1.3 km/s apart , and this leads to a  $3\sigma$  discrepancy between the measured line centre and that expected for the  $\text{SO}_2$  line.
- Simultaneous (for ALMA) and near simultaneous (for JCMT) observations of a different and stronger  $\text{SO}_2$  line , [?] provide predictions of the relative strength of the  $\text{SO}_2$  transition that might contaminate the Phosphine line.

They find that the level of contamination of the Phosphine line by  $\text{SO}_2$  is 10% for the JCMT data and  $< 2\%$  for the ALMA data. Given this conclusion it really seems likely that the detected line is indeed related to Phosphine.

There have been other analyses that tried to observe Phosphine at different transitions and have produced conflicting results, also because the observation at different wavelength and using very different facilities is probing the presence of Phosphine at different altitudes and times. However none of these observations have disproved the original ALMA or JCMT results. The observations are:

- the observations done with Nasa infrared telescope facility (IRTF) on Mauna Kea in Hawaii, at 10.471  $\mu\text{m}$  (28.65 THz). No Phosphine absorption was detected. The dataset was from 2015
- Observation from Venus express at 4.125  $\mu\text{m}$  above the cloud layers, failed to find any Phosphine absorption. The data came from 2006 to 2014.
- Observations in the far infrared at 534 and 1067 GHz with SOFIA observatory (stratospheric Observatory for infrared Astronomy). SOFIA observations were done in 2021. The first analysis of the data failed to find any sign of Phosphine, both for the J=4-3 line and J=2-1 line. Subsequent reanalysis corrected a precedent error and by analysing the line-to-continuum ratios, Phosphine was found at a level of  $1 - 2$  , averaged over altitudes from 75-110km, with  $6.5\sigma$  significance.

Surely one of the best way to understand the presence of Phosphine in the atmosphere of Venus is to probe it with in situ measurement. The pioneer Venus Multiprobe some years ago was carrying a mass spectrometer into the atmosphere. In 2021 the data were reanalysed , they were regarding the descent into the atmosphere in 9 december 1978. The data regarded an altitude of 51.3 km above the surface. A very important region for the search of life. The analysis found evidence for Phosphine at 0.1-2 parts per million (ppm) (an abundance which is much higher than the JCMT or ALMA observations). The data suggested also the presence of different chemical species like nitrite, nitrate, nitrogen and possibly ammonia. These ensemble of molecules might indicate the presence of chemical disequilibrium. An interest feature often associated with life that requires future investigations.

The reasons why the observations are partially contradictory are also because they sample the atmosphere of Venus at different altitudes and, in a very wide span of time, almost 40 years. The concentration of a molecule in the atmosphere can vary over a timescale of years or even days, as it happens with  $\text{SO}_2$ . Also Phosphine can vary with function of altitude and differently from in situ observations, it is difficult to extract this type of information from Earth. In principle an analysis of the pressure broadening of a particular line can reveal the altitude from the pressure,

since the greater the pressure, the broader the wings. However, there are different problems with this type of analysis:

- The pressure broadening for Phosphine in CO<sub>2</sub>, which is the dominant constituent of Venus atmosphere, is not currently known,
- the data reduction technique used to extract the absorption line remove any broad line wings as part of the process that removes baseline ripples. This causes the observation to being unable to catch broadened lines. [? ]

Another factor to consider is the timing of the observation. Currently we can't monitor the changes in the amount of Phosphine with time. But we can analyze if there are any correlations between the time of the observation and the different detections and non detection of the molecule with the illumination of atmosphere's of Venus by the Sun. Since it can modify the abundance of the molecule by photolysis.

### 4.3 hypothesis on the origins of Phosphine on Venus

Since Venus has an oxidised atmosphere, the presence of Phosphine, a compound of phosphorous with hydrogen should not naturally appear. As previously said, Phosphine on Earth is known to be produced only from industrial processes and from anaerobic life. However we do not know yet if there are any abiotic processes that can produce the observed amount of Phosphine in the atmosphere of the planet. A work that has explored a wide range of chemical processes to explain the Phosphine observations is [56]. The processes examined included gas reactions, geochemical reactions, photochemistry, volcanism, lightning and impactors. The results of these research point out that we currently do not know how it is possible to produce Phosphine on Venus in the quantity seen. The presence of anaerobic life is another potential explanation, but before we can do such a statement it is necessary to first exclude all the possible abiotic origins, and being able to explain how life is able to survive in the extremely acid environment of Venusian cloud droplets. It is possible that the ammonia present in the atmosphere of Venus can buffer the sulfuric acid. There is a possible detection by LNMS and in preliminary analysis of data from the Green Bank telescope, so this aspect is rather promising [9].



Until the next in situ observations that will search for life, with the VLF, it is important to establish , with our current knowledge about the clouds of Venus and microbial life, if there are the conditions for life to replicate. Since the medium temperature on Venus is  $424^{\circ}\text{C}$  , most biological organic molecules are pyrolyzed, enzymes are speedily inactivated and protein denatured. But , as previously said , since the clouds of Venus host , as shown in the figure 4.6, a temperate zone where the temperature can remain close to  $60^{\circ}\text{C}$  and the pressure of 1bar , the possibility of life must be scrutinized. On Earth there have been observed different types of life presence at high altitudes: bacteria, pollen, and algae in a region as high as 15km. [89]

Furthermore, evidence has been found for the growth of bacteria in the droplets sampled from a super cooled cloud near a meteorological station on a mountain top in the alps [42]. And the same mechanism that have brought these organism high in the atmosphere could have done the same with Venusian microorganism: evaporation, storms, eruptions, meteor impacts. Most importantly, on Venus the clouds are a stable , global phenomenon that can host aerosol particles for a long period of time, and not only few days as in the terrestrial atmosphere. In [28] it is has been supposed that the microorganism populating the Venusian atmosphere are not free floating but confined to the liquid environment inside cloud aerosols or droplets. In the study it has been constrained the maximum size of droplets that could be floating in the Venusian atmosphere and estimated whether their stokes fallout times to reach moderately high temperatures are larger than the microbe's replication time. For the Stokes fallout time the team has concluded that to maintain the colony of microbes alive the required fallout times is longer than half an Earth day. The team has also analyzed the possible influence of cosmic rays on the microbial life in the clouds of Venus. An important aspect since Venus is known to not have a magnetic field to shield from energetic particles coming from the space. For what concerns the temperate zone (51km to 62km) , numerical simulations show that cosmic radiation would not have had any hazardous effect on putative microorganism. [27]

In conclusion the team [28] has shown that for aerosols , the stokes fall-out times to reach the lower haze atmospheric layers is pronouncedly larger than the typical bacterium replication time on Earth. So they conclude that if in the past bacterial

life is emigrated from the surface to the clouds through updraughts , it is possible that now their remain confined in the aerosols.

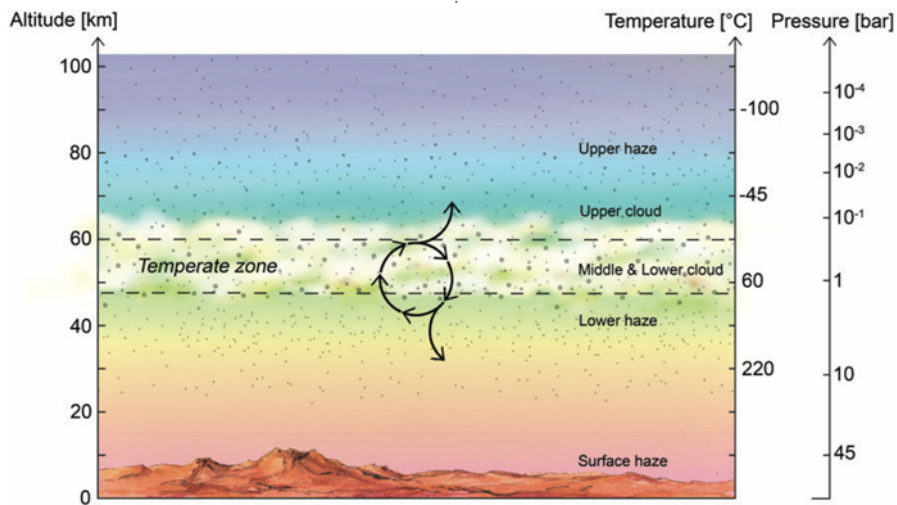


**Figure 4.6:** Plot showing the temperature and pressure conditions of different regions of the Venus atmosphere, with the temperate zone highlighted from [57]

## 4.4 The future of Phosphine study on Venus

Currently there is no solid conclusion neither on the presence of Phosphine on Venus and on the possibility of life in the clouds. Further missions need to constraint these aspects. The further missions should focus on the in situ observations and possibly return samples to Earth to acquire more solid informations.

### 4.4.1 Earth and space based studies

The largest of the projects currently studying phosphine is JCMT-Venus. The new receiver has a wider bandwidth than RxA3 so it is possible to observe simultaneously HD and SO<sub>2</sub> and search for other molecules such as SO and PO<sub>2</sub> to see how the different species vary in relation to each other. When complete, the JCMT-Venus will provide a major new database of observations of Venus in the mm band, including phosphine and other important molecules which will give us key informations of the origin of Phosphine.

There are also facilities that will study life on Venus that will not target Phosphine, for example the Green bank telescope (GBT) at radiowavelengths that will look for ammonia ( $\text{NH}_3$ ) in absorption.  $\text{NH}_3$  is another molecule that is not expected to be present in the oxidised atmosphere of Venus. In the future will also be important the laboratory studies regarding the formation and destruction of Phosphine and other hydrogen-rich compounds in Venus like conditions. In August 2025 the JUICE spacecraft, that plans to go on the moons of Jupiter will be make a flyby in August 2025. The submillimetre wave instrument (SWI) will be able to observe higher J transitions of phosphine, included those observed from the Earth by Sofia. In the 2030's three missions directly targeted at Venus will be launched: the ESA EnVISION mission and NASA VERITAS (Venus Emissivity, radio science, InSAR, Topography, Spectroscopy and imaging). Those two missions will be studying the surface and interiors of Venus, and will focus on study the history and role of volcanism on the planet. However they won't have much to say about the presence of Phosphine in the atmosphere. Davinci mission instead will focus on it. It will flight through the clouds and sample the atmosphere. The first to enter the atmosphere since the pioneer Venus probe in 1978. It will have a mass spectrometer that will improve the results of LNMS. Thanks to this it will be able to monitor the presence of Phosphine and other gases with altitude and other conditions. The four instruments combined with imagers on the orbiting mothership, will improve greatly our in situ knowledge of the atmosphere. Also private missions are about to come, the company Rocket lab for example is developing a series of missions called Venus life finder (VLF).<sup>[44]</sup> the first of these missions, will look for organic molecules using ultraviolet autofluorescence technique. On the mission there are not only spectrometer but also a microscope that will search cloud droplets for evidence of biological cells. The mission was planned for the 2023 but was delayed for the 2025. One of the most exciting mission planned by the VLF is the one that will use a balloon to collect samples of cloud droplets and gas. It will be a key to study the presence of life on Venus.

## 4.5 conclusion: Bayesian life detection on Venus

Since there are possible ways to produce Phosphine abiotically, to determine the biogenic origin on Venus it is necessary to constrain the likelihood that it has been produced abiotically. As previously stated, in the work of [22] it has been used a series of abiotic models based on thermodynamic calculations and photochemistry. The expected production rate for most of the mechanisms they tested, is much lower than the one that was extracted from the observations, often by several orders of magnitude. Even if it is not possible to rule out all the existing mechanisms that could produce Phosphine on Venus, most of them could be excluded, and so the hypothesis of life so far remains a valuable explanation. Nevertheless, it has not been done a Bayesian analysis so far, and so even if it is a plausible hypothesis, it is not possible to derive a conclusion yet.

In fact, constraining only  $P(obs|NL)$ , with the analysis of all the possible abiotic pathways could not be enough if  $P(life)$  has no constraint at all. As pointed out by [45], we are left with a conditional likelihood in the absence of context for assessing how it impacts our conclusion. Especially considering that there are many properties of the Venusian Atmosphere that are not completely understood.

We are in a situation where it is not possible to accurately constrain the strength of a claim on either side. This leads to various claims and subsequent debate about the origin of Phosphine on Venus, without the ability to moderate the strengths of those claims, from either side (life vs. non life), based on what we can reasonably infer about the likelihood of a biosphere on Venus.

We can understand how the Bayesian approach can help us by outlining the result obtained by [8], where it has been applied to quantify the probability that methanogenesis (biotic methane production) might explain the escape rates of molecular hydrogen and methane in Enceladus's plume, as measured by Cassini instruments. They find that the observed escape rates score the maximum likelihood under the hypothesis of methanogenesis, assuming that the probability of life emerging is high enough.

Instead if the probability of life emerging on Enceladus is low, the Cassini measurements are consistent with habitable yet unhabited hydrothermal vents and point

to unknown sources of methane.

The results obtained from [8] show how the application of the Bayesian model for inferring the presence of life within the solar system allows for a clear and rigorous conclusions regarding the biogenicity of the phenomenon , depending on the prior probability of life. In the future , it will be necessary to conduct a similar analysis for Venus, which can then benefit from future data collected by in situ missions.

## Chapter 5

# conclusions

As we have seen in chapter 2 the current state of gaseous biosignature science and biomarkers more in general contain many different critical aspect that currently undermine the strenght and reliability of the life detection claims. Some of the most crucial are:

- Need for a more rigorous definition of biomarkers that is based on strong theoretical framework.
- Need for a better universal accepted terminology in the field
- Need to clearly define our objectives when searching for biosignatures , whether we are aiming to detect signs of life or sumply identifying a biosphere on an exoplanet. This clarity is essential for effectively designing observations related to life detection. Because in most of the cases the observations won't teach us anything new about life but just improving our statistics about exoplanets biospheres. As outlined in [63].

The bayesian Framework , together with a strong theoretical theory of life, can help to solve this problems.

As we have seen, the Bayesian framework can be a flexible and powerful tool that helps guide and shape our future strategies for life detection, and solve many current problems of the field, as well as support more rigorous and realistic claims about our findings.

In Sections 3.1.9 and 3.2, we observed that in any situation where  $P(\text{molecule}|\text{life}) \ll P(\text{molecule}|\text{NL})$ , a high posterior probability can only be achieved by having a very high prior probability of life. However, this might never be a realistic scenario in the future.

In such cases, repeated observations would not lead to an increase in the posterior probability but rather to a steep decline.

Nevertheless, the subsequent results show that the combination of eliminating possible false positives for a biomarker, or selecting a biomarker without false positives, along with a large number of observations that build large statistical samples, can lead to obtaining posterior probabilities of high-confidence detection.

Furthermore, we saw that incorporating contextual information into the Bayesian framework can help create scenarios where  $P(\text{molecule}|\text{life}) > P(\text{molecule}|\text{NL})$ , leading to high-confidence detection based on high posterior probabilities. This is par-

ticularly helpful when we do not have the possibility of collecting a large number of observations.

The sensitivity analysis performed on equations 3.11 showed that when we have only a single observation, 60% of the uncertainty in biogenic assessment is due to the uncertainty of the prior. However, when the detection reaches 7 biosignatures, the effect of the prior becomes negligible, as demonstrated in [65]. The results of the sensitivity analysis for equation 3.16, where the likelihood of the error is also considered in the equation, shows that the influence of the prior's uncertainty becomes negligible only after detecting 15 biosignatures, which could pose problems when the likelihood of error is not negligible.

Finally, in Section 3.3.2, using the results from [54], we observed how different strategies can be followed depending on the value of  $P(\text{life})$ . If  $P(\text{life}) \gg 0$ , it may be sensible to target individual worlds and obtain high-resolution spectra. However, if  $P(\text{life})$  is very low, it might be more effective to take lower-resolution spectra of more worlds to generate better statistics.

As I have outlined in section 3.4, there are different aspects of the Bayesian framework that are critical and that come from the lack of a rigorous theoretical framework about life origin. In the first example presented, I outlined how the lack of a theoretical framework that could help to better constrain  $P(\text{life})$  makes the Bayesian framework conceptually unconstrained, allowing for the possibility of hypothesizing unknown metabolism, and life forms without a priori reasons within the model to exclude them. For this reason, to successfully apply the framework, it is necessary that the assumption regarding  $P(\text{life})$  are based on solid theoretical foundations. From this we can note how in one of the best strengths of the Bayesian framework, which is the flexibility, lies its biggest weakness. As I have highlighted, one example of this is the use of theories like Assembly theory. Then the biased coin example has showed how high confidence detection claims using the Bayesian hypothesis testing requires either a strong prior hypothesis on the existence of life in a given alien environment when we have false positives for the observation or a biosignature that lacks of false positives.

Then We have seen how the combination of the equation given by Bayesian hypothesis testing together with the ones provided by SDT can help to build a quantifiable framework to classify the biosignatures during an observation.

Finally, in the last chapter, I analyzed the recent alleged discovery of phosphine on Venus as a case study that helps to understand many critical issues and key aspects of life detection. As seen, it is not yet possible to infer with certainty the presence of life based on the observations that reported detecting phosphine, both due to the uncertainty of the observations itself and the current inability to rule out all the possible false positives, despite various efforts to study them, the subject is still highly debated. Phosphine on Venus remains a key example of how extremely difficult is it to make high confidence claims regarding the presence of life, even on planets so close to us. It also raises many doubts about the realistic possibility of making such claims regarding exoplanets, where in situ missions will not be possible in the near future, and where life detection will essentially be a study of the presence of biosphere in the galaxy rather than improving our theoretical framework on life. Nevertheless, it could help us better define the values of Bayesian parameters. The improvement of our theories on life and the science of life detection must start with

the study of life in the lab and in the solar system, through both in situ and remote mission, using a Bayesian framework to moderate conclusions about the presence or absence of life on a planet as rigorously as possible.

Here I present a list of the possible ways in which astrobiology can in the future better constrain the search for life:

1. Use Strong theoretical framework , like assembly theory to search for molecules that have no false positives
2. Plan mission to make statistical analysis on the presence of the biosignatures in order to better constrain the parameter of the bayesian framework and being able to do more rigorous claims about life.
3. Use the Bayesian framework in order to choose the best strategy for the search of exolife.
4. Trying to better define the difference between the search for life and the study of the distribution of terrestrial biospheres.
5. Study life in the solar system with in situ observations, this will be crucial to better constrain  $P(\text{life})$ .
6. Study life in the laboratory on Earth, exploring the chemical space in a systematic way in order to build stronger theoretical framework to asses biogenicity of other planets.



# Bibliography

- [1] Jayne L. Birkby. Exoplanet atmospheres at high spectral resolution. *arXiv: Earth and Planetary Astrophysics*, 2018. URL <https://api.semanticscholar.org/CorpusID:73580580>.
- [2] G. W. Marcy R. P. Butler. The planet around 51 pegasi. *The Astrophysical Journal*, 27(1379), 1995.
- [3] David Charbonneau. The rise of the vulcans. *proceedings of the international Astronomical Union*, 2008. doi: 10.1017/S1743921308026161.
- [4] Wenda chen. The comparison of five methods of detecting exoplanets. *Highlights in Science, Engineering and Technology*, 38, 2023.
- [5] David L. Clements. Venus, phosphine and the possibility of life, 2023. URL <https://arxiv.org/abs/2301.05160>.
- [6] Sara Seager Drake Deming.
- [7] Sara Seager Drake Deming. Illusion and reality in the atmospheres of exoplanets. *Journal of Geophysical Research: planets*, 122, 2017. doi: <https://doi.org/10.48550/arXiv.1701.00493>.
- [8] Affholden et al. Bayesian analysis of enceladus’s plume data to assess methanogenesis. *Nature Astronomy*, 5:805–814, 2021.
- [9] Bains et al. Production of ammonia makes venusian clouds habitable and explains observed cloud-level chemical anomalies. *Proceedings of the National Academy of Sciences*, 118(52), December 2021. ISSN 1091-6490. doi: 10.1073/pnas.2110889118. URL <http://dx.doi.org/10.1073/pnas.2110889118>.
- [10] Birkby et al. Detection of water absorption in the day side atmosphere of hd 189733 b using ground-based high-resolution spectroscopy at 3.2 $\mu$ m. *Monthly notices of the Royal Astronomical Society*, 436, 2013.
- [11] Borucki et al. Characteristics of planetary candidates observed by kepler ii. analysis of the first four months of data. *The astrophysical journal*, 736(19):22, 2011.
- [12] Cassan et al. One or more bound planets per milky way star from microlensing observations. *Nature*, 481:167–169, 2012. doi: <https://doi.org/10.1038/nature10684>.

- [13] Catling et al. Exoplanet biosignature: a framework for their assessment. *Astrobiology*, 18(6), 2018.
- [14] Charbonneau et al. Detection of an extrasolar planet atmosphere. *The astrophysical journal*, 2002. doi: 10.1086/338770.
- [15] Charbonneau et al. Detection of thermal emission from an extrasolar planet. *The astrophysical journal*, 2005. doi: 10.1086/429991.
- [16] Chen et al. The gtc exoplanet transit spectroscopy survey ix. detection of haze, na, k, and li in the super-neptune wasp-127b. *Astronomy and Astrophysics*, 2018. doi: <https://doi.org/10.1051/0004-6361/201833033>.
- [17] Cristophe Malaterre et al. Is there such a thing as a biosignature? *Astrobiology*, 2023.
- [18] Davaille et al. Experimental and observational evidence for plume-induced subduction on venus. *nature geoscience*, 10:349–355, 2017.
- [19] Des Marais et al. The nasa astrobiology roadmap. *Astrobiology*, 2008.
- [20] Foucher et al. A statistical approach to illustrate the challenge of astrobiology for public outreach. *life*, 2017.
- [21] Greaves et al. Addendum: Phosphine gas in the cloud deck of venus. *Nature astronomy*, 5:726–728, 2021.
- [22] Greaves et al. Phosphine gas in the cloud decks of venus. *Nature Astronomy*, 5:655–664, 2021. doi: [https://ui.adsabs.harvard.edu/link\\_gateway/2021NatAs..5..655G/doi:10.1038/s41550-020-1174-4](https://ui.adsabs.harvard.edu/link_gateway/2021NatAs..5..655G/doi:10.1038/s41550-020-1174-4).
- [23] Greaves et al. Re-analysis of phosphine in venus’ clouds. *Nature astronomy*, 5(7):636–639, 2021.
- [24] Greaves et al. Low level of sulphur dioxide contamination of venusian contamination spectra. *MNRAS*, 514:2994–3001, 2022.
- [25] Green et al. Call for a framework for reporting evidence for life beyond earth. *Nature*, 598, 2021.
- [26] Grillmair et al. Strong water absorption in the dayside emission spectrum of the planet hd 189733b. *Nature*, 456, 2008.
- [27] Herbst et al. Revisiting the cosmic-ray induced venusian radiation dose in the context of habitability. *Astronomy and Astrophysics*, 663, 2020. doi: <https://doi.org/10.1051/0004-6361/201936968>.
- [28] Jennifer J. Abreu et al. Necessary conditions for earthly life floating in the venusian atmosphere, 2024. URL <https://arxiv.org/abs/2404.05356>.
- [29] Kane et al. On the frequency of potential venus analogs from kepler data. *Astrophysical journal*, 2014.

- [30] Kane et al. Venus as a laboratory for exoplanetary science. *Journal of Geophysical research*, 124:2015–2028, 2019.
- [31] Kathie L. Thomas Keppta et al. Magnetofossils from ancient mars: a robust biosignature in the martian meteorite alh84001. *Applied and Environmental Microbiology*, 2002.
- [32] Knutson et al. A map of the day–night contrast of the extrasolar planet hd 189733b. *Nature*, 447:183–186, 2007.
- [33] Kopparapu et al. Habitable moist atmospheres on terrestrial planets near the inner edge of the habitable zone around m-dwarfs. *Astrophysical journal*, 2017.
- [34] Krissanse-Totton et al. Was venus ever habitable? constraints from a coupled interior–atmosphere–redox evolution model. *The planetary science Journal*, 2021. doi: <https://doi.org/10.3847/PSJ/ac2580>.
- [35] Krissansen-Totton et al. On detecting biospheres from chemical thermodynamic disequilibrium in planetary atmospheres. *Astrobiology*, 16(1), 2016.
- [36] Lebrun et al. Thermal evolution of an early magma ocean in interaction with the atmosphere. *Journal of Geophysical research: planets*, 118:1155–1176, 2013. doi: 10.1002/jgre.20068,2013.
- [37] Mashusudhan et al. *Exoplanetary atmospheres*. University of Arizona Press, 2014.
- [38] Meadows et al. Exoplanet biosignatures: Understanding oxygen as a biosig nature in the context of its environment. *Astrobiology*, 18(630), 2018.
- [39] Omran et al. Phosphine generation pathways on rocky planets. *Physics faculty publications and presentations*, 2021.
- [40] O’Rourke et al. Prospects for an ancient dynamo and modern crustal remanent magnetism on venus. *Earth and Planetary science letters*, 502:46–56, 2018. doi: <https://doi.org/10.1016/j.epsl.2018.08.055>.
- [41] Petigura et al. Prevalence of earth-seza planets orbiting sun-like stars. *PNAS*, 2013.
- [42] Sattler et al. Bacterial growht in the supercooled cloud droplets. *Geophysical research letters*, 28:239–242, 2001.
- [43] Seager et al. Toward a list of molecules as potential biosignature gases for the search for life on exoplanets and applications to terrestrial biochemistry. *Astrobiology*, 16(6), 2016.
- [44] Seager et al. Venus life finder missions motivation and summary. *Aerospace*, 9 (7):385, 2022.
- [45] Searra Foote et al. False positives and the challenge of testing alien hypothesis. *Astrobiology*, 23(11), 2023.

- [46] Showman et al. Atmospheric circulation of hot jupiters: Coupled radiative-dynamical general circulation model simulations of hd 189733b and hd 209458b. *The Astrophysical journal*, 699:564–584, 2009. doi: <http://dx.doi.org/10.1088/0004-637X/699/1/564>.
- [47] Snellen et al. The fast spin-rotation of a young extrasolar planet. *Nature*, 2014.
- [48] S.Seager et al. A biomass-based model to estimate the plausibility of exoplanet biosignature gases. *The astrophysical journal*, 775(104):28, 2013.
- [49] Stuart M. Marshall et al. Identifying molecules as biosignatures with assembly theory and mass spectrometry. *Nature communications*, 12, 2021.
- [50] Swain et al. Methane present in an extrasolar planet atmosphere. *Nature*, 2008.
- [51] Taylor et al. Venus: The atmosphere, climate, surface, interior and near-space environment of an earth-like planet. *Space science reviews*, 214(35), 2018.
- [52] Vidal-Madjar et al. An extended upper atmosphere around the extrasolar planet hd209458b. *Nature*, 422:143–146, 2003. doi: <http://dx.doi.org/10.1038/nature01448>.
- [53] Villanueva et al. No evidence of phosphine in the atmosphere of venus by independent analyses. *Nature astronomy*, 5:631–655, 2021.
- [54] Walker et al. Exoplanets biosignatures:future directions. *Astrobiology*, 18(6), 2018. doi: 10.1089/ast.2017.1738.
- [55] Snellen et al. 2010. The orbital motion, absolute mass, and high-altitude winds of exoplanet hd209458b. *Nature*, 465:1049–1051, 2010.
- [56] Bains et al.2021. Phosphine on venus cannot be explained by conventional processes. *Astrobiology*, 10:1277–1304, 2021. doi: 10.1089/ast.2020.2352.
- [57] Seager et al.2021. The venusian lower atmosphere haze as a depot for desiccated microbial life: A proposed life cycle for persistence of the venusian aerial biosphere. *Astrobiology*, 21(2), 2021. doi: 10.1089/ast.2020.2244.
- [58] A. Wolszczan D. A. Frail. A planetary system around the millisecond pulsar psr1257 + 12. *Nature*, 355, 1992.
- [59] Nicholas F.Wogan and David C. Catling. When is chemical disequilibrium in earth-like planetary atmospheres a biosignature versus an anti-biosignature? disequilibria from dead to living worlds. *The astrophysical journal*, 2020.
- [60] B. S. Gaudi. *The Demographics of Exoplanets*. IOP Publishing, 2020.
- [61] Jane S Greaves, Paul B Rimmer, Anita M S Richards, Janusz J Petkowski, William Bains, Sukrit Ranjan, Sara Seager, David L Clements, Clara Sousa Silva, and Helen J Fraser. Low levels of sulphur dioxide contamination of venusian phosphine spectra. *Monthly Notices of the Royal Astronomical Society*, 514(2):2994–3001, May 2022. ISSN 1365-2966. doi: 10.1093/mnras/stac1438. URL <http://dx.doi.org/10.1093/mnras/stac1438>.

- [62] guedel et al. Astrophysical conditions for planetary habitability. *Protostars and Planets*, VI:24, 2014.
- [63] Cole Mathis Harrison B.Smith. The futility of exoplanet biosignatures: Astrobiologist need to stop and ask themselves, what are we looking for when we look for life? *BioEssays*, 2023.
- [64] Julie Hartz and Simon George. Quantitative framework for astrobiology strategies and in situ biogenic assessments. *Frontiers in Astronomy and Space Sciences*, 9:769607, 03 2022. doi: 10.3389/fspas.2022.769607.
- [65] Julie Hartz and Simon George. Quantitative framework for astrobiology strategies and in situ biogenic assessments. *Frontiers in Astronomy and Space Sciences*, 9:769607, 03 2022. doi: 10.3389/fspas.2022.769607.
- [66] H. D. Holland. *The Chemical Evolution of the Atmosphere and Oceans*. Princeton University Press, 1984.
- [67] Mahima Kaushik, Aditee Mattoo, and Ritesh Rastogi. Exoplanet detection : A detailed analysis, 2024. URL <https://arxiv.org/abs/2404.09143>.
- [68] Vivien Parmentier Laura Schalker. The air over there: exploring exoplanets atmospheres. *Geoscience beyond the Solar System*, 17(4), 2021.
- [69] Amedeo Balbi Manasvi Lingam. Beyond mediocrity:how common life is? *Monthly notices of the ROYAL ASTRONOMICAL SOCIETY*, 522:3117–3123, 2023.
- [70] R. Luger and R. Barnes. Extreme water loss and abiotic o<sub>2</sub> buildup on planets throughout the habitable zones of m dwarfs. *Astrobiology*, 15(2): 119–143, February 2015. ISSN 1557-8070. doi: 10.1089/ast.2014.1231. URL <http://dx.doi.org/10.1089/ast.2014.1231>.
- [71] Ryan J. MacDonald and Natasha E. Batalha. A catalog of exoplanet atmospheric retrieval codes. *Research Notes of the AAS*, 7(3):54, March 2023. ISSN 2515-5172. doi: 10.3847/2515-5172/acc46a. URL <http://dx.doi.org/10.3847/2515-5172/acc46a>.
- [72] Madhusudhan. Exoplanetary atmospheres: Keyinsights,challenges and prospects. *Annual Review of Astronomy and Astrophysics*, 2019. doi: <https://doi.org/10.1146/annurev-astro-081817-051846>.
- [73] Brandon Carte William H. McCrea. The anthropic principle and its implications for biological evolution. *Philosophical Transactions of the Royal Society of London. Series A, Mathematical and Physical Sciences*, 310:347–363, 1983.
- [74] Therese M.Donovan Ruth M. Mickey. *Bayesian statistics for beginners: a step by step approach*. Oxford university press, 2019.
- [75] Hervé Monod, C. Naud, and David Makowski. Uncertainty and sensitivity analysis for crop models. *Working with Dynamic Crop Models*, pages 55–100, 01 2006.

- [76] S.Krishnamoorthy P.Byrne. Estimates on the frequency of volcanic eruptions on venus. *Journal of geophysical research:planets*, 2021. doi: <https://doi.org/10.1029/2021JE007040>.
- [77] Michael perryman. *Exoplanet Handbook*. Cambridge university press, 2018.
- [78] Andrew Pohorille and Joanna Sokolowska. Evaluating biosignatures for life detection. *Astrobiology*, 20(10), 2020.
- [79] Edward W. Schwieterman and Michaela Leung. An overview of exoplanets biosignatures. *Reviews in mineralogy geochemistry*, 91, 2024.
- [80] Schwietermann. An overview of exoplanet biosignatures. *Exoplanets:compositions,mineralogy,and evolution*, 90, 2024. doi: <https://doi.org/10.48550/arXiv.2404.15431>.
- [81] D. K. Sing1 and M. López-Morales. Ground-based secondary eclipse detection of the very-hot jupiter ogle-tr-56b. *Astronomy and Astrophysics*, 2009. doi: <http://dx.doi.org/10.1051/0004-6361:200811268>.
- [82] Clara Sousa-Silva, Sara Seager, Sukrit Ranjan, Janusz Jurand Petkowski, Zhuchang Zhan, Renyu Hu, and William Bains. Phosphine as a biosignature gas in exoplanet atmospheres. *Astrobiology*, 20(2):235–268, February 2020. ISSN 1557-8070. doi: 10.1089/ast.2018.1954. URL <http://dx.doi.org/10.1089/ast.2018.1954>.
- [83] David S. Spiegel and Edwin L. Turner. Bayesian analysis of the astrobiological implications of life’s early emergence on earth. *Proceedings of the National Academy of Sciences*, 109(2):395–400, December 2011. ISSN 1091-6490. doi: 10.1073/pnas.1111694108. URL <http://dx.doi.org/10.1073/pnas.1111694108>.
- [84] Paul K.Byrne Stephen R. Kane. Venus as an anchor point for planetary habitability. *Nature Astronomy*, 8:417–424, 2024.
- [85] David S. Spiegel Edwin L. Turner. Bayesian analysis of the astrobiological implications of life’s early emergence on earth. *PNAS*, 109:395–400, 2011.
- [86] Douglas A. Vakoch. *Archaeology, Anthropology, and Interstellar Communication*. NASA History Office, 2015.
- [87] Peter D. Ward and Donald Brownlee. *Rare Earth: Why Complex Life is Uncommon in the Universe*. Copernicus Books, 2000.
- [88] way et al. Was venus the first habitable world of oursolar system? *Geophysical research letters*, 43(16):8376–8383, 2016. doi: <https://doi.org/10.1002/2016GL069790>.
- [89] Ann M. Womack, Brendan J. M. Bohannon, and Jessica L. Green. Biodiversity and biogeography of the atmosphere. *Philosophical Transactions of the Royal Society B: Biological Sciences*, 365:3645 – 3653, 2010. URL <https://api.semanticscholar.org/CorpusID:294351>.

- [90] Alice Zurlo. Direct imaging of exoplanets, 2024. URL <https://arxiv.org/abs/2404.05797>.